Politecnico Di Milano

School of Industrial and Information Engineering Master's Degree in Materials Engineering and Nanotechnology

Investigation of carbon nanotubes reinforced thermosetting resins for better tribological properties

Thesis Supervisor:

Professor Giovanni Dotelli

Co-supervisor:
Professor Luca Andena

Master of Science

Sundas Ismaeel

Matricola: 877273

July 2019

Academic Year 2018-2019

Investigation of carbon nanotubes reinforced thermosetting resins for better tribological properties

By

Sundas Ismaeel

Thesis Supervisor

Professor Giovanni Dotelli

Co-supervisor

Professor Luca Andena

This page is intentionally left blank

This thesis work is dedicated to my late grandfather who believed in my abilities

ABSTRACT

The aim of the present study is to develop nanocomposite based on thermosetting resin, with multi-walled carbon nanotubes (MWCNTs) as a reinforcing agent and cellulose as a lubricating agent for the better mechanical and tribological performance. The idea of developing such polymer composites is to make slip rings with them, and replace the ones made of metals in the future. These slip rings will be integrated into an aeronautical "Full Integrated Ice Protection System" as an end application.

As polymer nanocomposite provides high interface area between polymer matrix and nano sized filler thus resulting in better bonding between the two phases and better mechanical properties as compared to pristine polymer or other conventional polymer composites.

For this purpose, four set of samples were prepared using hot compression molding press with different composition of fillers (functionalized carbon nanotubes, unfunctionalized carbon nanotubes, cellulose), thermosetting polymers (melamine formaldehyde, phenol formaldehyde) at molding conditions of 8 minutes, 165ºC, 8 minutes 160ºC and 7minutes 165ºC with constant pressure of 75kg/cm^2 (7.35MPa). Chemical functionalization of the MWCNTs was done and verified by Fourier Transform Infrared Spectroscopy (FTIR). Surface morphology of functionalized and unfunctionalized carbon nanotubes, and molded sample was examined under Scanning Electron Microscopy (SEM).The tribological behavior of these set of samples is investigated by performing tensile, three point bending and scratch tests using Instron 1185 screw driven dynamometer and CSM Microscratch tester.

To develop a composite material for the slip rings that also possess high electrical conductivity, is beyond the scope of this research work. Indeed, electrical performance of the composite developed here, will be investigated in a further work.

Keywords: composite, multi-walled carbon nanotubes, tribology, slip rings, melamine formaldehyde, phenol formaldehyde

ACKNOWLEDGEMENTS

First and foremost, I would like to thank the Almighty God to bless me with an opportunity to pursue the academic path I wished. Secondly, I would like to express my sincere gratitude to Prof. Giovanni Dotelli for giving me the chance to work under his kind supervision, guiding me, sparing his valuable time whenever I needed, suggestions to keep me in the right direction to achieve the desired targets.

I would also like to express heartiest indebtedness to the Gasti Giuseppina for helping me through laboratory experiments also, Professor Luca Andena and researchers from his laboratory for their time and guidance throughout mechanical testing required for this research activity.

I am glad that I fulfilled my father's dream to study in a multi-cultural and internationally renowned university. I would really thank my family and friends for their continuous support, prayers and motivation throughout my master degree and specially thesis.

Last but not the least, I would also like to thank Politecnico Di Milano for awarding me with platinum scholarship so that I could pursue my dream of higher education in an international environment comfortably. I would also take this opportunity to extend my gratitude to university's academic and organizational staff for humble dealing in all aspects with international students.

TABLE OF CONTENTS

LIST OF FIGURES

LIST OF TABLES

LIST OF GRAPHS

LIST OF ABBREVIATIONS

MWCNTs- Multi-walled carbon nanotubes

EDS- Energy Dispersive X-ray Spectroscopy

PTFE- Polytetrafluoroethylene

FTIR- Fourier Transform Infrared Spectroscopy

SEM- Scanning Electron Microscopy

HNO_3- nitric acid

H_2SO_4 - sulphuric acid

$KMnO_4$ - potassium permanganate

This page is intentionally left blank

CHAPTER 1- INTRODUCTION TO RESEARCH

1. INTRODUCTION

1.1 Motivation and Relevance

This research work is for the development of a material with high tribological properties i.e. high mechanical sliding wear resistance, to make a slip ring that has to be integrated into an aeronautical "Full Integrated Ice Protection System".

The "Full Integrated Ice Protection System" is an ice protection system for the main and tail rotor, pitot tubes and the defrosting of the helicopter cockpit windows, including slip rings, which are totally integrated with the electric generation, ice detection system, external temperature sensors, and on board avionics. Usually, deicing is important to prevent asymmetrical ice collection which leads to the imbalance in the propeller blades, destructive vibration and pressure on several parts of plane/aircraft by elevating their weight.

The slip ring not only has to transfer the electric power to the heating elements of the tail rotor blades, but also has to do data transfer from the sensors to the on-board avionics.

1.1.1 Electrical de-icing system in aircrafts

An electrical de-icing system in aircrafts is made up of an electrical energy source, heating elements, system controls and necessary wiring as shown in the figure 1-1. Electrical energy from the aircraft system gets transferred to its propeller hub via electrical connections, which ends in the portion of slip rings and brushes. There are heating elements that are mounted on the aircraft’s spinner and blades, either internally or externally.

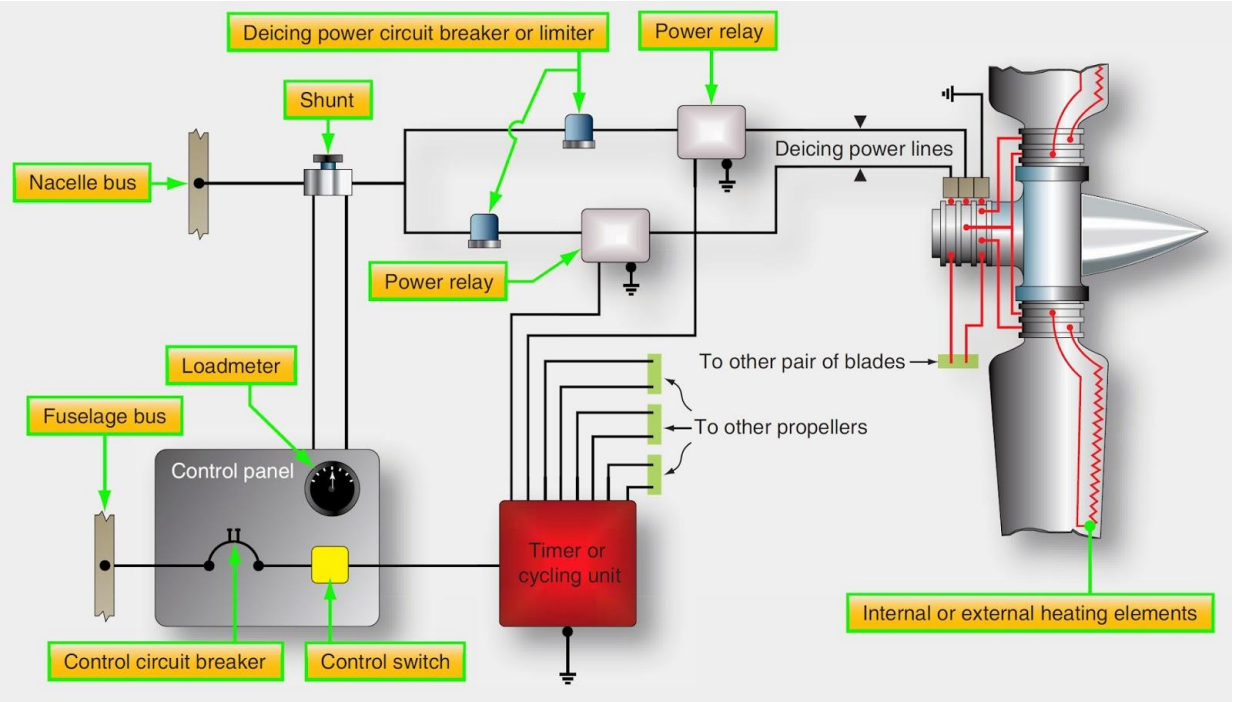

Figure 0-1-1: Typical electrical de-icing system [29]

A deicing system (figure 1-1) generally has some on-off switches, a master switch, and a toggle switch for each propeller. Internal heating elements are present inside a deice boot. A deice boot is attached with an adhesive to the leading edge of each blade.

Slip rings basically are made of two parts, rotating metal ring and carbon/metal brushes. A slip ring and brush block assembly is shown in Figure 1-2. The brush holder guides the carbon brushes. A brush block transfers electrical energy to the slip ring, while slip ring rotates with the propeller and supplies current to the deice boots attached to the blades [29].

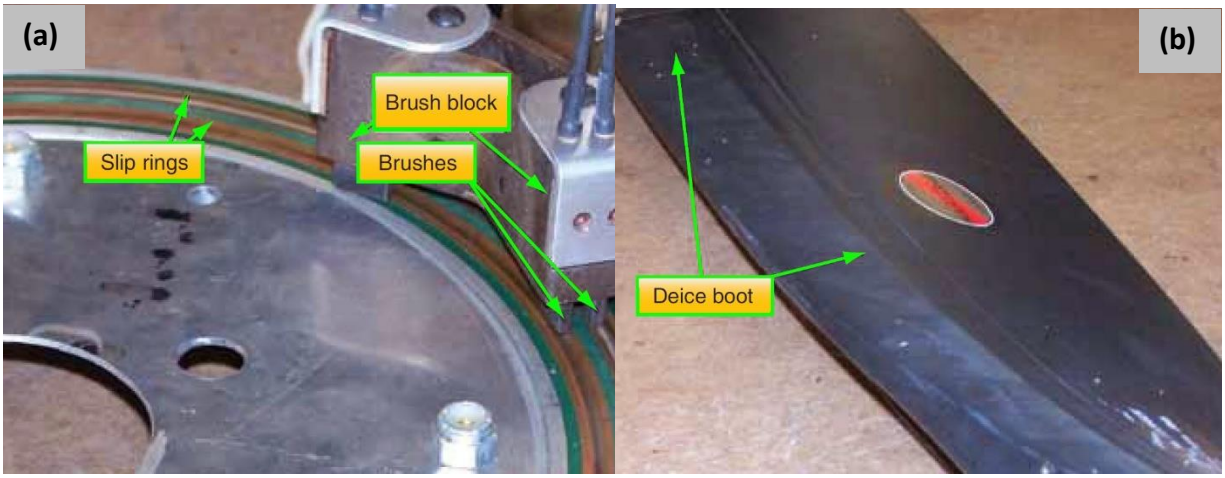

Figure 1-0-2 (a) Deicing brush block and slip ring assembly (b) Electric deice boot

The role of carbon brushes in the slip rings is very important. The polymer composite to be developed during this research mainly targets the replacement of these carbon brushes in the slip ring. Below are the peculiar properties of different grades of carbon brushes which are generally used.

1.1.2 Grades of carbon brushes

The main five grades of the brushes are as follows:

MAIN GRADES	COMPOSITION	PROPERTIES	APPLICATIONS
Electrographitic Brushes (EG)	carbographitic materials produced at high temperature (~2500ºC)	• medium contact drop • low to medium friction coefficient (μ) • high strength • high temperature resistant [30]	Used in • DC stationary or traction industrial machines, operating with low, medium, or high voltage and constant/variable loads. • AC synchronous and asynchronous slip ring
Carbographitic Brushes	mixture of graphite powders and coke, agglomerated with resins or pitch	• moderate contact drop • withstand high temperatures & variable loads	Used in • old designed machines (operating at slow speed and low voltage) • low voltage battery-powered motors • modern but small machines operating with permanent magnets/servomotors/universal motors [30]
Soft Graphite Brushes	purified natural graphite & artificial graphite mixed along with additives and suitable binders	• low shore hardness • good shock absorption properties • low friction coefficient	Used in • steel and stainless steel slip rings for synchronous motors [30]
Resin-Bonded Brushes	natural or artificial graphite mixed along with thermo-setting resin	• high electrical resistance • high mechanical strength • high contact drop	Used in • AC Schrage-type commutator motors • medium-speed DC motors operating at medium voltage
Metal Graphite Brushes (CG-MG-CA)	powdered natural or artificial graphite mixed with copper powder and/or other metal	• low friction • low contact drop	Used in: • low speed and low voltage DC motors

	powders and thermo-setting resins		• medium speed and highly-loaded AC asynchronous motors (e.g. wind turbine generators) • medium speed AC synchronous motors slip rings

Table 1 1Grades of carbon brushes

1.2 Research Objective

The present work revolves around the idea of developing such a material for the ring and sliding brushes that is light in weight, have an adequate life span, possess high tribological properties (wear resistance, scratch hardness, abrasion resistance) and good mechanical strength. For this purpose, polymer composite is prepared using thermosetting polymer resins and CNTs. Cellulose is used as a lubricating agent in such composites. From the range of different thermosetting polymer resins, melamine formaldehyde and phenol formaldehyde are chosen to work with, which were supplied by Chemisol Italia. Melamine formaldehyde used in this research work is named as MF-200 by Chemisol.

1.3 Structure of the thesis

The work on this thesis has been divided into several chapters. Explanation of the chapters is mentioned below:

Chapter 1 talks about the objective of this research and the main motivation behind replacing conventional slip rings with the ones based on polymer composite.

Chapter 2 introduces the main thermosetting resins used in the desired polymer composite.

Chapter 3 explains about the reinforcing filler i.e carbon nanotubes which is used in the desired polymer composite.

Chapter 4 discusses the state of the art on tribological behavior of polymer matrix composites reinforced with different fillers.

Chapter 5 includes the instruments used in this work, experimental techniques employed to prepare the samples, explanation of all the steps involved in preparing samples and finally the measurements performed on them.

Chapter 6 includes results of the experiments and mechanical tests along with its discussion.

Chapter 7 concludes this research work and discuss the improvements that could be made in the future to obtain better tribological properties.

CHAPTER 2- THERMOSETTING POLYMERS

2. Thermosetting polymer resins

Replacing metal slip rings with polymer composites seems a good alternative as polymer composites are light in weight, easily replaceable, have less lead time i.e. needs less time and low cost to fabricate, good corrosion resistivity [40], and low friction coefficient [41].

There are many different thermosetting resins which are being used industrially, but the ones based on formaldehyde and produced as a result of polycondensation are dominating the field for many decades. Formaldehyde based thermosetting resins like melamine formaldehyde (MF), phenol formaldehyde (PF), urea formaldehyde (UF) and melamine urea formaldehyde (MUF) are widely used because of their relative ease of manufacture and relatively low plant investment necessary to produce such resins. During their hardening and gelling phase, insoluble and non-melting 3D cross linked network gets created irreversibly. Depending on the hardening conditions, different resin types are made, for instance: for amino plastic resins based on urea and melamine, acidic environment is needed, for phenolic resins highly alkaline or acidic conditions are required while neutral to light alkaline condition is preferred for resorcinol resins and tannins [34].

2.1 Melamine Formaldehyde (MF)

Melamine (1, 3, 5-triamino-2, 4, 6-triazine) formaldehyde (MF) is among the toughest and most rigid thermosetting polymers having good properties. It is an amino resin with many industrial applications. Some of its advantages are:

- Better hardness
- Thermal stability
- Transparency
- Flame retardant
- Abrasion resistance
- Scratch resistance
- Moisture resistance and surface smoothness

Initially, melamine formaldehyde was used as wood adhesives but later on it has found applications in molding compounds, adhesives, coatings, decorative laminates and flooring. MF resins are involved in a wide range of products which are valued for their relative manufacturing ease and toughness. The relation of MF resin and the curing behavior determine the customized product properties such as electrical, thermal and

mechanical properties. MF polymers that are cured are hard; temperature, chemical and hydrolysis resistant; which makes them suitable for indoor working surfaces. MF lacks surface finishes and mechanical resistance, if it is not properly cured. As an example, MF impregnated papers lack durability, hardness, hydrolysis and chemical resistance. Reaction conditions like temperature, pH, reactant molar ratios, and resin preparation profiles affects the condensation reaction and thus the resultant structure of MF resins. Curing studies of MF resins therefore finds enormous importance. Insolubility of cured resins makes it difficult to chemically characterize them [7].

2.1.1 Resin Chemistry

MF and MUF resins possess high resistance to water attacks, and this characteristic distinguish them from urea-formaldehyde (UF) resins. As MF adhesives are expensive, therefore adding more or less urea in MF leads to MUF resins which is cheaper and thus most commonly used. Some of their main uses are in:

- semi-exterior and external wood panels
- bonding and formation of high and low-pressure paper laminates and overlays [4].

Two main steps are involved in the synthesis of MF resin: methylolation and condensation. Initially, Okano and Ogata attempted to investigate these steps [9].

1. In the methylolation step, melamine reacts with formaldehyde to form a series of nine distinct methylol melamine, utilizing monohexamethylol melamine.

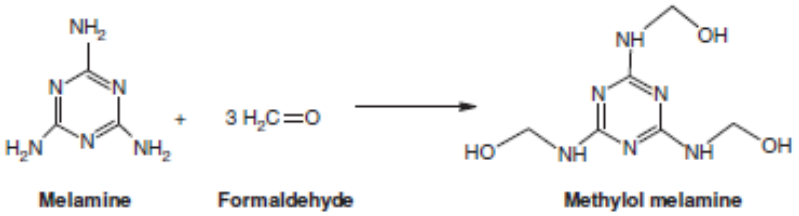

Reaction 1: Melamine and formaldehyde are reacting in the methylolation step

2. The condensation reaction step results in the establishment of many different oligomers containing methylene and methylene ether bridges. pH of the reaction medium dictates the formation of bridges, as methylene bridges are favored in case of low pH i.e 7-8, but if the pH is high i.e above 9, ether bridges are expected to be formed [7]. Ether links can be converted into methylene links by removing formaldehyde as explained in reaction 2.

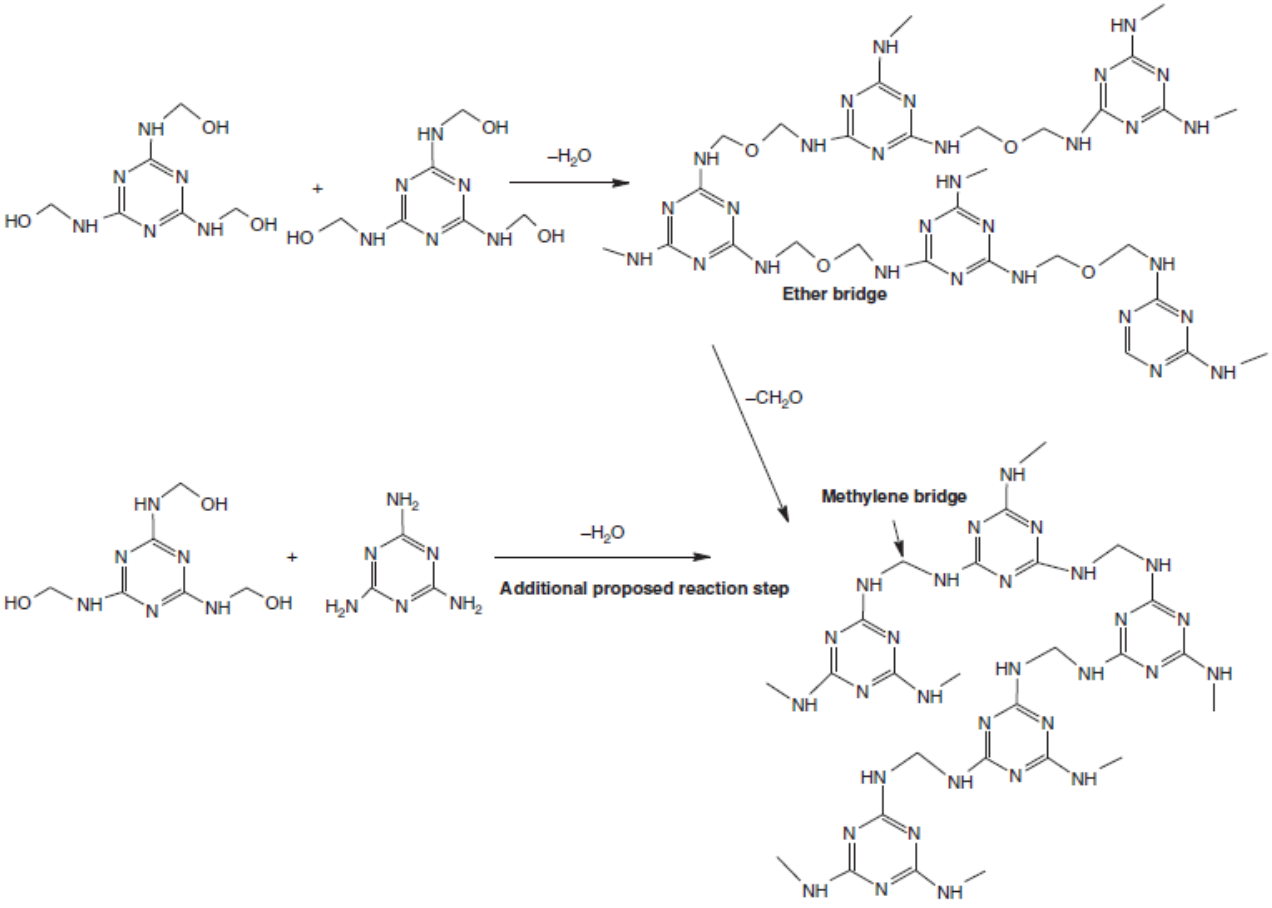

Reaction 2: Condensation step involved in preparation of MF resin.

Melamine as compared to urea is less soluble in water, thus the hydrophilic stage proceeds more quickly in the formation of MF resin. Thus, hydrophobic intermediates appear early in the reaction of the MF condensation.

The condensation reaction involving formaldehyde with melamine is similar as well as a little different from reaction of urea with formaldehyde. With urea, formaldehyde targets the amino groups present in melamine first, resulting in compounds of methylol. The addition of formaldehyde with melamine happens easily and entirely as compared to that with urea. The amino groups in melamine can easily accept up to two molecules of formaldehyde. As a result, there is possibility of complete methylolation of melamine. One molecule of melamine can be attached to 6 molecules of formaldehyde [4].

MF polycondensate prepared by using variable ratios of melamine: formaldehyde (1:1.33 to 1:4), possesses high molecular weight and high processing thermal stability, thus acts as formaldehyde absorbent by the addition reaction of hydrogen (attached on amine group) and formaldehyde (result of polyoxymethylene decomposition in the presence of oxygen and heat). Lower crosslinking MF polycondensates are produced at lower ratio of formaldehyde (melamine: formaldehyde of 1: 1.33), which are unstable and get

decomposed during the analysis of thermal weight loss. In contrary, the unreacted hydrogen on MF molecules is not enough to act as a formaldehyde absorbent of polyoxymethylene at a very high formaldehyde ratio [7].

The formation of melamine depends on the decomposition of methylol melamine, at a temperature that is above 140ºC as displayed in the reaction 3, -NH2 groups are seen in the FTIR spectrum to confirm this reaction step for the partially cured sample (T<160ºC) [7].

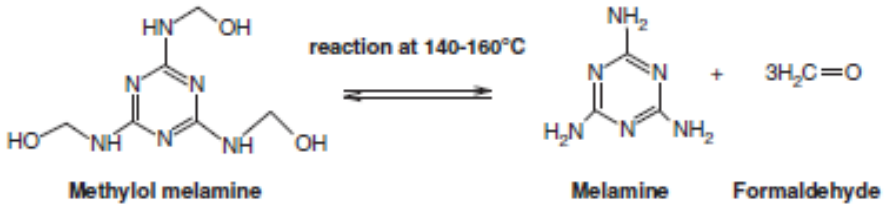

Reaction 3: Formation of melamine by decomposition of methylol melamine.

Koehler [5] and Frey [6] have presented a simplified formula for cured MF resins. They have emphasized on the presence of numerous ether bridges which are present besides methylene bridges and unreacted methylol groups.

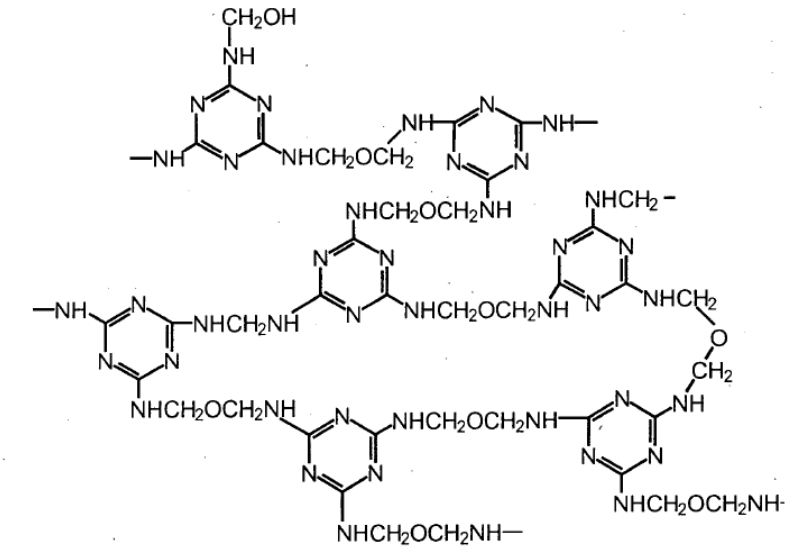

Figure 2 1: Structure of MF resin as proposed by Koehler and Frey (1943)

The idea behind was the fact that no significant amount of formaldehyde is liberated, in MF curing temperatures till 100ºC. Only a little quantity is liberated while curing up to 150ºC [4]. Studies related to MF resins' curing using high-resolution solid state 13C NMR spectra has indicated the conversion of free methylol groups to methylene linkages throughout the process of curing. However, due to the overlapping of residual methylol

groups with methylene ether links, these spectra doesn't provide evidence of enough residual unreacted methylol groups [7].

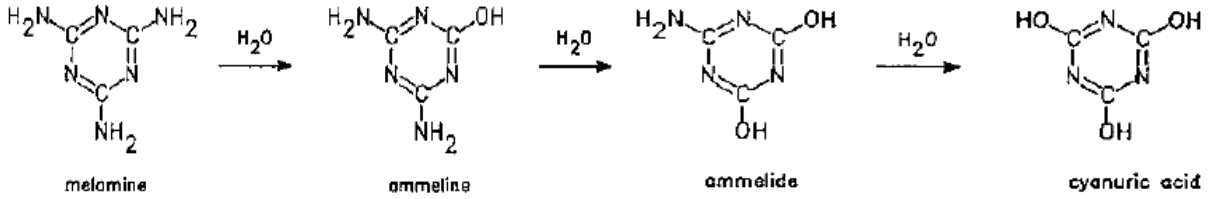

Figure 2 2 By-products during melamine production

Special attention should be paid to the hydrolysis products of melamine, before their preparation starts. To obtain such products, amino groups of melamine gets steadily replaced by hydroxyl groups. Complete hydrolysis produces cyanuric acid (Fig.4), while ammelide and ammeline can be regarded as partial amides of cyanuric acid. Due to acidic nature of MF resin production reaction, such by-products of melamine can be very undesirable for the manufacturer of melamine as they are of no use in MF resin production. These by-products must be removed in the crude form by crystallization of the crude melamine or by an alkali wash [4].

2.1.2 Mechanisms and Kinetics

Melamine reacts with formaldehyde and results in the formation of methylol melamines. The mechanism of acid catalyzed condensation reaction of methylol melamines has been explained by Naito and Sato [4]. It has been observed that the main product of the reaction between formaldehyde and melamine i.e. methylol melamines, are only favoured at higher or ambient temperature, exception is only in acid pH ranges. Although throughout pH range, this is a reversible reaction.

As per the pH used, forward rate of reaction is proportional to either[melamine][H^+CHOH] or [melamine][HCHO] or [melamine$^+$][HCHO].

Condensation reaction between methylol melamine and melamine produces ''dimers'' as a result of an irreversible process, in acidic and neutral conditions at around 70ºC. The hydroxymethylation initially is very rapid and its rate is determined by the condensation of melamine with the conjugated acids of methylol melamines. The rate of reaction is proportional to [melamine]^2[HCHO].

When the ratio of [mineral acid]/[melamine] is between the range of 0.0 to 1.0, the initial stage hydroxymethylation of melamine is relying on the concentration of the molecules of melamine (base species) MH and it's conjugated acid MH_2^+ in the subsequent order:

$$\text{rate} = k_{H_2O}[MH][HCHO] + k_H[MH_2^+][HCHO] + k_{MH_{2+}}[MH_2^+][MH][HCHO] + \\ + k_{MH}[MH]^2[HCHO]$$

If no acid is added, the ratio of [mineral acid]/[melamine] is equal to 0 and the reaction rate can be represented as:

$$\text{rate} = k_{H_2O}[MH][HCHO] + k_{MH}[MH]^2[HCHO]$$

Regarding the formation of methylol compounds as a result of hydroxymethylation, the observed melamine functionality is 6 compared to formaldehyde. Likewise, formaldehyde and malamine react easily with each other to form MF3; while if the formaldehyde is concentrated we get MF6.

2.1.3 Fillers for Melamine Formaldehyde Resins

As MF resins are brittle and rigid in their cured state, so copolymerizing them with a minor amount (3%-5%) of modifying compounds can give the finished product a better flexibility and an improved viscoelastic dissipation of stress in joint. Most commonly used fillers for this purpose are p-toluenesulfonamide, acetoguanamine and e-caprolactam.

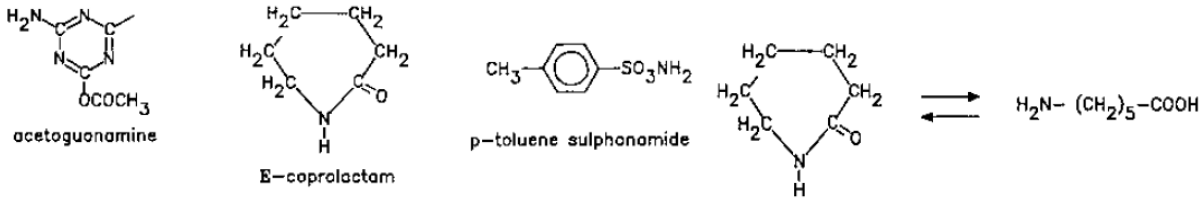

Figure 2 3 Fillers used for melamine formaldehyde resins

Adding fillers results in the reduction of cross-linking density of the cured resin because of reducing the number of aminic or amidic groups in their molecules. The fillers reaches such segments of resins where they can promote linear chains, thus resulting in the reduction of brittleness and rigidity of the resin. For the high-pressure paper laminates, acetoguan amine is most widely used for the modification of resins, whereas for particleboard's low-pressure overlays, caprolactame is used, which is subjected to equilibrium in water. Dimethylformamide acts as a good solvent for melamine, that's why it is often added to melamine in a little amount, to ensure it is completely dissolved and ready for the use [4].

2.2 Phenol Formaldehyde

2.2.1 Raw materials

Phenol-formaldehyde resins are produced as a result of polycondensation reaction between phenols and formaldehyde solutions. Mainly phenolic resins are being made by three raw materials mentioned below:

1. Phenol
2. Formaldehyde
3. Hexamethylene Tetramine (HMTA)

There are some other phenols that can be used as its alternative like monomethyl-phenols (cresols), dimethyl-phenols (xylenols), alkylated-phenols and m-dihydroxybenzene (resorcinol), but phenol being less expensive and easily available limits their usage. Alkylated phenols like p-tertiary butyl phenol and p-tertiary octyl phenol are used as tackifiers in the pressure sensitive tapes and automobile tires respectively. While resorcinol-based resin that can be cured at room-temperature usually find their use in the laminated beams for boat keels, churches etc. [34].

2.2.1.2 Phenol

The primary source of phenol is the fractional distillation of coal tar and various other synthetic processes. Commercially known synthetic processes for producing phenol are at least six, out of which the most common are four i.e Cumene, Raschig, Dow, and Sulfonation. The Sulfonation process which used to be popular at one time, isn't in use anymore [34].

Cumene Process for Making Phenol

Cumene process which was commercialized by H. Hook in 1952, is the reaction between propylene and benzene in the presence of an aluminum chloride catalyst producing isopropyl benzene i.e. cumene. Cumene oxidizes to hydroperoxide which then breaks down to acetone and phenol as a result of acidification.

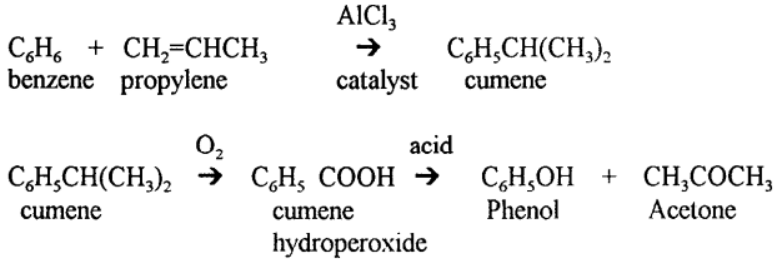

Dow Process

This process involves the direct reaction of chlorobenzene with sodium hydroxide solution at 4000 psi and 300°C. It was established in 1920.

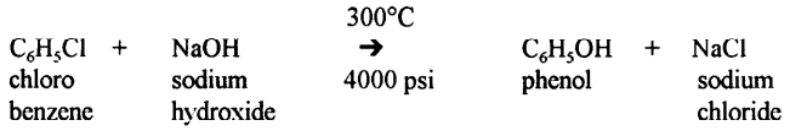

Raschig Process

The Raschig process involves the passing of hydrogen, benzene and air at 200-300°C over a heated copper catalyst. Water in the gaseous state and chlorobenzene as an intermediate product is produced as a result of this reaction. The chlorobenzene gets hydrolyzed by water to produce hydrochloric acid (HCl) and phenol, when it is passed over hot silica catalyst at 500ºC.

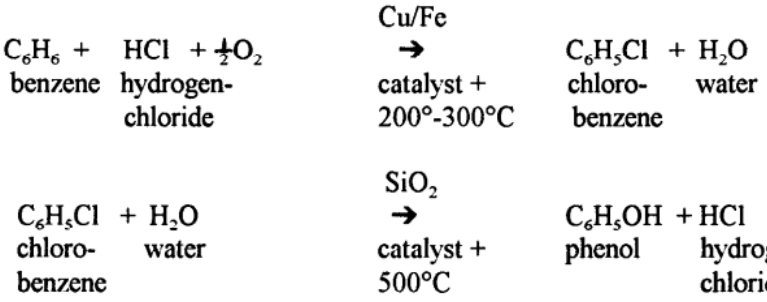

2.2.1.3 Formaldehyde

Formaldehyde is produced as a result of dehydrogenation of methanol in the presence of copper oxide catalyst. This process is carried out at 300-600ºC and the product produced is a 37% formaldehyde solution which is then further enriched to produce formalin i.e. a 40% formaldehyde solution.

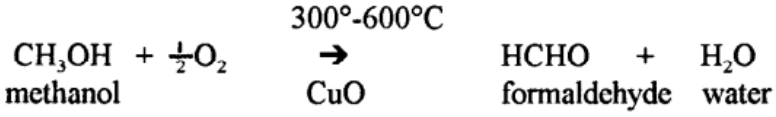

Formalin produced contains impurities like formic acid and methanol. Formic acid gets removed while residual methanol acts as a stabilizer during storage. Rcichhold Chemical, Inc. commercialized this process in late 1950s by the name ‘Formox process’ [34].

2.2.1.4 Hexamethylene Tetramine (HMTA)

It is produced when ammonia gas passes into a formaldehyde solution (30%) at room temperature. Hexamethylene Tetramine is a crosslinking agent and used as an adhesive in organic-inorganic composites.

$6CH_2O$	+	$4NH_3$	→	$(CH_2)_6N_4$	+	$6H_20$
formal-dehyde		ammonia		HEXA		water vapor

2.2.2 Production of phenol-formaldehyde resins

2.2.2.1 Reaction Chemistry

The reaction chemistry between phenol and formaldehyde is not yet known completely. But the known fact is the initiation step of this reaction, which involves benzene ring activation by hydroxyl group like a methylol group (CH_2OH) which get attached to the benzene ring at the ortho and para positions. Resol is produced if an alkaline catalyst is used in the reaction otherwise a novolac is produced if an acid catalyst is used. As work of Baekeland and Lebach suggests, three basic stages are observed in the phenol-formaldehyde reaction:

1. A-stage or resole
2. B-stage or resitol
3. C-stage or resite

At the A-stage, the initial condensation products are mainly alcohols. The resin at this point is thermoplastic and soluble in inorganic solvents. At the B-stage, there is a higher degree of condensation and some crosslinking, with a consequent increase in molecular weight and viscosity, and a decrease in solubility. The resin is not fully cured; it is soft and fusible when hot but hard and brittle when cold. At the C-stage, the degree of polymerization and crosslinking is very high, and there is almost a complete cure. The resin is infusible and insoluble [34].

2.2.2.2 Polymerization Process

Phenols (trifunctional) in the presence of either alkali or acid undergo condensation with formaldehyde (difunctional) producing methylolphenol first and then dimethylolphenol. The initial attack may be at ortho/meta or para position but the next step is the reaction involving methylol groups with other available methylolphenol or phenol, forming linear polymers first and then highly branched and cured structures.

There are two main types of phenolic resins:

1. Resoles or one-stage resins
2. Novolacs or two-stage resins

Resole phenolic resins

They are produced as a result of polymerization reaction between phenol and formalin (1:1) in a reactor for almost 1hour at 100°C (Fig. 6).

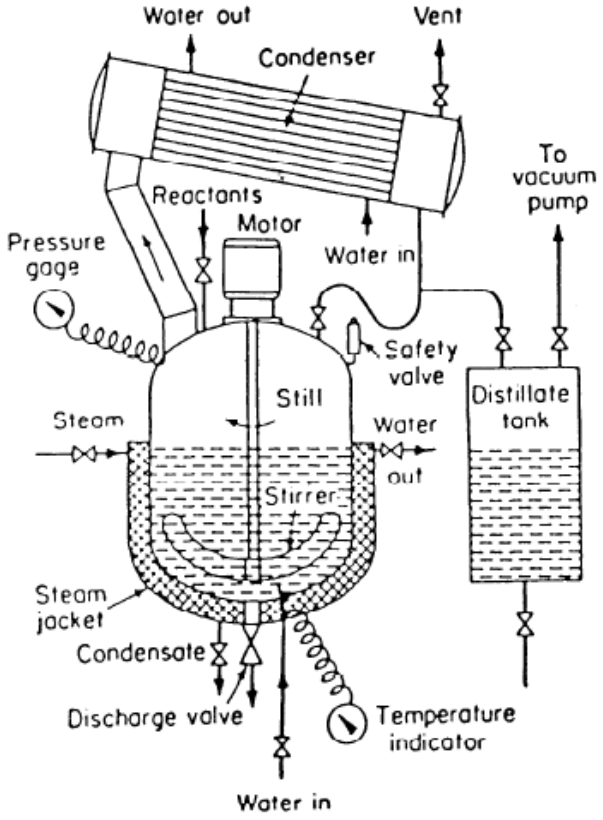

Figure 2 4 Schematic of the reaction chamber for the production of bulk-polymerization of phenolic resins

The reaction takes place in an alkaline catalyst environment, catalyst could be sodium hydroxide, ammonia or sodium carbonate.

Phenol to formaldehyde ratio can also vary from 1:1.1 to 1:1.5. The reaction is concluded short of the gel point via cooling (that's B-staging). The product obtained at this point is an intermediate resin. To obtain a solid product, the same intermediate is dried under a vacuum for 3-4 hours to prevent heat hardening.

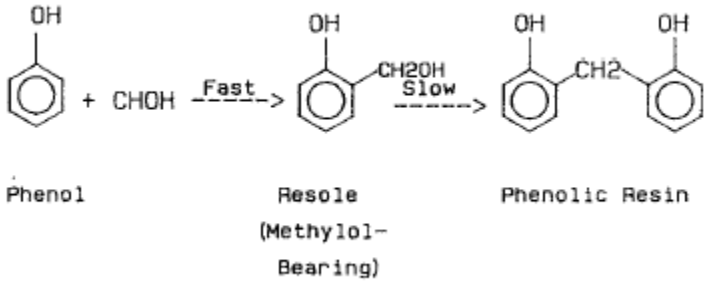

Figure 2 5 Resinification reaction for the production of resole phenolic resins

Resole phenolic resin is a water soluble methylol bearing resin. To obtain the final thermoset material, the resole must be heated in the mold beyond its gel point. The resultant resole resins form large molecules containing methylene crosslinks without the need of a curing agent. The reason of calling them one-step phenolics is their ability to be cured only by heat, without the need of curing agents. This resinification reaction produces water as a by-product, thus a typical polycondensation reaction [34].

Novolac Phenolic Resins

For the production of novalac phenolic resins, acidic catalyst is required such as oxalic acid and sulfuric acid (most commonly used). Other acids that can be used are formic acid and hydrochloric acid. In the pre-polymerization step, phenol-formaldehyde ratio of 1:0.8 is most commonly used.

Polymerization occurs by heating the mixture at reflux for 2-4 hours, with removing water at high temperature of 160°C (Fig. 6). The intermediate produced is low-molecular weight molten material, which is then cooled, crushed and blended with powdered hexamethylene tetramine (HMTA) to produce a molding compound. As novolac phenolic resins needs HMTA as crosslinking agent that is why such phenolic resins are termed as two-step resins.

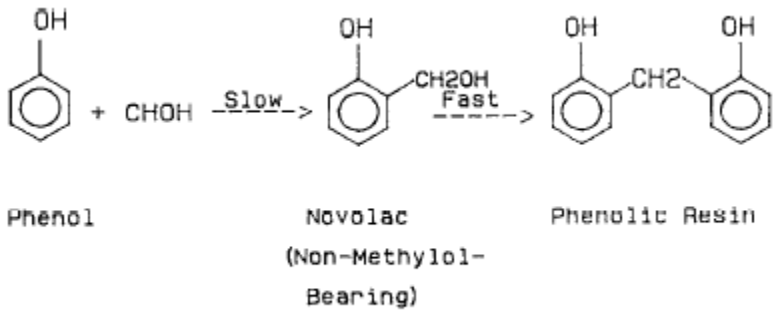

Figure 2 6 Resinification reaction for the production of novolac phenolic resins

When novolac resins are heated at about 165°C in a mold, the HMTA decomposes to give the formaldehyde needed for the final curing, thus obtaining final working ratio of phenol-formlaldehyde i.e. 1: 1.5. As schematic in figure 6, shows steam jacket which fulfills the temperature requirement for the polycondensation reaction of phenol and formaldehyde. The condenser helps in condensation and in removing water vapors coming from the phenol/formalin reaction. Water removal from the system takes the phenol/formaldehyde reaction forward thus causing the formation of more of the product, otherwise product formation would be suppressed. The table below lists the basic differences between resoles and novolac phenolic resins [34].

Points	Resole Phenolic Resins	Novalac Phenolic Resins
1	Produced by alkaline catalyst	Produced by acidic catalyst
2	Produced by B-staging	Made by pre-polymerization
3	Methylol-bearing resins	Non-methyl-bearing resins
4	Shelf-life of less than a year	Have infinite shelf-life
5	Produces water while curing	Produces ammonia while curing
6	Less dimensional stability	More dimensional stability
7	Usually liquids	Usually solids
8	Mainly used for casting and bonding (For example: resins for laminating wood and paper)	Mainly used for manufacturing molding compounds

Table 2 1Differences between resoles and novolac phenolic resins

2.2.3 Properties of Phenolic resins

Phenolic resins are usually opaque and their color ranges from pale/dark brown to black. They are available in the form of powder, flakes, liquid and films. As they are able to be compounded into engineering structural materials that's why they are general-purpose thermosets. Phenolic resins are brittle without the addition of fillers, so additives are supposed to be added while compounding phenolics to get their desired characteristics. For instance, the compressive strength of unfilled phenolic molding resin is around 10,000-30,000 psi while the ones filled with glass fibers shows the compressive strength of about 26,000-70,000 psi.

There are different grades of phenolic resins:

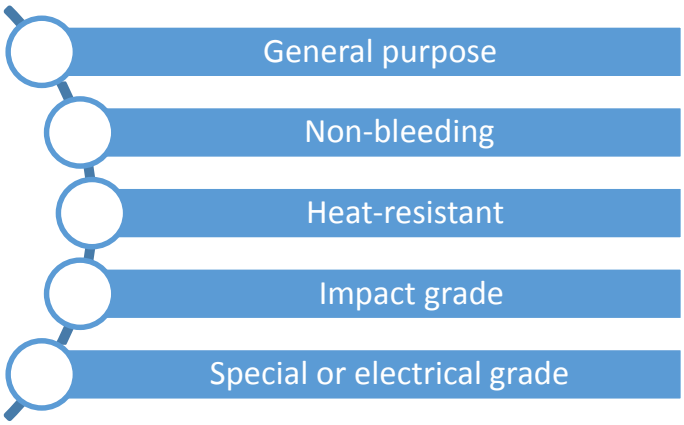

Wood flour filled resin is an example of general-purpose grade of phenolic resins, glass filled resoles belong to non-bleeding grade, while mica/mineral filled resins are from heat-resistant grade. Fillers like rubber, cellulose, glass, fabric makes the Impact grade phenolics. For special or electrical grade resins, mica/glass filled resins are preferred [34].

Properties	Casting Resin Unfilled	Molding Resin Unfilled	Molding Resin Cellulose Filled	Molding Resin Wood flour Filled	Molding Resin Glass fiber Filled
Tensile strength (at break) (psi)	5000-9000	7000-8000	5000-9000	5000-9000	7000-18000
Impact strength izod (notched) (ft-lb/in.)	0.24-0.4	0.2-0.36	0.2-0.6	0.24-0.6	0.5-18
Compressive strength (at rupture) (psi)	12000-15000	10000-30000	22000-31000	25000-31000	26000-70000
Flexural strength (at yield) (psi)	11000-17000	11000-14000	7000-14000	7000-14000	15000-60000
Elongation (at break) (%)	1.5-2.0	-	0.4-0.8	0.4-0.8	0.1-0.2
Hardness (Rockwell)	M93-120	M124-128	E64-95	Ml00-115	E54-101
Heat deflection temperature (at 264 psi) (°F)	165-175	-	300-350	300-370	350-600
Coefficient of linear thermal expansion lo^{-6} (in/in.°C)	1700-1800	640-1520	30-45	30-45	8-21
Thermal conductivity (10^{-4} cal/sec cm °C)	3-5	-	-	4-8	8-14
Linear mold shrinkage (in./in.)	0-0.01	0-0.01	0.004-0.006	0.004-0.009	0.001-0.004
Dielectric strength (V/mm)	250-400	200-350	300-380	260-400	140-400
Dissipation factor (at 60Hz) (*= 1 KHz)	0.10-0.15	0.06-0.10	* 0.04-0.20	0.03-0.3	0.01-0.1
Water absorption (24 H) (%)	0.2-0.4	0.1-0.2	0.05-0.9	0.3-1.5	0.03-1.2
Specific gravity	1.236-1.320	1.25-1.30	1.37-1.46	1.30-1.35	1.69-2.0

Table 2 2: Different properties of the phenolic resins

Most important properties of phenolic molding resins are mentioned below:

1. They are easily molded into complex shapes and provide finished dimensions without additional finishing touches.
2. They possess very good dimensional stability and accuracy at atmospheric conditions. Normally, molding compounds formed by novolacs shows double dimensional stability than the ones produced using resoles. As novolacs give off ammonia as a result of curing, while resoles give off water. Water molecule being larger than that of ammonia molecule, causes less stability in the overall structure of the resin.
3. Phenolic resins possess high creep resistance. When phenolic resin is tested at condition of 2000 psi, 73ºF, and for over 400 hours, the maximum total strain (%) observed is < 0.1, while the strain at the same conditions for polycarbonate is 0.4, > 1.4 for polyacetal and > 0.6 for polyphenylene oxide.
4. Phenolic resins possess high resistance to deformation under the application of load. Compressive and flexural strengths for phenolic molding resin (general purpose) are 25000 - 31000 psi and 7000-14000 psi respectively.
5. Phenolic molding resins act as good heat insulation materials because of having low thermal conductivities.
6. Phenolic resins are good materials to be used for electrical insulation, with a dissipation factor of 0.03-0.3 and 260-400 V/mm of dielectric strength for general-purpose grades. So they are suitable for low voltage (260-400 V/mm) electrical insulation the most.
7. Phenolic molding resins have really good chemical resistance i.e towards common solvents, weak alkalis and acids, hydrocarbons, but are affected by concentrated acids and strong alkalis.
8. Phenolic compounds absorb water in the low range of about 0.03-1.75%, which is quite low. Although resoles tend to be more water resistant but the unpreheated powdered preforms generally absorb water in an environment with high humidity level while they become stiff by losing moisture in the presence of dry conditions. That's why recommended storage conditions for phenolics are room temperature and relative humidity of about 50-60%.
9. Phenolics are weather resistant materials so they can be used for the outdoors applications but nonetheless heat and prolonged sun exposure may alter its properties and can lead to failure.
10. Phenolics possess fairly good machining qualities specially for casting resins.

2.2.4 Fillers for Phenolic Resins

Adding fillers to the phenolic resins improves their performance. It is observed that the resins filled with glass fiber are more stable than the resins filled with cellulose i.e. lower cellulose content produces more stable resin. Typically used fillers for adding into the phenolic resins are:

Fillers used for phenolic resins	Characteristics
Wood flour	Least expensive, provides good appearance, has low heat conductivity and poor impact strength
Cellulose	Imparts good impact strength
Silica	Increases viscosity, reduces cracks, possess abrasive and heat insulation properties
Mineral based fillers	*Mica:* possess good heat insulation and electrical properties, to be used with wetting agent *Clay:* provides dimensional stability, improves heat and chemical resistance, helps control viscosity
Graphite fiber	Expensive, Improves frictional properties, provides lubrication

Table 2 3: Types of fillers used in the processing of phenolic resins [34]

2.2.5 Processing methods for Phenolic Resins

The three most commonly used methods for processing of phenolic resins are:

1. **Compression molding**

   Compression molding as per Leo Baekeland's heat and pressure patent, is mostly used method to produce phenolic resins as the product is strong and dimensionally stable. The controlled pressure and heat throughout the process results in the product with less internal stresses and warpage. Process conditions for compression molding usually are 290-400ºF and 2000-20000 psi.

2. **Injection molding**

   In the screw injection molding, preheated material is injected and conveyed into the mold by rotation and grinding motion of the screw. Phenolic resins are heated around 220-240ºF and processed at the pressure of 10,000-20,000 psi through this method. Productivity of this process can be increased by feeding the material inside the mold automatically and directly thus no need to store and pre-heat the material.

3. **Transfer molding**

   Transfer molding is widely used for manufacturing intricate parts. This process utilizes a separate heated transfer charger which allows to push pre-weighed and preheated resin into the mold via plunger or auxiliary ram. This process can be used for producing the parts with both thin- and thick-walled sections.

4. **Runnerless injection compression (RIC)**

   RIC is a runnerless method, which implies less material loss. It combines the advantages of injection molding and compression molding i.e automated feeding system and dimensional stability respectively. With low pressure the material is

injected into a partially open mold and with the compression force the mold is closed [34].

2.2.6 Applications of Phenolic Resins

Phenolic resins have their applications in different areas, some of them are as follows:

1. Phenolic resins are mostly used in bonding and adhesive applications i.e in the composite wood and lamination.
2. Phenolics are good heat insulators because they have low thermal conductivity.
3. Phenolics are used in the preparation of wear resistant products like brake linings, grinding wheels and clutch facings. Typically, the phenolic resins are rubber modified to introduce properties like toughness and elasticity.
4. Phenolic resins are used in bonded and coated abrasives. For example in grinding wheel and emery paper because the bonding ability of phenolic resins are more water, thermal, and mechanical shock resistant than other bonding materials like elastomers and powdered clay.

   A grinding wheel consists of the synthetic fused alumina or silicon carbide as grit, phenolic resins as bonding material, and fillers. Emery paper is a polishing material for the coatings of body of automobiles, its substrate is rubber or acrylic-modified paper bonded with phenolic resin and iron oxide as the grit.
5. Phenolic resins in laminating applications are used mostly in the building, furniture, electrical, and electronics industries. Specifically, laminates are used in printed circuit boards, laminated tubes and rods, decorative laminates, filters, separators, and molded parts. A laminate essentially consists of a substrate (support material) and an impregnating material. In phenolic-resin-based laminates, the impregnating material is phenolic resin or phenolic resin blends, and the substrate is typically a cellulose-based fiber such as cotton fiber or paper fiber.
6. Phenolic resins are molded to produce intricate parts like electrical appliances, housewares and automobile parts. The compounds molded out of resoles are preferred in the making of housewares as it releases water unlike ammonia (in case of novolacs). The molding compounds could be produced by different grades of phenolic resins for example the ones formed by impact grade phenolics are electrical switch blocks and gears, fuse holders, motor housings and frames. Electrical grade of phenolics, because of their high dielectric strength, are used for producing brush holders, wiring device parts, commutators, circuit breakers, automotive ignition parts and electronic connectors.
7. Phenolic resins are also used for coating applications. Their coatings have properties like temperature resistance, adhesion, chemical resistance, anti-corrosion, electrical insulation and abrasion resistance [34].

CHAPTER 3-CARBON NANOTUBES

3.1 Introduction to carbon nano-materials

Carbon nano materials like zero-dimensional (0D) fullerenes, one-dimensional (1D) carbon nanotubes (CNTs), two dimensional (2D) graphene and three-dimensional (3D) nano diamonds have been extensively studied in optics, electrochemistry, mechanics and tribology because of their properties like good corrosion resistance, excellent mechanical behaviors, and high thermal conductivity. Fig 2.shows technological applications of carbon nanomaterials. Fullerenes have the high electron mobility and availability for chemical modification that is why it has been applied to different fields including medical science and optics. C60 is the most stable form of fullerenes, with twenty hexagons and twelve pentagons [5]. But focus from C60 has been shifted to CNTs and graphene because of lots of ongoing research on them [7]. CNTs and graphene are the allotropes of carbons with sp^2-hybridization and they have been widely used for electronics, chemical separation, catalysis support, superlubricity, etc. Some of their peculiar characteristics are their extraordinary charge carrier mobility [8-11], electrochemical stability [12,13] and mechanical flexibility [14,19].

Unlike others nano diamonds contains both sp^2 and sp^3 carbon atoms, where sp^2 carbons undergoes reconstruction and makes the structure of nano diamonds stable [20]. These days, nano diamonds have been explored in biocompatible and wear resistant coatings [21-23] because of their high hardness and tunable surface structures. Nano diamonds have the potential to achieve as many application areas as CNTs [24].

The use of solid lubricants, as components for coatings or as additives in bulk materials has attracted great attention in the field of tribology. Different efficient ways to reduce energy consumption by using carbon nano materials as solid lubricants are being explored.

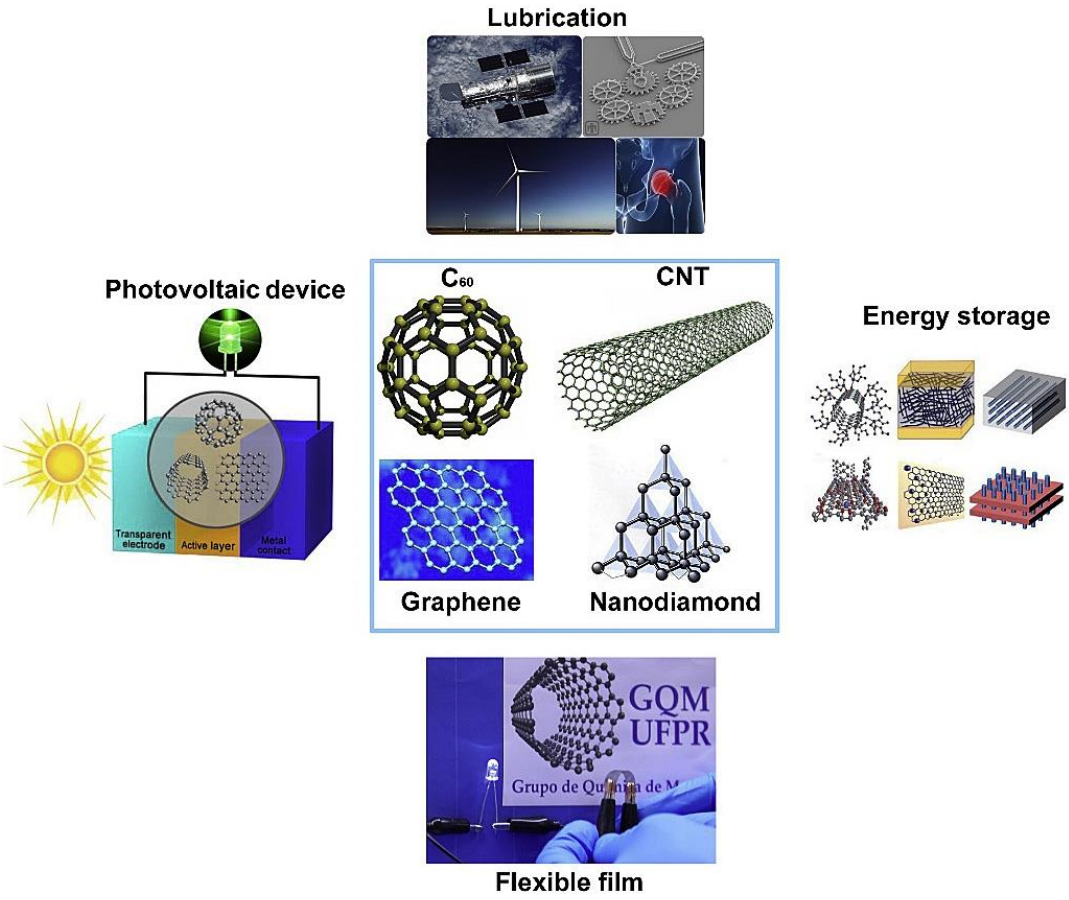

Figure 3 1 Different applications of carbon nanomaterials like fullerenes (C60), Carbon NanoTubes, Graphene and nanodiamond [3-7]

3.2 Properties of Carbon nanotubes (CNTs):

In 1991, CNTs were first prepared employing an arc-discharge evaporation method. The structure of CNTs consists of cylindrical graphite as sp2 carbon which can easily undergo linear and rotational nano-bearings during the nano-sliding or nano-rotating regime [32].

In the present study multi-walled carbon nanotubes (MWCNTs) are used due to their unique structure and possibility of modifications. But there are other forms as well like single wall (SWCNTs), double wall (DWCNTs) carbon nanotubes, where van der Waals forces keeps the cylindrical concentric planes interacting with each other [1].

3.2.1 Functionalization of CNTs

The use of CNTs as reinforcements has been severely limited due to poor van der Waals interaction between CNTs and polymer matrix. CNTs have high aspect ratio (>1000) i.e. nano scale diameter and thus large surface area, so their dispersion is rather different from other conventional fillers, such as spherical particles and carbon fibers. While, the commercialized CNTs have inherent difficulties in dispersion because they are in the form of heavily entangled bundles. In order to improve the interaction of CNTs and foreign molecules, functionalization is done which can be broadly classified as: physical (non-

covalent) and chemical (covalent) functionalization [3]. Different chemical modification methods are used as per required products. This can be done using wet chemical reactions, usually with aqueous solution of HNO_3, H_2SO_4, HCl or their mixtures, oxidation in ozone, oxygen, oxygen plasma and electrochemical reaction. Functionalized MWCNTs, containing oxygen groups, were found to be more active than non-functionalized MWCNTs. As surface groups attached to MWCNTs and surface defects are the active sites for other functionalization and catalytic reactions [1].

3.2.1.1 Covalent Functionalization

The end caps of nanotubes tend to be composed of highly curved fullerene-like hemispheres, which are therefore highly reactive, as compared with the side walls [8,9]. The sidewalls themselves contain defect sites such as pentagon-heptagon pairs called Stone-Walls defects, sp3-hybrideized defects, and vacancies in the nanotube lattice (Figure 1) [8]. Chemical functionalization is based on the covalent bond of functional groups onto carbon form of CNTs. It can be performed at the end caps of nanotubes or at their sidewalls which have many defects. Direct covalent sidewall functionalization is associated with a change of hybridization from sp2 to sp3 and a simultaneous loss of p-conjugation system on graphene layer (Figure 2). This process can be made by reaction with some molecules of a high chemical reactivity. In the first approach, fluorination of CNTs has become popular for initial investigation of the covalent functionalization because the CNTs sidewalls are expected to be inert [10,11].

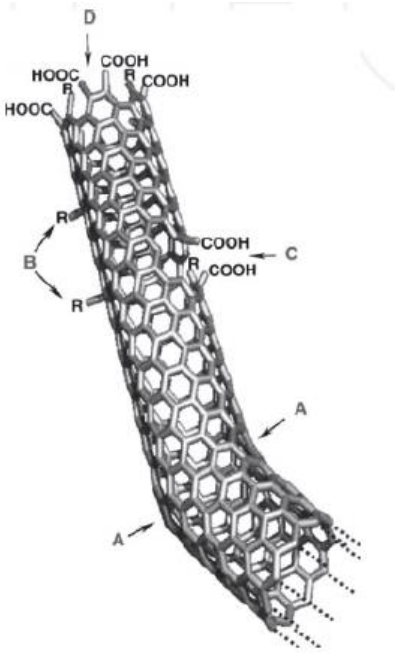

Figure 3 2 Typical defects in a Single Walled Carbon Nanotube. A) Bend in the tube because of 5 or 7-membered rings instead of 6 (normal case) in carbon framework, B) sp^3- hybridized defects (OH & R=H). C) Damage (seen as a hole lined with –COOH groups), caused in the carbon framework due to the oxidative conditions. D) open end of the SWNT, terminated with COOH groups. Besides carboxyl termini, the existence of which has been unambiguously demonstrated, other terminal groups such as -NO2, -OH, -H, and =O are possible [8].

The fluorinated CNTs have C-F bonds that are weaker than those in alkyl fluorides [12] and thus providing substitution sites for additional functionalization. Successful replacements of the fluorine atoms by amino, alkyl and hydroxyl groups have been achieved [13].

Other methods, including cyclo-addition, such as Diels-Alder reaction, carbene and nitrene addition, chlorination, bromination, hydrogenation, azomethineylides [16] have also been successfully employed.

Another method is defect functionalization of CNTs. These intrinsic defects are supplemented by oxidative damage to the nanotube framework by strong acids which leave holes functionalized with oxygenated functional groups [3]. In particular, treatment of CNTs with strong acid such as HNO_3, H_2SO_4 or a mixture of them, or with strong oxidants such as $KMnO_4$ [18], ozone [19], reactive plasma [20] tend to open these tubes and to subsequently generate oxygenated functional groups such as carboxylic acid, ketone, alcohol and ester groups, that serve to tether many different types of chemical moieties onto the ends and defect sites of these tubes. These functional groups have rich chemistry and the CNTs can be used as precursors for further chemical reactions, such as silanation, esterification, thiolation [17], and even some biomolecules. The CNTs functionalized by the covalent methods has good advantage which that was soluble in various organic solvents because the CNTs possess many functional groups such as polar or non-polar groups [3].

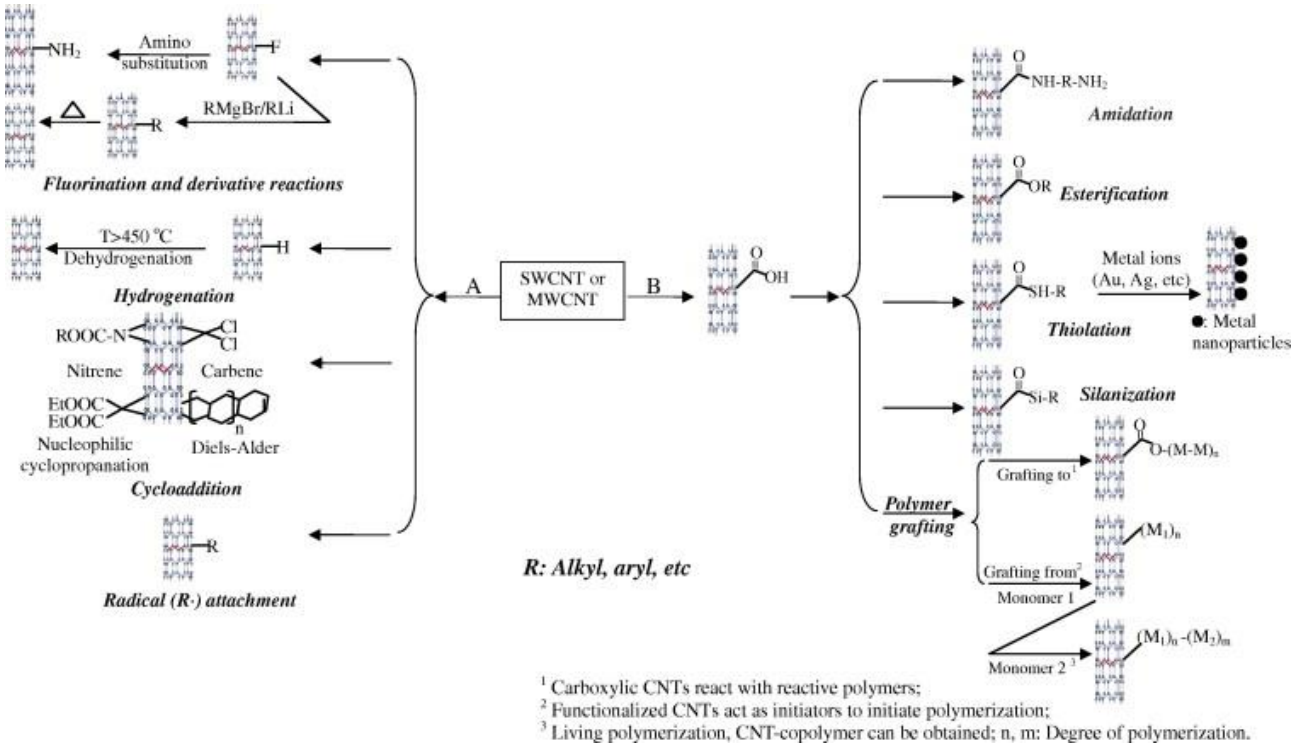

Figure 3 3 Strategies for covalent functionalization of CNTs. A: direct sidewall functionalization;

However these methods have two major drawbacks.

1. During the functionalization reaction, especially along with damaging ultrasonication process, a large number of defects are inevitably created on the CNT sidewalls, and in some extreme cases, CNTs are fragmented into smaller pieces. Namely, the carbon hybridization of CNTs was changed from sp2 to sp3. These damaging effects result in severe degradation in mechanical properties of CNTs as well as disruption of π electron system in nanotubes. The disruption of electrons is detrimental to transport properties of CNTs because defect sites scatter electrons and phonons that are responsible for the electrical and thermal conductions of CNTs, respectively [3].
2. Concentrated acids or strong oxidants are often used for CNT functionalization, which are environmentally unfriendly. Therefore, many efforts have been put forward to developing methods that are convenient to use, of low cost and less damage to CNT structure [3].

3.2.1.2 Non-covalent Functionalization

The advantage of non-covalent functionalization is that it does not destroy the conjugated system of the CNTs sidewalls, and therefore it does not affect the final structural properties of the material. The non-covalent functionalization is an alternative method for tuning the interfacial properties of nanotubes. The CNTs are functionalized non-covalently by aromatic compounds, surfactants, and polymers, employing π-π stacking or hydrophobic interactions for the most part. In these approaches, the non-covalent modifications of CNTs can do much to preserve their desired properties, while improving their solubilities quite remarkably. It will summarize as followed: aromatic small molecule absorption, polymer wrapping, surfactants, biopolymers and endohedral method [3].

Aromatic molecules, such as pyrene, porphyrin, and their derivatives, can and do interact with the sidewalls of CNTs by means of π-π stacking interactions, thus opening up the way for the non-covalent functionalization of CNTs. Polymers, especially conjugated polymers, have been shown to serve as excellent wrapping materials for the non-covalent functionalization of CNTs as a result of π-π stacking and van der Waals interactions between the conjugated polymer chains containing aromatic rings and the surfaces of CNTs (Figure 10) [3]. Those has reported some organic-soluble conjugated poly(m-phenylenevinylene)- co-(2,5-dioctoxy-pphenylene) vinylene (PmPV) poly(2,6-pyridinlenevinylene)- co-(2,5-dioctoxy-p-phenylene)vinylene (PPyPV) (Steuerman et al.; 2002),poly-(5-alkoxy-m-phenylenevinylene)-co-(2,5-dioctoxy-p-phenylene)-vinylene (PAmPV) and stilbene-like dendrimers to investigate their non-covalent functionalization for CNTs [3].

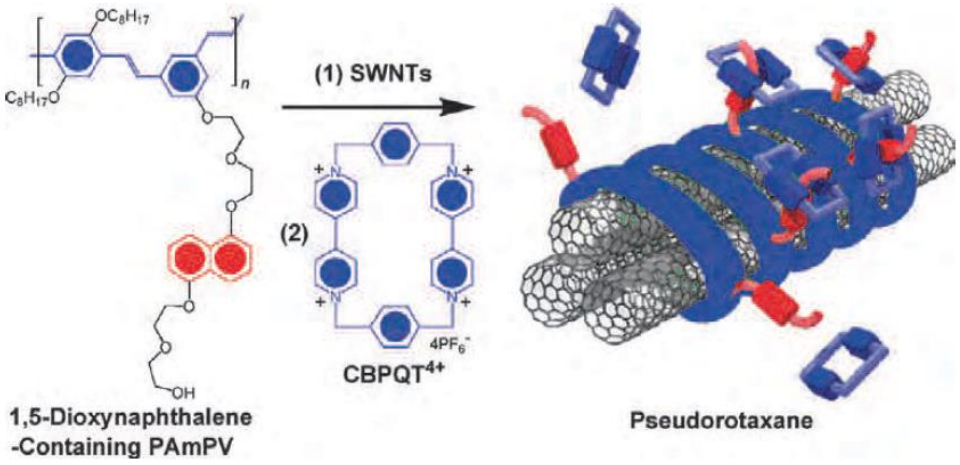

Figure 3 4 The side arms of the 1,5-dioxynaphthalene containing PAmPV-decorated CNTs hybrids associate with cyclobis(paraquat-p-phenylene) (CBPQT4+) rings [3].

In addition, surfactants polymers have also been employed to functionalize CNTs (Figure 11). The physical adsorption of surfactant on the CNTs surface lowered the surface tension of CNTs that effectively prevented the aggregation of CNTs. Furthermore, the surfactant treated CNTs overcame the van der Waals attraction by electrostatic/steric repulsive forces.

The efficiency of this method depended strongly on the properties of surfactants, medium chemistry and polymer matrix. Although surfactants may be efficient in the solubilization of CNTs, they are known to be permeable plasma membranes. They are toxic for biological applications. Therefore, the use of surfactant-stabilized CNTs complexes is potentially limited for biomedical applications [20].

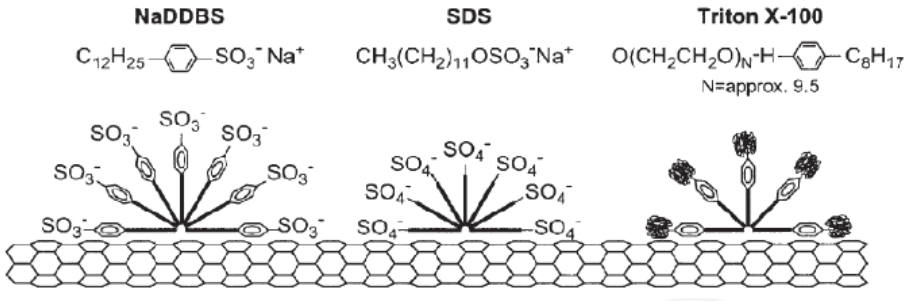

Figure 3 5 The schematic representation of how surfactants may adsorb onto the CNTs surface [15].

3.2.1.3 Alternative routes for the functionalization of carbon nanotubes

The traditional covalent functionalization strategy of CNT is most frequently initiated by chemical acid oxidation acid treatment.

However, dramatic amounts of induced defects during functionalization hinder the intrinsic mobility of carriers along CNTs, which is not preferred in any case. This method

not only functionalizes the nanotube surfaces with carboxylic acid groups but leaves behind detrimental structures, hence hampering their potential for practical applications and can also compromise the mechanical properties of the nanotubes. Therefore, as a common rule, and a now widespread approach to alleviate these problems is to find alternative routes such as an effective functionalization method that can not only introduce high density and homogenous surface functional groups, which enhance the compatibility between CNTs and the foreign matrix, but allow direct grafting and has little or no structural damage to the CNTs, thus, optimizing their properties for various applications [3].

METHOD		PRINCIPLE	POSSIBLE DAMAGE TO CNTs	EASY TO USE	INTERACTION WITH POLYMER MATRIX	RE-AGGLOMERATION OF CNTs IN MATRIX
Chemical Method	Side wall	sp^2 to sp^3 hybridization	Yes	No	S	Yes
	Defect	Defect transformation	Yes	Yes	S	Yes
Physical method	Polymer wrapping	Vanderwaal force, Π-Π stacking	No	Yes	V	No
	Surfactant adsorption	Physical adsorption	No	Yes	W	No
	Endohedral method	Capillary effect	No	No	W	Yes

Table 3 1 Advantages and disadvantages of various CNT functionalization methods. ***S:*** *Strong,* ***W:*** *Weak,* ***V:*** *variable as per matrix-polymer interaction on CNTs [14].*

To overcome this challenge, efficient route to covalently functionalize CNTs have reported a via direct Friedel-Crafts acylation technique (Figure 13). This kind of covalent grafting of the nanotubes is a promising strategy to not only improve nanotube dispersion but also provide a means for creating microscopic interlinks. On the whole, this kind of surface functionalization not only enhances the reactivity, but also improves the specificity and provides an avenue for further chemical modification of CNTs. Not only a mild and an alternative route to functionalize CNTs, this strategy was previously shown to be a less-destructive and/or nondestructive reaction condition for the efficient dispersion and functionalization of carbon nano-materials. As a result, CNT damage from severe chemical treatments including oxidation and sonication can be avoided to a larger extent. Thus, maximum enhanced properties can be expected from improved dispersion stability as well as chemical affinity with matrices [3].

3.2.2 Conclusion

In light of the continuous progress of nanotechnology and material science over the last two decades, CNT based materials have opened new pathways for developing novel functional materials. In summary, CNTs were always been regarded as new and interesting type of materials, especially for energy and electronic applications. All types of CNTs are being investigated with equal importance. While few strategies have been developed so that the handling and manipulation of CNTs be relatively easier, on the whole there is much room for investigations in areas such as supercapacitors. Very recent reports show CNT based supercapacitor devices with better capacitor performance. Precisely, the combination of CNTs with particular macromolecules that offer to enhance the conductivity of the material is one interesting research [3].

3.3 Methods for CNTs characterization

Morphology of CNTs can be characterized by transmission electron microscopy (TEM) or scanning electron microscopy (SEM). The former one can give the structures of CNT walls, and the latter can exhibit the CNT outside sketch. UV-vis scanning spectra can be used to examine the fuctionalized CNTs to check the stability of the complex covalently attached to the CNTs and possible leaching of the complex. FT-IR spectroscopy can show that which kinds of groups are introduced on the CNT surfaces. X-ray diffraction (XRD) patterns of MWNTs can prove that if the modified MWNTs still have the same cylinder wall structure as raw MWNTs and inter-planner spacing of all samples remains the same. The mass loss given by the thermogravimetric analysis (TGA) also can show which groups grow on the CNT surfaces. Evidence for the modification of MWNTs coming from the XPS spectrum can reveal the surface chemical state, and can be used to calculate the content of elements on surface of MWNTs by area of each element. The weight content of elements can indicate the presence of groups [22].

3.4 Applications of carbon nanotubes as functional materials

The possibility to combine the remarkable specificity and parallel processing of biomolecules with carbon nanotubes has attracted considerable attention for several types of applications, including the creation of new types of biosensors, the fabrication of drug or vaccine delivery devices, medical treatment, and so on. Furthermore, the functionalized carbon nanotubes can be also used in fuel cells, and in the field of thermal management. Pantarotto et al. [23] has shown that peptide–carbon nanotube complexes can enhance the immune (antibody) response against the peptides with no detectable crossreactivity to the carbon nanotubes. It has shown that the functionalized carbon nanotubes can cross cell membranes accumulate in the cytoplasm without being toxic for the cell.

CNTs have been increasingly considered as an advanced metal catalyst support for proton exchange membrane fuel cells (PEMFCs), owing to their outstanding physical and mechanical characteristics. Reddy and Ramaprabhu [25] have designed and developed a metal hydride-based hydrogen storage device. For the first time, good quality of

MWCNTs have been synthesized by pyrolysis of acetylene over hydrogen decrepitated alloy hydride catalyst. Pt-supported MWCNTs (Pt/MWNTs) electrocatalysts have been prepared by chemical reduction method using functionalized MWCNTs. MWCNTs have very high thermal conductivity, which make it excellent candidate to prepare thermal conductivity enhanced nanofluids.

Briefly the present steps involved in the preparation of MWCNTs nanofluids include:

1. Disentangle the nanotube aggregates and introduce hydrophilic functional groups on the surface of the nanotubes by mechanochemical reaction
2. Disperse the chemically treated MWCNTs into a base fluid. Potassium hydroxide has been used to modify the surfaces of MWCNTs.

Study found that aspect ratios of the SWNTs and DWNTs could be tailored by adjusting the ball milling parameters. Chemical surface effects of CNTs play the main roles in improving the thermal conductivity enhancement with the increase of temperature [21].

CHAPTER 4- STATE OF THE ART ON TRIBOLOGICAL BEHAVIOUR

4.1 Introduction to tribology

Tribology is the study of two solid surfaces in contact with each other in the relative motion, introducing many complex issues like friction, wear, stiction, scratch, adhesion and surface fatigue. Tribology comes from a Greek word called 'Tribos' which means rubbing. Use of polymers for the tribological applications is increasing because of its properties, like elasticity, shock absorbance, wear resistance and low friction. But polymers, being time dependent and visco-elastic are quite different than other materials like metals etc. Their ability to get chemically modified helps in achieving the required wear properties.

4.1.1 Economic aspects of tribology

Friction, wear and corrosion causes huge cost to the economy of a country. To quantify the impact of these tribological properties on the economics all over the world, Kenneth Holmberg and Ali Erdemir in 2017 [39] considered the four sectors which consume most of the energy i.e manufacturing, residential, power generation and transportation.

They concluded the following facts:

- Tribological contacts consumes 23% of the world's total energy. Out of that 20% is being used to overcome friction while 3% is employed in remanufacturing the parts which undergo wear.
- By employing different ways to reduce friction and wear like creating new surfaces, altering the materials, and their lubrication properties, energy losses could be reduced by 18% in the short term i.e. ~ 8 years while they can exceed to 40% in the long term i.e. ~15 years. Thus, 1.4% of GDP annually and 8.7% of the total energy consumption in the long term can be saved up globally.
- 25% energy can be saved up in the transportation sector, ~10% in the manufacturing and residential sectors, while 20% in the power generation. As per the investigation, these savings would be 55%, 40%, 25%, and 20%, respectively in the long term [38].

As now a days metals parts in automotive sector, housing and flexures are rapidly replaced by polymer components. Therefore, more attention is required for polymer/polymer and metal/polymer tribo-contacts.
Polymer tribology is less well understood and more complex as compared to metal [38]. Although well-established 'Friction Laws' govern the tribology of metal and also ceramic contacts in relative motion, but polymer/metal tribo-contacts usually do not follow such laws due to some reasons mentioned below:

- lower melting points of polymers
- relative softness of polymers

- much lower thermal conductivities associated with heat generation in contacts

4.2 Wear modes of polymers

The reasons of the changes occurring in the surface layer are chemical reactions, mechanical stresses and temperature. Polymers are more sensitive to these factors due to their mechanical behavior and specific structure. Wear raises the local temperature at the interface thus elevating the wear of polymers [36]. Wear mechanisms can be classified as the following

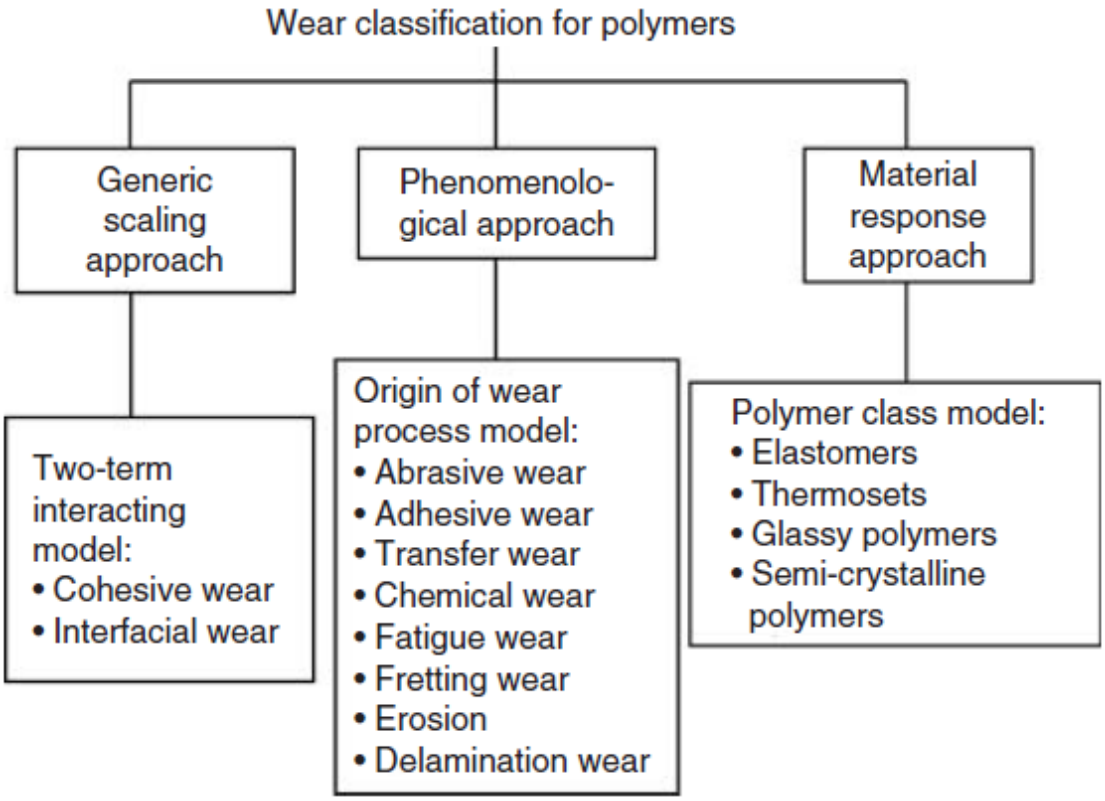

Figure 4 1 Simplified approach to classification of the wear of polymers

Most common types of wear in polymers are:

- abrasion,
- adhesion, and
- fatigue

4.2.1. Abrasive wear

Abrasive wear includes cutting or plowing of the surface by some harder particles or asperities. These cutting points may either be embedded in the counterface called two-body abrasion, or loose within the contact zone called three-body abrasion.

Abrasion results in the scratches, gouges, and scoring marks on the substrate, thus producing debris that appears as finer fine cutting chips. Many models that deals with abrasive wear describe the geometric asperities, like apex angles and shape of the

abrasive points that moves along the substrate surface. Whenever an abrasive particle acts on the plastic material, there are two deformation modes [36].

1. Plastic grooving (ploughing) in which a prow is pushed ahead of the particle, thus displacing the material continuously in the sideways to form ridges just adjacent to the groove. But in this mode no material is removed from the surface.
2. Cutting, here material is removed as a chip because this mode is quite similar to micromachining.

4.2.2 Adhesion wear

Adhesion wear occurs due to the shearing of the friction junctions. In this mode of wear, the material transfer from one surface to another occurs due to localized bonding between the contacting the two. Bely et al. [37] noted that the transfer of polymer is the most important characteristic of adhesive wear in polymers.

If micrometer sized particles get transferred from one surface to another, then the wear rate varies to only a small extent. Whenever hard material is transferred on the soft surface like bronze is transferred on polymer. The hard particles get into soft material acting as abrasive, thus scratching the parent's material.

Polymers are more prone to friction transfer when rubbed both against metals and polymers.

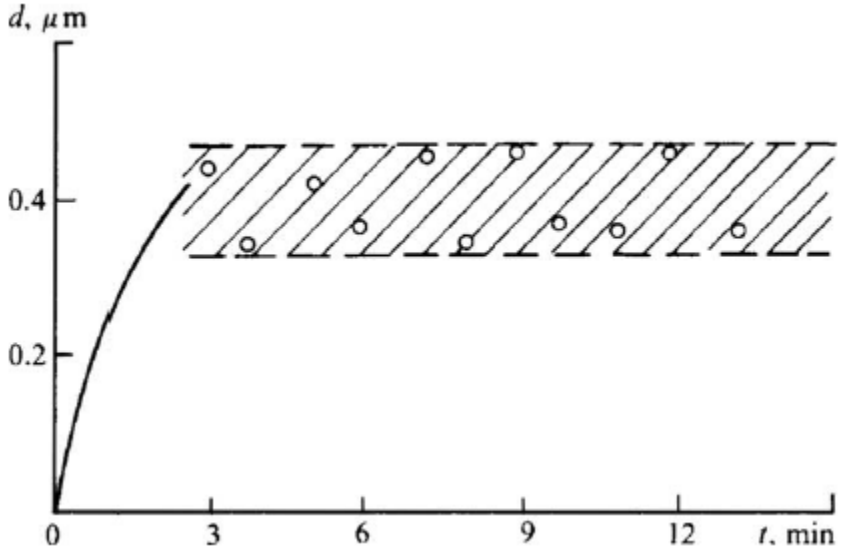

Figure 4 2 The thickness of PTFE layer transferred on PE as a function of friction time (load =0.05 MPa, sliding velocity = 0.35 m/s).

Considering experimental results of the wear test between polyethylene (PE) and polytetrafluoroethylene (PTFE), with cylindrical block-shaft geometry [37], It was found that PTFE is transferred in a very small sized flakes initially but then the thickness of the transferred layer increases monotonically and later it stays at a mean value depending

specially on sliding velocity and load (Fig. 8). Polymer transfer results in a change in roughness of both the contact surfaces [36].

4.2.3 Fatigue wear

Fatigue is cyclic stressing of the material that results in progressive fracture. Fatigue results in accumulation of irreversible changes, leading to formation and development of cracks. Reciprocal sliding and rolling at a friction contact leads to cyclic stressing. Each asperity of friction surface faces sequential loading from the countersurface's asperities, thus creating two different stress fields in surface and sub-surface regions. These fields create material fatigue in these regions resulting in formation and propagation of cracks and wear particles. This process is friction fatigue and the loss of material it causes in the solid surfaces is termed as fatigue wear [36].

Generally, the fatigue cracks originate at the points of maximum tangential stress or the tensile strain. As per theoretical and experimental studies, under contact loading the maximum tangential stress position depends on the friction coefficient. With low friction coefficient ($\mu<0.3$), this point is located below the surface, while with high friction coefficient ($\mu>0.3$), the point is on the surface.

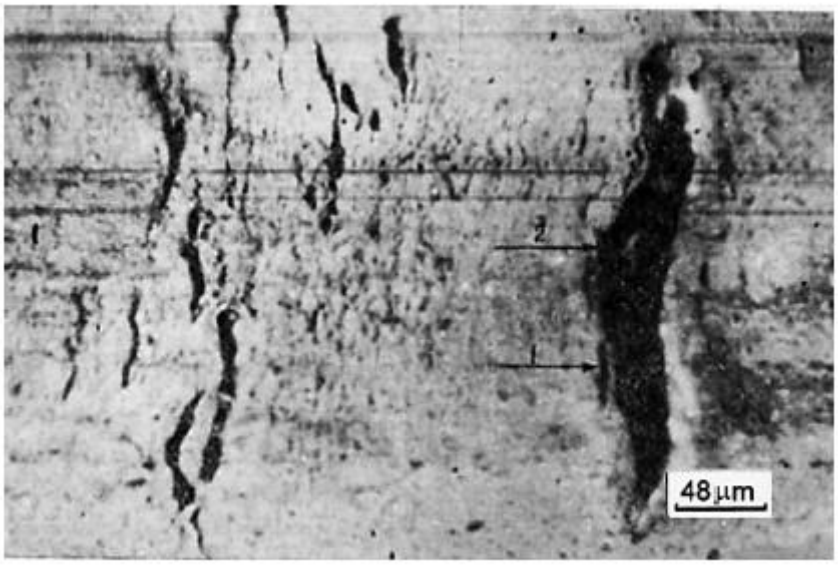

Figure 4 3 Fatigue damage beneath the surface for the epoxy resin with $\mu=0.17$ (source: Bogdanovich PN, Sov J Friction Wear 1982;3(2).

But if a solid is under combined normal and tangential loading, surface and sub-surface regions appear where the tensile strain and frictional heating occur. Thus, cracks can nucleate in surface and/or beneath as shown in the figure above.

Defects like scratches, dents, surface pits, impurities, voids, cavities in sub-surface region assist the fatigue crack initiation thus concentrating the stress [36].

Thermoplastics can be used without any reinforcing agent in the tribological applications, as they possess high wear resistance and low friction coefficient, as compared to thermosets. PEEK and UHMWPE are the ones extensively used. PEEK has relatively high friction coefficient. Nylons and PTFE also find use in wear applications.

Thermosetting polymers possess high hardness and strength but at the same time they have high friction coefficient and high wear rate due to very low elongation at failure values. They are usually used as fiber reinforced composites thus having reduced wear [43].
Use of fibers result in the improvement of resistance towards crack initiation and propagation at the sub-surface level thus less plowing by the fatigue cracking or counterface asperities. To reduce interface friction solid lubricant in a suitable percentage can be added in the composite. In the recent times, this trend has shifted the focus of research on developing composite or hybrid materials for improved tribological performance using epoxy or phenolic resins as the matrix [42].

4.3 Polymer composites for tribological applications

PTFE, can be made wear resistant by reinforcing with fillers like ceramics/metals particles or carbon fiber/aramid fiber or glass fibers. These fillers increase the load-bearing capacity of the resultant composite thus strengthening polymer matrix. The friction coefficient remains lower while wear resistance can be improved up to an order of magnitude. Optimization of the tribological and mechanical properties is needed because the particulate fillers makes composites less tough as compared to the pristine polymer and increase the possibility of fatigue [43].

Addition of hard fillers to a softer matrix results in slight increase of friction coefficient while prominent increase in the wear resistance as in the case of PTFE/GF and Nylon 11/GF. These composites have less load-carrying capacity due to decrease in the strength. To reduce the friction coefficient and increase the wear resistance, fillers should be self-lubricating and interactive at the interface with the matrix. It is important to find an optimum ratio of the filler and the matrix that can help achieve maximum wear resistance along with high bulk strength [43].

As per previous research, single walled carbon nanotubes (SWCNTs) can be considered as quite promising additives for the coatings for example on the silicon surface for the applications with a good wear resistance [31]. CNTs having large contact area, provides excellent bonding between them and the polymer matrix. Satyanarayana et al. [31] have studied how the addition of SWCNTs influences the tribological properties of the polyimide (PI) coating on silicon surface, while the thickness of the coating was 6-7 μm applied at the contact pressure of ~370 MPa using a ball-on-disk tribometer. As SWCNTs

were added to the PI coating, a slight increase in the friction coefficient of the coating was observed, but it was still less than that of the bare silicon substrate. This composite coating showed an exceptional wear life time up to ~7.2 x 10^3 cycles with the friction coefficient of less than 0.30, in comparison to the bare silicon (100 cycles) and pristine polyimide coating (3000 cycles), and didn't show any obvious sign of wear even after 10^5 cycles with the friction coefficient reaching up to 0.5. SWCNTs reinforced PI coating resulted in improved wear durability thus better mechanical properties like hardness and elastic modulus (by 60-70%).

CHAPTER 5 – MATERIALS AND METHODS

5.1 Chemicals

The chemicals used in this work are listed as follows:

1. Melamine Formaldehyde
2. Phenol Formaldehyde
3. Multi-Walled Carbon Nanotubes (MWCNTs)
4. Cellulose
5. Nitric acid
6. Sulphuric acid

5.1.1 Melamine Formaldehyde

Melamine formaldehyde named as HIPERESIN MF-200 obtained from Chemisol (Italia) was used to prepare the samples.

5.1.2 Phenol Formaldehyde

CELLOBOND™ J1115H which is Phenolic novalac resin/Hexamine was obtained from HexionTM (United Kingdom) and it was used in the experiments.

5.1.3 Multi-Walled Carbon Nanotubes (MWCNTs)

In this work, MWCNT's with the purity >95% produced by PlasmaChem GmbH (Germany) has been used. Further characteristics of MWCNTs are presented below:

Number of walls	3-15
Outer Diameter	5-20 nm
Inner Diameter	2-6 nm
Length	1-10 µm
Apparent Density	0.15-0.35 g/cm^3
Loose agglomerate size	0.1-3 mm

Table 5 1 Specifications for the MWCNTs used in this work

5.1.4 Cellulose

Cellulose named JELUCEL® HM 150 T1 produced by JELU-WERK J. Ehrler GmbH & Co. KG (Germany) was used in preparing the samples. It is added to the composite to absorb moisture that is produced during polymerization inside the mold, provide lubricating effect and good surface finish of the final product.

Appearance	Cellulose content	Brightness before tempering	Brightness after tempering	Residue on ignition	Loss of drying	Bulk density	pH-value (10% suspension)
White powder	~ 99.5 %	~ 92 %	~ 87 %	~ 0.3 %	~ 5 %	~ 190 g/l	~ 6

Table 5 2 Specifications of cellulose JELUCEL® HM 150 T1.

5.1.5 Nitric Acid

Nitric acid from MERCK (Germany) was consumed for the experimentations. It was % concentrated.

5.1.6 Sulphuric Acid

Sulphuric acid from Carlo Erba reagents (Italy) was consumed for the experimentations. It was 98% concentrated.

5.2 Instruments

Following are the instruments used for making and testing the samples.

1. Hot Molding Press
2. Ball Mill
3. Vacuum Oven
4. Fourier Transform Infrared Spectroscopy (FTIR)
5. Optical Microscopy
6. Scanning Electron Microscopy (SEM)
7. Dynamometer
8. Micro Scratch Tester

Below is the detailed description of the instruments used for the work.

5.2.1 Hot Molding Press

The hot molding press used for making the samples for this research work, has been manufactured by Jbt Engineering (United Kingdom). This is a pneumatic press with options of heating, cooling, temperature and pressure control.

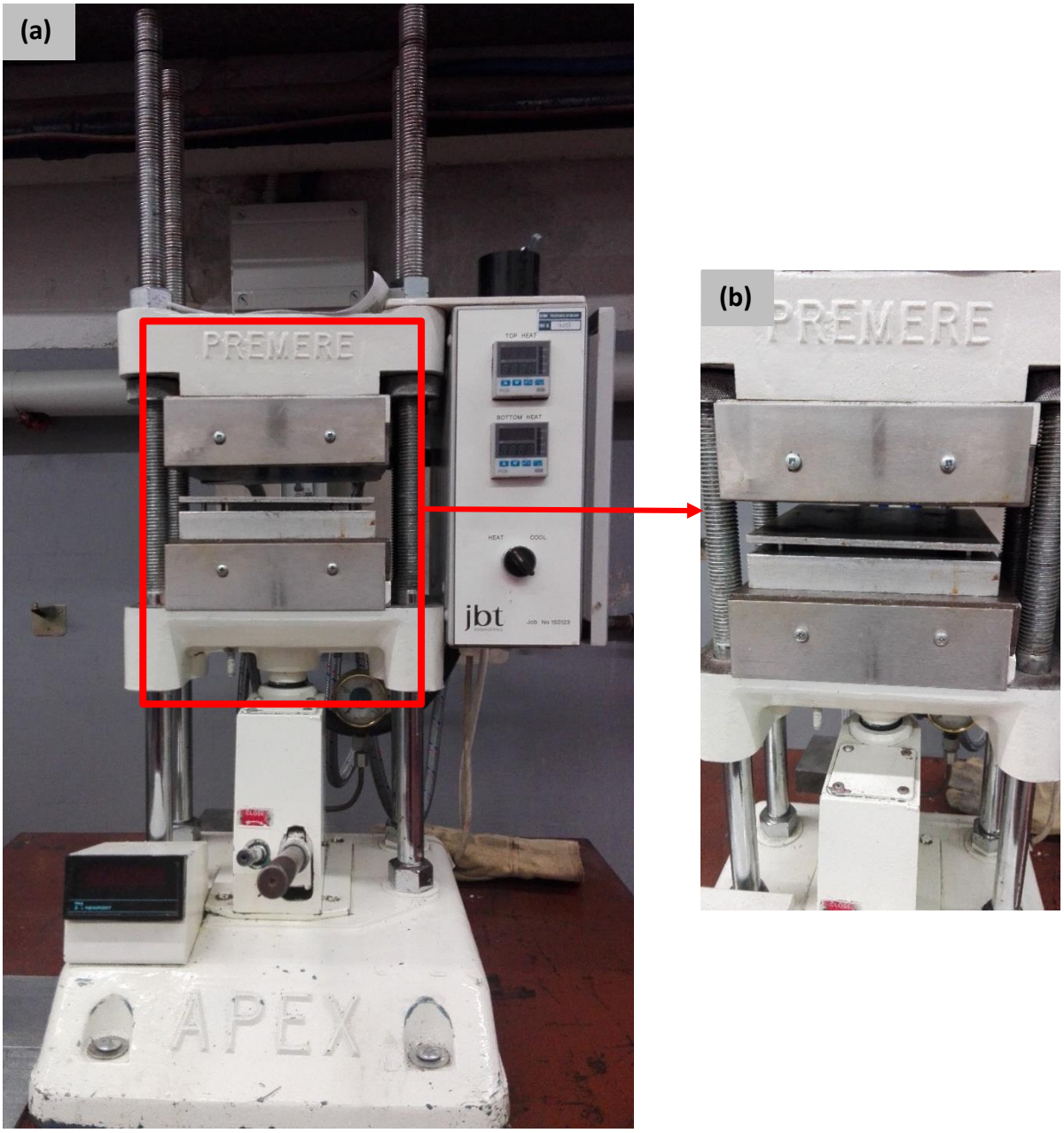

Figure 5 1: (a) Hot molding press (b) close-up of the mold placed between the hot plates of the molding press

5.2.2 Ball Mill

The ball mill is manufactured by an Italian company named MGS SRL, the plastic bottles containing sample powders along with zirconia balls are placed in the brown chamber to get milled.

Figure 5 2 Ball mill apparatus

5.2.3 Vacuum oven

The manufacturer of the vacuum oven is Fratelli Galli (Italy). It is equipped with control AG system i.e it is programmable, and contains platinum probe PT100 Class A. The working chamber is made up of Stainless steel AISI 304 and it has two shelves. There is double display to show both the set temperature and actual inner temperature of the oven. The model of the oven is G-2100 [33].

Figure 5 3 Vacuum oven used for drying the powders during the experimentation [33].

5.2.4 Fourier Transform Infrared Spectroscopy (FTIR)

FTIR studies were performed in a Thermo Scientific (JASCO) FT/IR 615 spectrophotometer (United States). The samples were scanned in the form of KBr pellets containing 2mg of the sample and mg of KBr powder. Spectrum was recorded in the wavenumber range of 4000–400cm^{-1}. The spectra were recorded as percentage transmittance versus wavenumber.

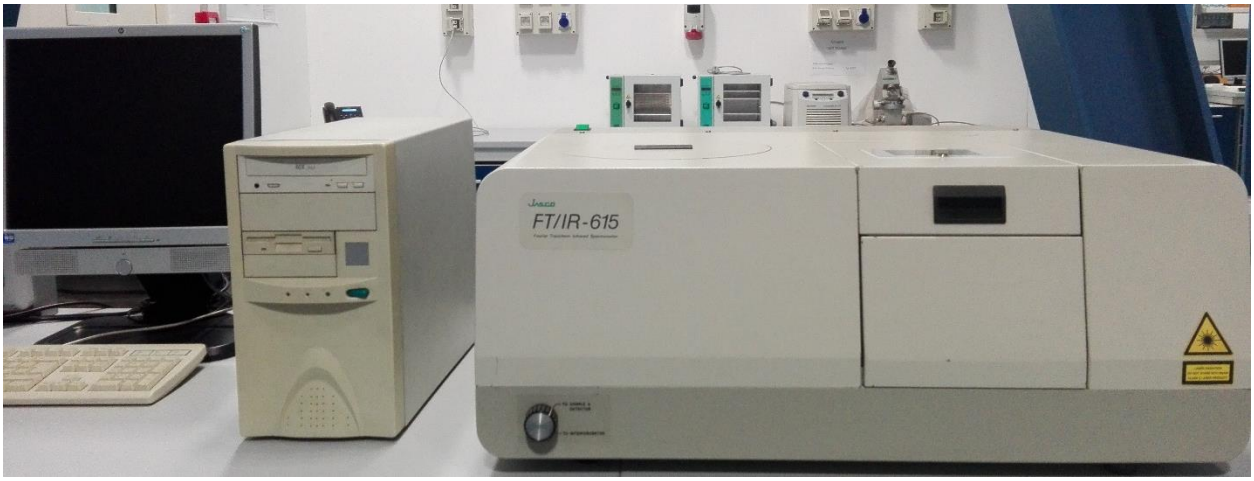

Figure 5 4 JASCO FTIR-615 attached with computer system

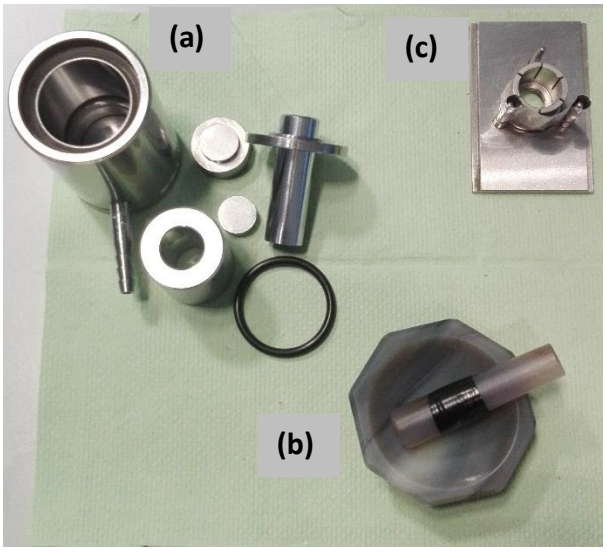

Figure 5 5(a) pellet making assembly (b) mortar to mix and grind the specimen powder (c) holder for the pellet to be placed inside the FTIR equipment

5.2.5 Optical Microscopy

Top view optical microscopy images were taken by using an Olympus BX60 optical microscope (Japan) in reflection mode with multiple magnifications to observe:

1. the uniform mixing of the powders during ball milling
2. the surface of the molded samples to know about the possible defects

Figure 5 6 Optical microscope attached with the computer system

5.2.6 Scanning Electron Microscope (SEM)

Scanning Electron Microscopes (SEM) applies focused electron beam on a sample and tells about its topography and composition. SEM from Carl Zeiss AG - EVO® 50 Series (Germany) was used for the analysis. Powders of functionalized MWCNTs and unfunctionalized MWCNTs are spread on the graphite tape and put inside the test chamber of SEM.

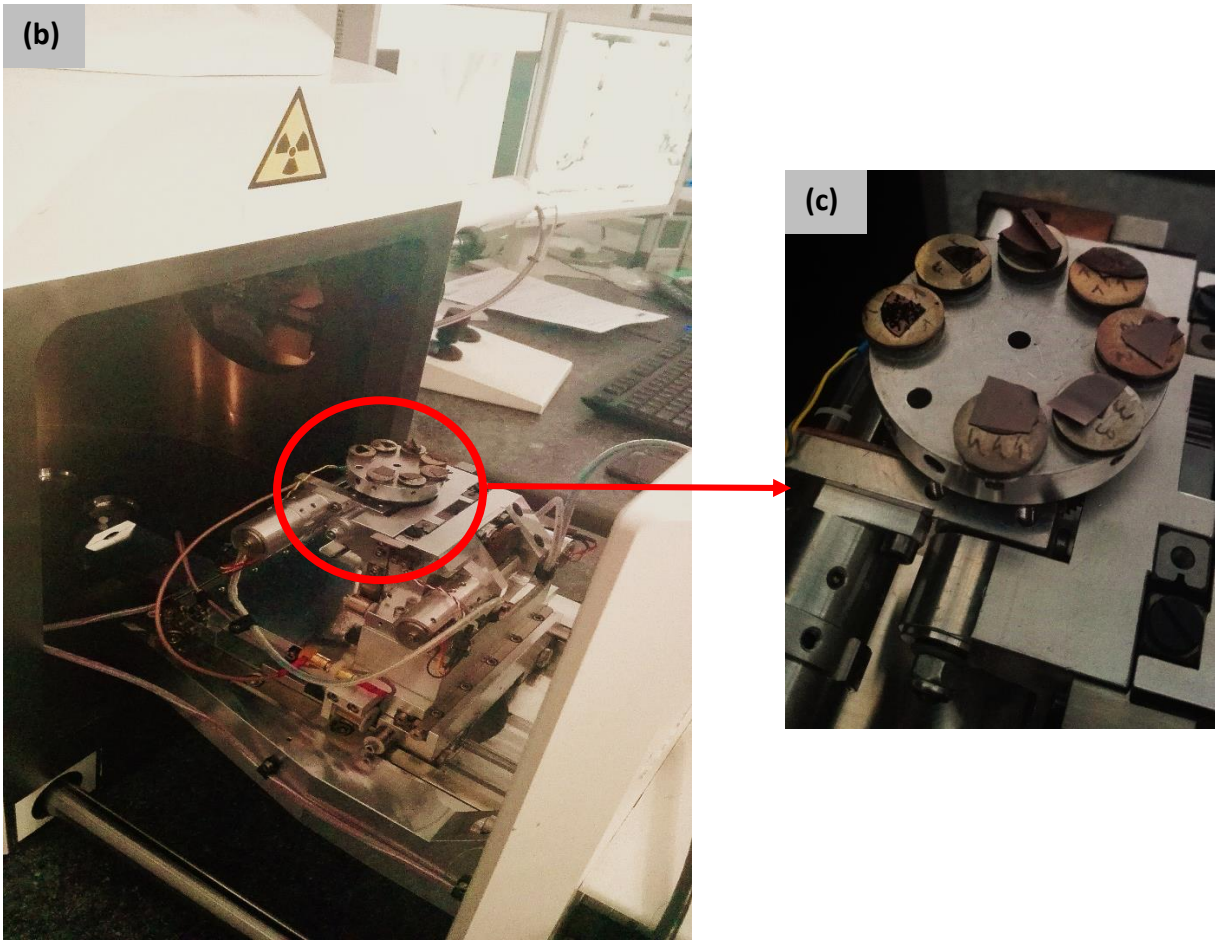

Figure 5 7(a) A typical Scanning Electron Microscope (SEM) showing the electron column, sample chamber, EDS detector and electronic consoles (b) Closer view of sample assembly and chamber (c) Closer view of sample holder mounted with samples for testing

5.2.7 Dynamometer

Instron 1185 screw driven dynamometer (United States) 100kN model was used for mechanical testing in this research work. All the tests were performed at 23ºC. This instrument comes with clip-on extensometer to measure the deformation while the sample is straining.

Figure 5 8 Instron 1185 screw driven dynamometer

5.2.8 MicroScratch Tester

The instrument used for the scratch test is CSM Microscratch tester (United States) equipped with a conical indenter having an apex angle of 120º and a spherical tip with the radius R of 200µm. Constant sliding tip velocities varying between 0.25 and 250mm/min are available. Load from 1-200N is available. It measures the load normal to the surface F_N, the tangential or friction force F_T, penetration depth P_d, residual depth R_d. These parameters, together with the acoustic emission ΔE, constitute a unique signature of the sample under test.

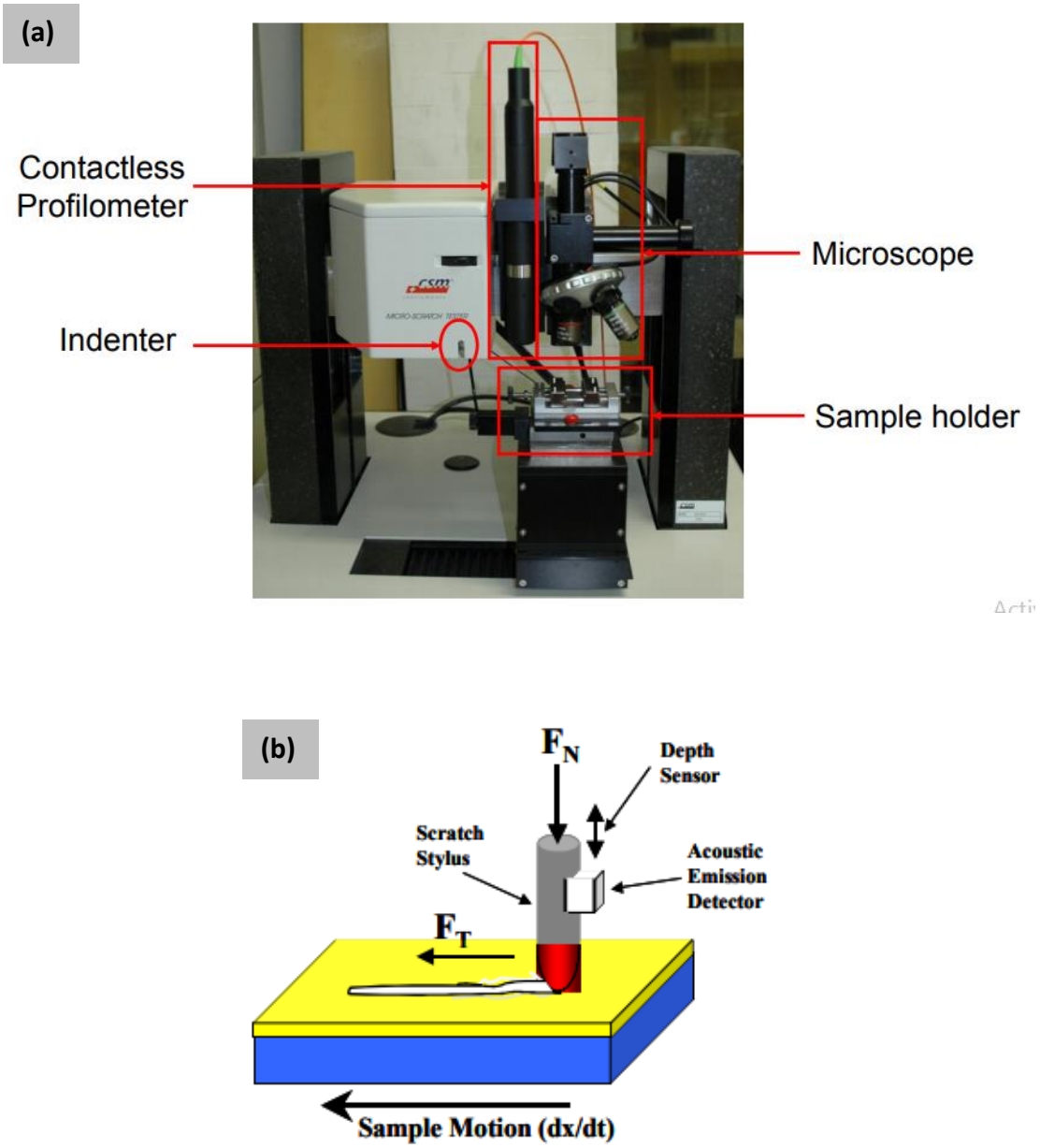

Figure 5 9: (a) Microscratch tester assembly (b) mechanism of forces applied on the sample during the scratch tests

5.3 Experimentation

5.3.1 Functionalization of MWCNTs

169.2mg of as-received MWCNTs were added to a 20ml concentrated mixture of sulphuric acid and nitric acid (75:25 volume %). The suspension was refluxed at 60ºC and 460rpm for 2hr. The suspension was cooled and washed with distilled water, followed by filtration with a filter paper (pore size = 20µm) and a careful rinse with distilled water till the filtrate was neutral. The yield on the filter paper was dried at the temperature of 70

ºC in a vacuum oven for 20 minutes. The obtained functionalized MWCNTs was kept in flask and stored in the desiccator.

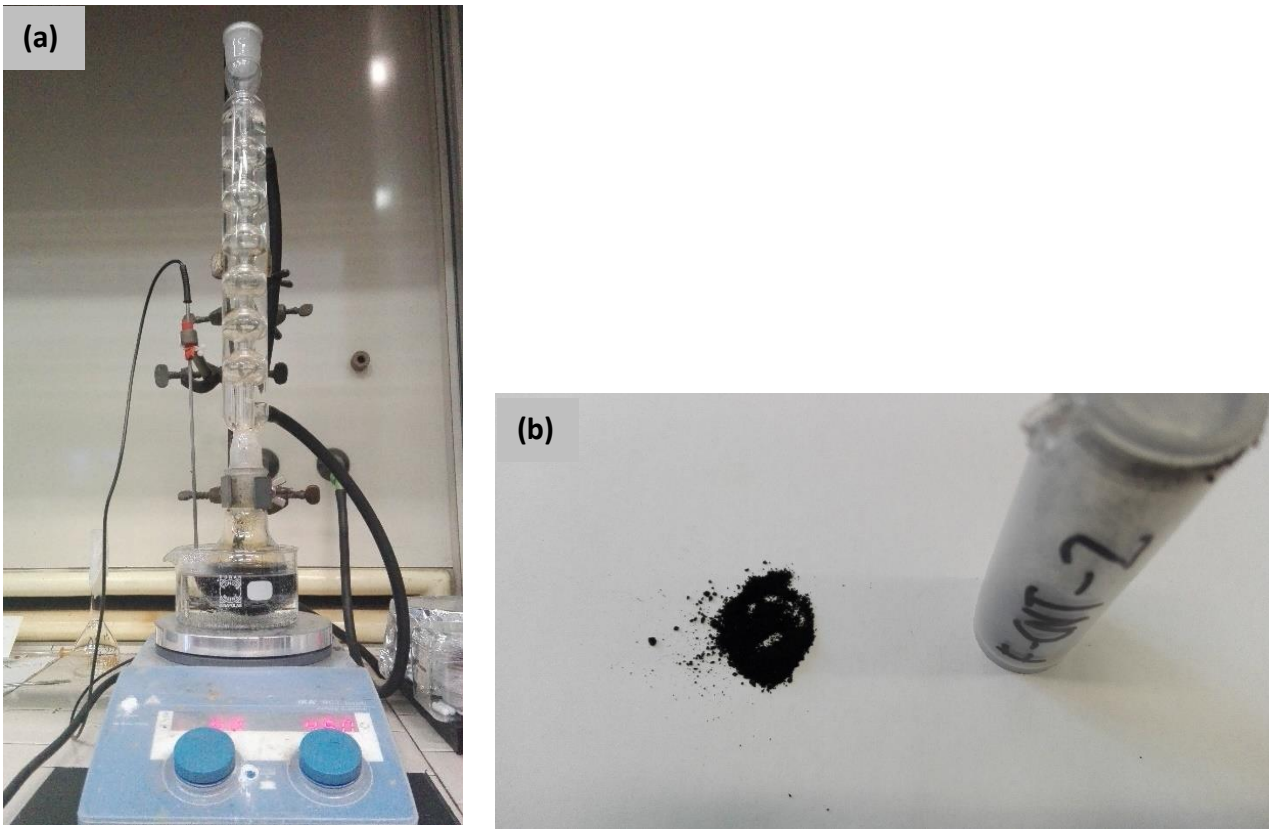

Figure 5 10 (a) Experimentation assembly for the production of f-MWCNTs (b) Dried powder of f-MWCNTs

5.3.2 Preparation of samples

Melamine formaldehyde, phenol formaldehyde, cellulose, unfunctionalized MWCNTs and functionalized MWCNTs are the main ingredients used for making the composites samples. Initially 41 samples were prepared mixing melamine formaldehyde and phenol formaldehyde in different proportions and at different temperature and time conditions, keeping the pressure of constant i.e 75kg/cm^2 (7.35MPa) to find the best suited combination of parameters for the final set of samples.

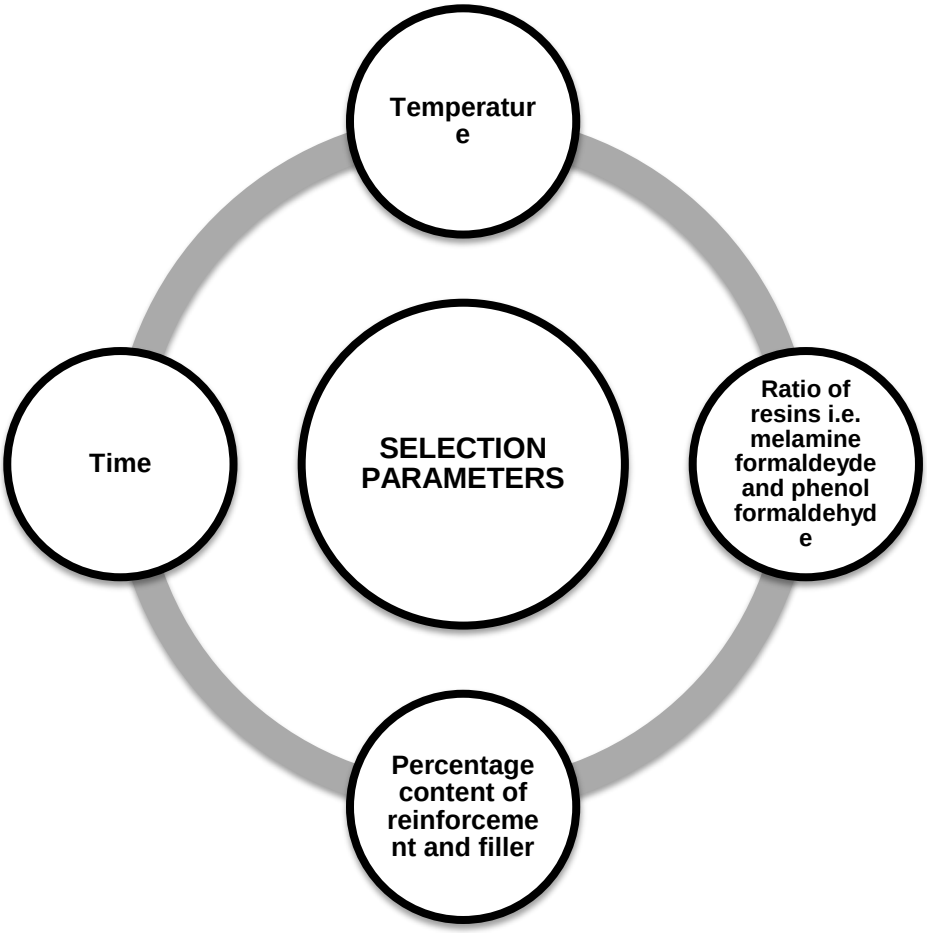

Figure 5 11 Few of the selection parameters considered for making the final set of samples.

Finally, the best conditions were chosen to make the four set of samples, as shown in the tables below:

Sample number	Molding Conditions: 8minutes, 165°C
S1	Base: MF-200
S2	MF+20% cellulose
S3	MF+20% cellulose + 2% unfunctionalized MWCNTs
S4	MF+20% cellulose + 2% functionalized MWCNTs

Sample number	Molding Conditions: 8minutes, 160°C
S9	Base: MF&PF (1:1)
S10	MF&PF (1:1)+20% cellulose
S11	MF&PF (1:1)+20% cellulose + 2% unfunctionalized MWCNTs
S12	MF&PF (1:1)+20% cellulose + 2% functionalized MWCNTs

Sample number	Molding Conditions: 8minutes, 165°C
S5	Base: MF&PF (1:1)
S6	MF&PF (1:1)+20% cellulose
S7	MF&PF (1:1)+20% cellulose + 2% unfunctionalized MWCNTs
S8	MF&PF (1:1)+20% cellulose + 2% functionalized MWCNTs

Sample number	Molding Conditions: 7minutes, 165°C
S13	Base: MF&PF (1:1)
S14	MF&PF (1:1)+20% cellulose
S15	MF&PF (1:1)+20% cellulose + 2% unfunctionalized MWCNTs
S16	MF+PF (1:1)+20% cellulose + 2% functionalized MWCNTs

Total weight of each sample mixture was 30g. Powders were weighed on the laboratory scale weigh balance. 20 weight % of cellulose was decided to be added in the samples, after observing the problems of poor surface finish and bubbles between the polymer interface. As cellulose provides lubricating effect at the interface by decreased shear stress. 2 weight % of functionalized MWCNTs and unfunctionalized MWCNTs was added in all of the samples.

30g of the sample mixtures were put in plastic bottles along with the zirconia balls. These bottles were then placed in a ball mill to get the well mixed powder. Milling time for all of the samples was 2 hours. After the powders were finely milled, they were weighed again, 30g of the powder mixture was taken out for making each sample. Mold is uniformly pre-heated around 45ºC and temperature was checked by non-contact digital laser infrared thermometer gun manufactured by FLOUREON (USA) (figure (b)). Then the mixture powder was poured in a cast iron mold of dimensions 10cm by 10cm (figure (c)) and as per above mentioned molding conditions, the four set of samples are prepared. After the samples are taken out of the mold, they are allowed to get cooled and release thermal stresses. There is a release of colorless and pungent formaldehyde vapors in the environment as a result of polymerization reaction between the ingredients. As per

Environmental Protection Agency (EPA) formaldehyde belongs to Group B1 i.e. probably carcinogenic to humans [35], therefore full face mask with the suitable cartridge filter, by Spasciani Italy, is used to avoid inhaling of formaldehyde gas during molding the samples, as shown in the figure ().


(a)


(b)
FLUKE

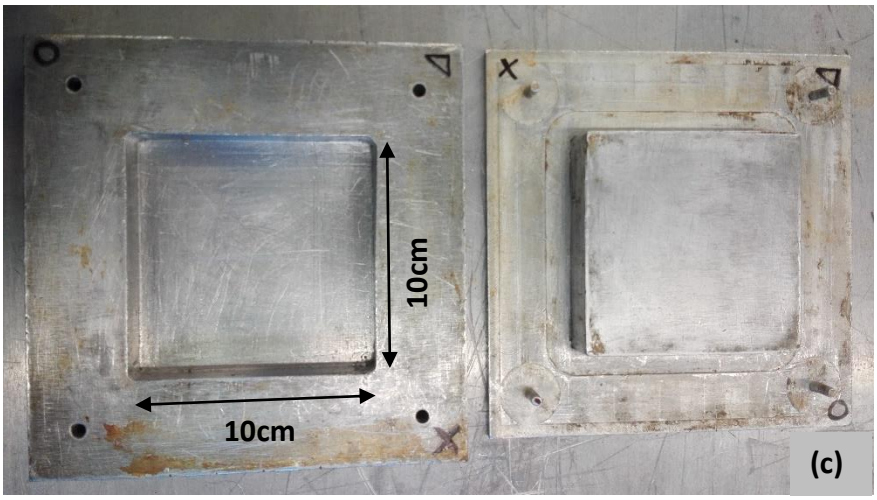
10cm
10cm
(c)

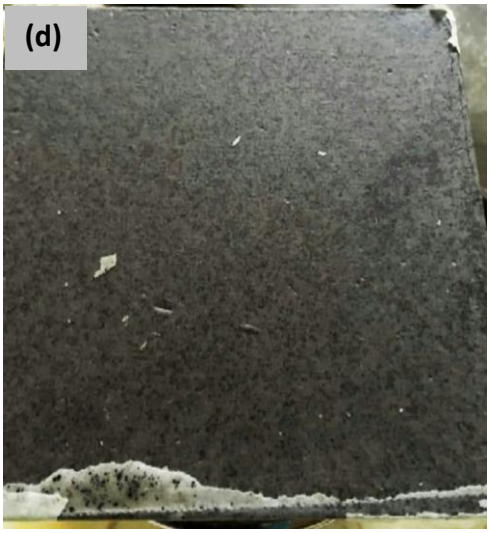
(d)

*Figure 5 12 (a) TR-2002 full face safety mask with the A2 class cartridge filter (Spasciani Italy) (b) Non-contact gun style Infrared thermometer ranging from -50ºC to 380ºC from FLOUREON (USA)(c) 10cm*10cm iron-mold (d) molded sample containing melamine formaldehyde, phenol formaldehyde, cellulose and functionalized carbon nanotubes (MWCNTs)*

5.4 Mechanical testing

5.4.1 Tensile tests

ASTM-638 entitled ''Standard Test Method for Tensile Properties of Plastics'' was used to determine the tensile properties of unreinforced and reinforced plastic. Specimens used for the testing are in standard dumbbell shape and the conditions of humidity, temperature, pretreatment, and machine speed need to be specified. The specimens are subjected to controlled tension and test speed (depends on material specifications) until they fail, while extensometer attached to the specimen determines the change in length observed once the specimen fails.

To avoid the specimen slippage relative to the grips, serrated grip surfaces should be used. Finer serrations tend to be work well with harder plastics, such as the thermosetting materials (phenol formaldehyde, melamine formaldehyde in our case). In this research work, yellow sand paper is used to keep the specimen well griped. At the end of the test, resulting tensile test data reveals essential material properties such as ultimate tensile strength, yield strength, elongation and reduction in area. Poisson's ratio and Young's modulus can also be calculated with this data. Specimens with length 100mm, width 15mm and thickness of 2.5mm are tested under Instron 1185R5800 dynamometer fitted with compression plates. The tests were performed at constant crosshead speeds of 100mm/min and 23ºC. Deformation between the two plates was measured using a strain-gauge extensometer.

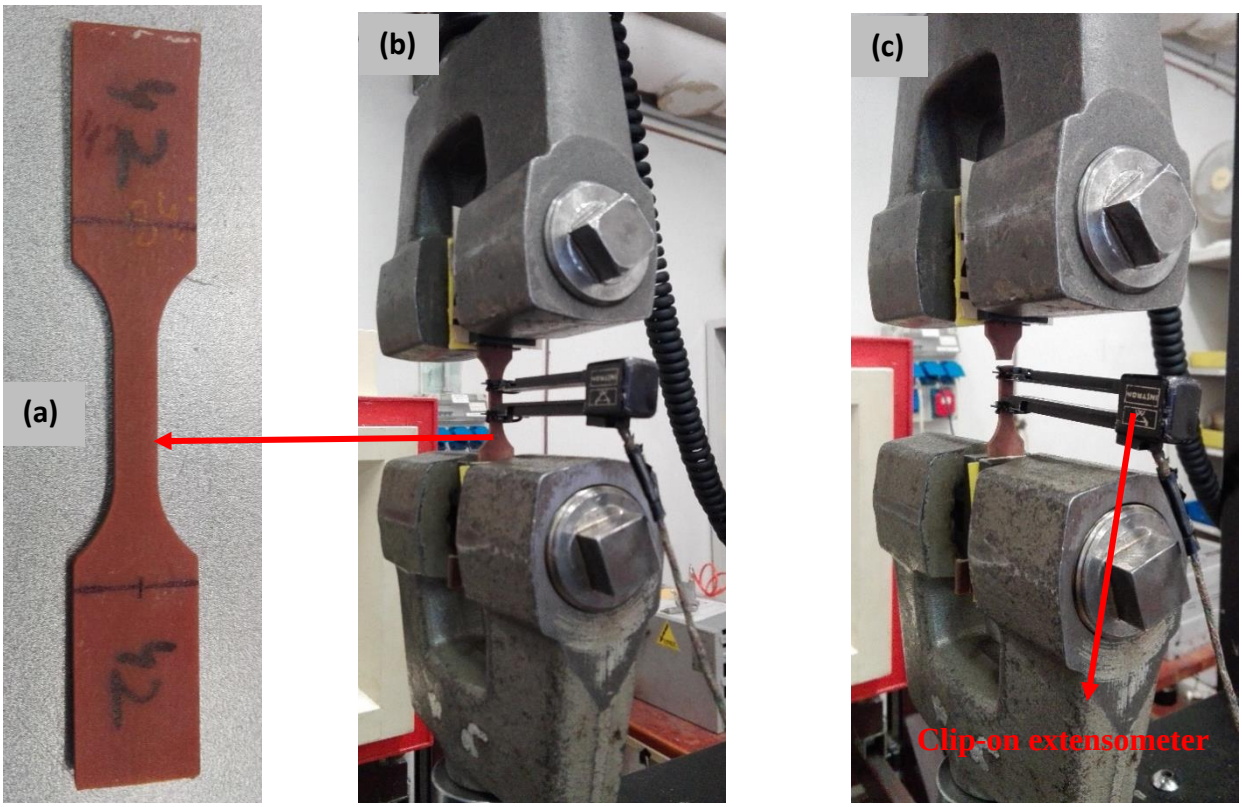

*Figure 5 13: (a) Dumbbell shape of a reinforced composite specimen (b) The specimen held between the serrated grips, **before** the application of the load (c) The broken specimen held between the serrated grips, **after** the application of the load.*

5.4.2 Bending tests

Specifications from ISO/DIS 178 entitled 'Plastics — Determination of flexural properties' was used to perform the bending test.

Principle

A specimen having rectangular cross-section which rests on two supports, observes deflection when a loading edge acts on the specimen midway between the supports. The deflection continues at a constant midspan rate (L) until specimen goes through rupture either at its outer surface or until a maximum strain of 5% is reached. Applied force and the resulting deflection of the specimen at midspan were measured.

It is expressed in megapascals (MPa). L is the distance between the test specimen supports. It is expressed in millimetres (mm). L should be adjusted as per following equation:

$$L = (16 \pm 1)h$$

To calculate the test speed to obtain a specified flexural strain rate, the following equation is used.

$$v = rL^2/600h$$

Where,

v is the test speed,(mm/min)

r is the flexural strain rate, (%/min)

h is the specimen thickness, (mm)

Test speed of 1mm/min was used for these tests.

Supports and loading edge

The arrangement of two supports and central loading edge should be parallel to within ±0.2 mm over the specimen width, as per specified in the standard.

Radius of the loading edge = R1 = 5.0 mm ± 0.2 mm;

Radius of the supports = R2 = 2.0 mm ± 0.2 mm (for specimen having thickness ≤ 3 mm)

Preferred sample dimension (mm)	Sample dimensions used (mm)
Length l: 80.0 ± 2	Length l: 70
Width b: 10.0 ± 0.2	Width b: 10
Thickness h: 4.0 ± 0.2	Thickness h: 2.5

Table 5 3 Test parameters

σ_{fM} is the maximum flexural stress a specimen sustains during a bending test. While for calculation of flexural-stress, following equation is used:

$$\sigma_f = 3FL/2bh^2$$

Where,
σ_f is the flexural-stress parameter
F is the applied force, (N)
b is the width, (mm)

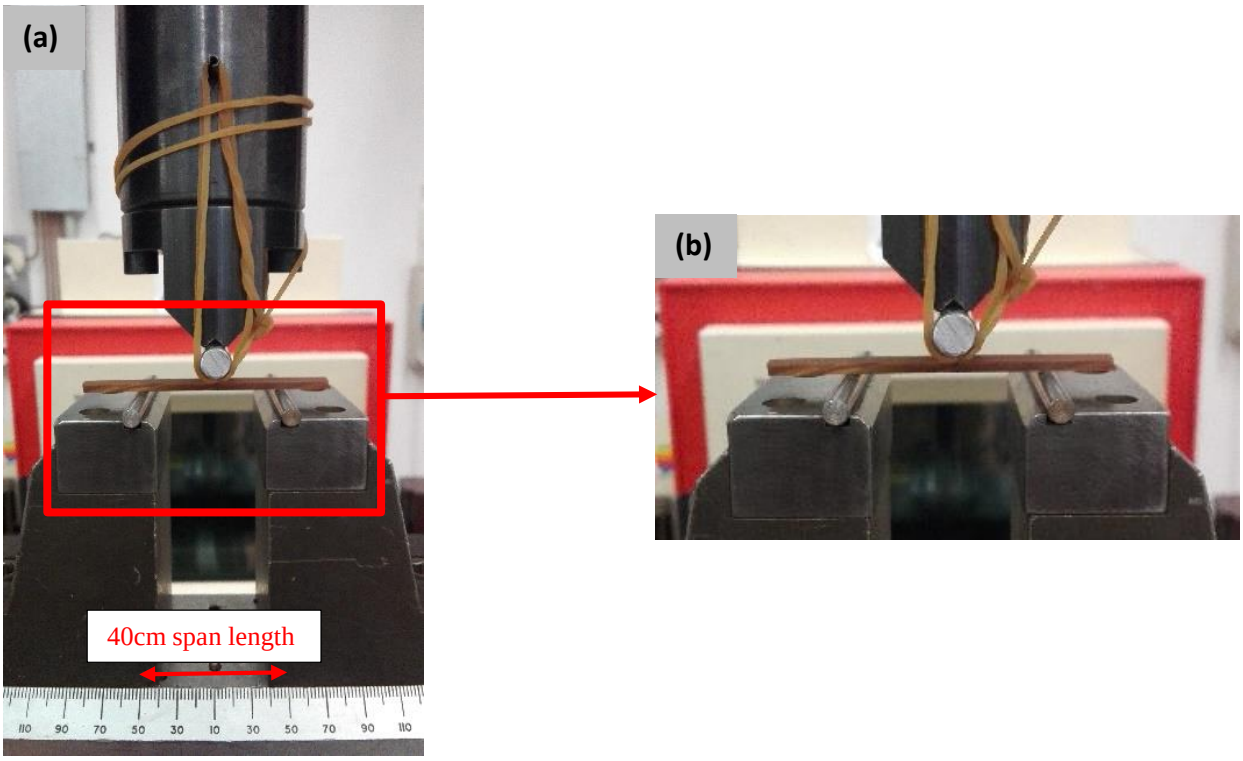

Figure 5 14(a) Specimen in the three point bending mode with the span length of 40cm (b) close up of the sample between the three supports

5.4.3 Scratch Properties

For the mechanical stability of the components, their scratch resistance is one of the essential features. The presence of scratches affects the performance of polymer components badly. Scratches are not only aesthetically undesirable, but they can also impair the functionality of the component or can be a threat to their structural integrity. To quantify and qualify the surface damage occurring during a scratch test, different analytical models and evaluation technique are used. Commonly used methods include:

a) Observation of the change in the optical properties like grey level, reflectivity, and gloss.
b) Making scratch deformation maps which can show how the deformation modes change as the indenter geometry and testing condition varies.
c) Analyzing the rest of the scratch groove either using a profilometer or some microscopy methods, then determining scratch hardness at the end.

Scratch behavior of polymers depends on different factors, which are categorized in two main groups:

a) Geometry of the indenter and testing conditions like normal load F_N, sliding tip velocity '*v*', and temperature during the test.
b) Material properties like modulus, yield stress, ductility, hardness, crystallinity, surface roughness, and surface tension. Many authors correlates material's

modulus/hardness ratio with the recovery and pile-up characteristics and penetration depth which is calculated during scratch test [2].

Penetration depth 'h_{max}', tangential force 'F_t', residual depth 'h_r' and acoustic emission are the major parameters which are calculated from the scratch tests. Whenever a material undergoes some damage, it emits acoustic radiations thus releasing elastic energy suddenly, hence indicating the material failure. In composites, the filler breakage, matrix cracking, and filler–matrix de-bonding are the possible failure mechanisms causing acoustic emissions [2].

To have an idea about the scratch performance of the materials, usually its scratch hardness is determined. Scratch hardness defines an average response of the material towards the load applied by the indenter on its surface. It is calculated as: ''the normal load over the contact area''. But there is a difficulty in evaluating scratch hardness because finding the true contact area isn't easy. As per the assumptions of classical approach:

a) only the front half of the indenter is actually in contact with the material,
b) the shape of the contact is circular for a conical or spherical indenter and
c) one half of the residual scratch width can be considered as contact radius.

The above assumptions of classical approach are applicable for plastically deformable materials like metals, but are not appropriate for viscoelastic materials such as polymers. As in polymers, the back side of the indenter has a partial contact with the material because there is both elastic and viscoelastic recovery of the indentation.

On the other hand, while taking into consideration the recovery occurring at the back side of the indenter and the pile-up forming in front of the indenter, Pelletier et al. [26] suggested a model to predict the true contact area. The model uses a parameter X which was defined by Johnson [27] as the ratio of the strain applied by the indenter to the maximum strain a material can withstand before yielding. This X, was later called as the ''rheological factor'' by many authors. It depends on the indenter geometry and modulus/yield stress ratio of the material.

For a conical indenter, X can be found using the following expression:

$$X = \frac{E}{\sigma_Y} \tan \beta$$

Where, E is the Young modulus, σy being the yield stress and β is the attack angle as shown in Fig. 1.

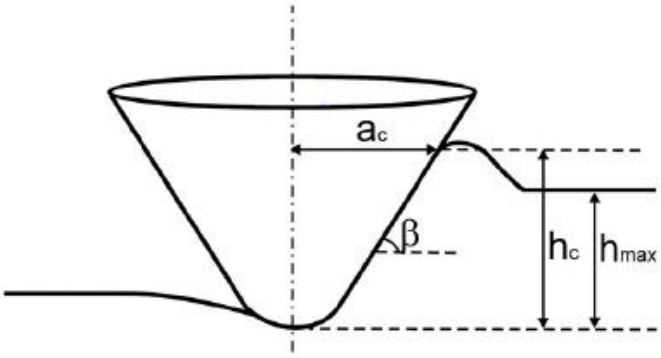

Figure 5 15 schematic representation of deformation during scratch test.

Shape ratio, represented by c^2 is the ratio of contact depth (h_c) to the penetration depth (h_{max}). It characterizes the pile-up which is formed during indentation tests. By numerical analysis, Bucaille et al. [28] computed the value of c^2 for scratch tests using a conical indenter for model materials having the same yield stress but different values of X. Plotting the dependence of the c^2 on X, two different behaviors were observed keeping X below/above 80. The behavior is represented in the form of equations below:

$$c^2 = \frac{h_c}{h} = 0.25339 \ln X + 0.5017 \quad X < 80$$

$$c^2 = \frac{h_c}{h} = 0.0684 \ln X + 1.2984 \quad X \geq 80$$

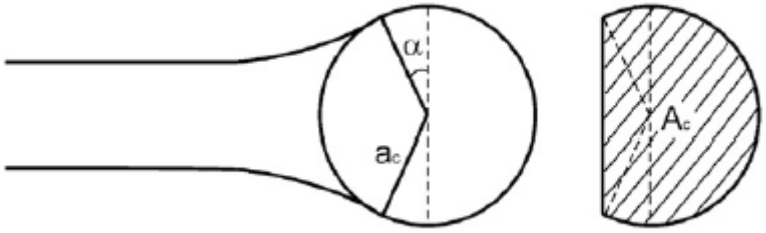

Figure 5 16 Schematic representation of recovery angle (α) and contact area (A_c)during scratch test.

Recovery at the back side of the indenter, was defined by angular parameter α (fig) and it can be found using the rheological factor, X as per following equation:

$$\alpha = \frac{1}{b + dX}$$

with b = 8.54 x10^{-3} and d = 4.3 x 10^{-3}. α = 0°, shows fully plastic nature of the material while α = 90°, shows purely elastic nature.

To determine contact radius a_c for the conical part of the indenter, the following formula is used:

$$a_c = \sqrt{2Rh_c - h_c^2}$$

To determine the contact area, A_c, following formula was used

$$A_c = a_c^2\left(\frac{\pi}{2} + \alpha + \sin\alpha\cos\alpha\right)$$

In this study, Pelletier's model was instrumentally used to determine the scratch hardness HC. It is the ratio between the applied normal load (F_N) and the predicted contact area (A_c).

$$Hc = \frac{Fn}{Ac}$$

5.4.3.1 Performance of Scratch Test

Specimens with the dimensions of 15mm x 30mm x 2.5mm in the thickness were prepared for the scratch tests. Prior to testing, the test surface of all samples was cleaned with the ethanol. Tests were performed in load-controlled mode. Sample surface is oriented parallel to the indenter motion with the aid of automated procedure. Force (F_N) of 15N normal to the sample surface was applied at room temperature. Total scratch length was 4mm in each test. Three scratches (1mm apart) were applied using geometry of Rockwell Diamond Indenter V-227 with 200µm radius. Experiments were performed with a scratch speed i.e. sliding tip velocity 'v' of 20mm/min. At the end of each test, the profiles of the transverse section of the scratch tracks was obtained using a CONSCAN contactless profilometer.

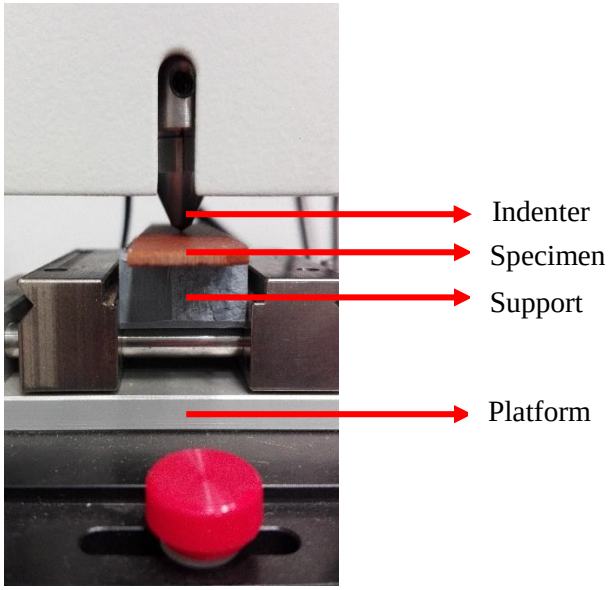

Figure 5 17 Close up image of sample while performing the scratch test

CHAPTER 6-RESULTS AND DISCUSSION

The four set of samples prepared in this research work along with the composition and molding conditions, are presented in the tables below:

Sample number	Molding Conditions: 8minutes, 165°C
S1	Base: MF-200
S2	MF+20% cellulose
S3	MF+20% cellulose + 2% unfunctionalized MWCNTs
S4	MF+20% cellulose + 2% functionalized MWCNTs

Sample number	Molding Conditions: 8minutes, 160°C
S9	Base: MF&PF (1:1)
S10	MF&PF (1:1)+20% cellulose
S11	MF&PF (1:1)+20% cellulose + 2% unfunctionalized MWCNTs
S12	MF&PF (1:1)+20% cellulose + 2% functionalized MWCNTs

Sample number	Molding Conditions: 8minutes, 165°C
S5	Base: MF&PF (1:1)
S6	MF&PF (1:1)+20% cellulose
S7	MF&PF (1:1)+20% cellulose + 2% unfunctionalized MWCNTs
S8	MF&PF (1:1)+20% cellulose + 2% functionalized MWCNTs

Sample number	Molding Conditions: 7minutes, 165°C
S13	Base: MF&PF (1:1)
S14	MF&PF (1:1)+20% cellulose
S15	MF&PF (1:1)+20% cellulose + 2% unfunctionalized MWCNTs
S16	MF+PF (1:1)+20% cellulose + 2% functionalized MWCNTs

6.1 Characterization of functionalized MWCNTs (f-MWCNTs)

To investigate the bond formation after functionalization MWCNTs were characterized by different ways. FTIR and SEM results demonstrated a good functionalization.

6.1.1 FTIR of f-MWCNTs

The dried functionalized MWCNTs was grinded with Potassium Bromide (KBr) with the ratio of and pressurized to produce KBr pellet for FTIR analysis. The functionalized MWCNTs had indicated a peak at the range of **3455-3390cm^{-1}** to be **–COOH**. A sharp peak at **1634cm^{-1}** corresponding to **C=O** stretching vibration confirmed the existence of carboxyl group on MWCNTs surface. Another peak at **1295cm^{-1}** indicates **C-O** stretch, i.e the formation of oxygenated species which may rise from hydroxyl, carboxyl or carbonyl. Further evidence of functionalization of MWCNTs is the appearance of strong peak at **1380cm^{-1}**assigned to the methyl **–C-H** asymmetric/symmetric bend. There are less prominent transitions at **2915-2852cm^{-1}** for methyl **–C-H** asymmetric/symmetric stretch.

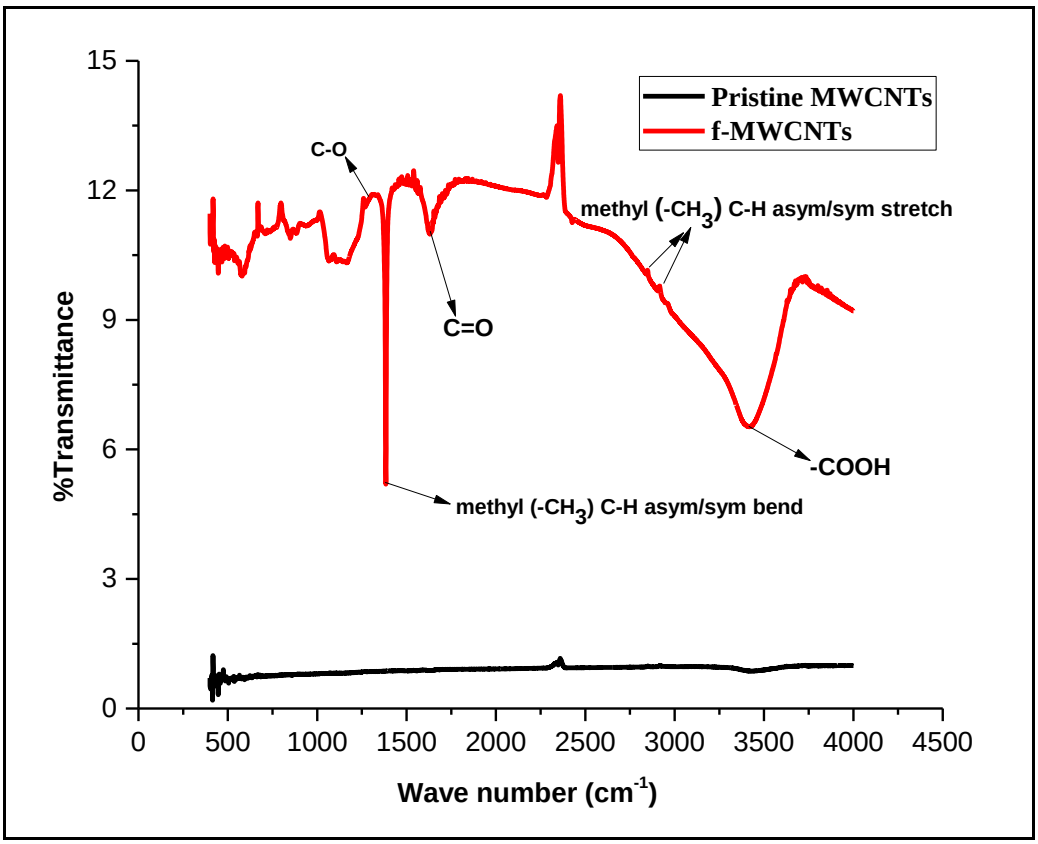

Graph 6 1 Comparison between the pristine and functionalized MWCNTs to know about the functional groups attached to the MWCNTs as a result of chemical treatment

6.1.2 SEM images of f-MWCNTs

Specimens were observed under SEM to get an idea about the surface morphology of the pristine MWCNTs, and what changes can occur on the surface after the chemical functionalization of MWCNTs. Also a molded sample was observed under SEM to check the mixing of the powders that can be observed from the surface.

Morphology of pristine MWCNTs, functionalized MWCNTs and molded sample was observed at an accelerating voltage of 20 kV in a Carl Zeiss AG - EVO® 50 Series scanning electron microscope as shown in the micrographs below.

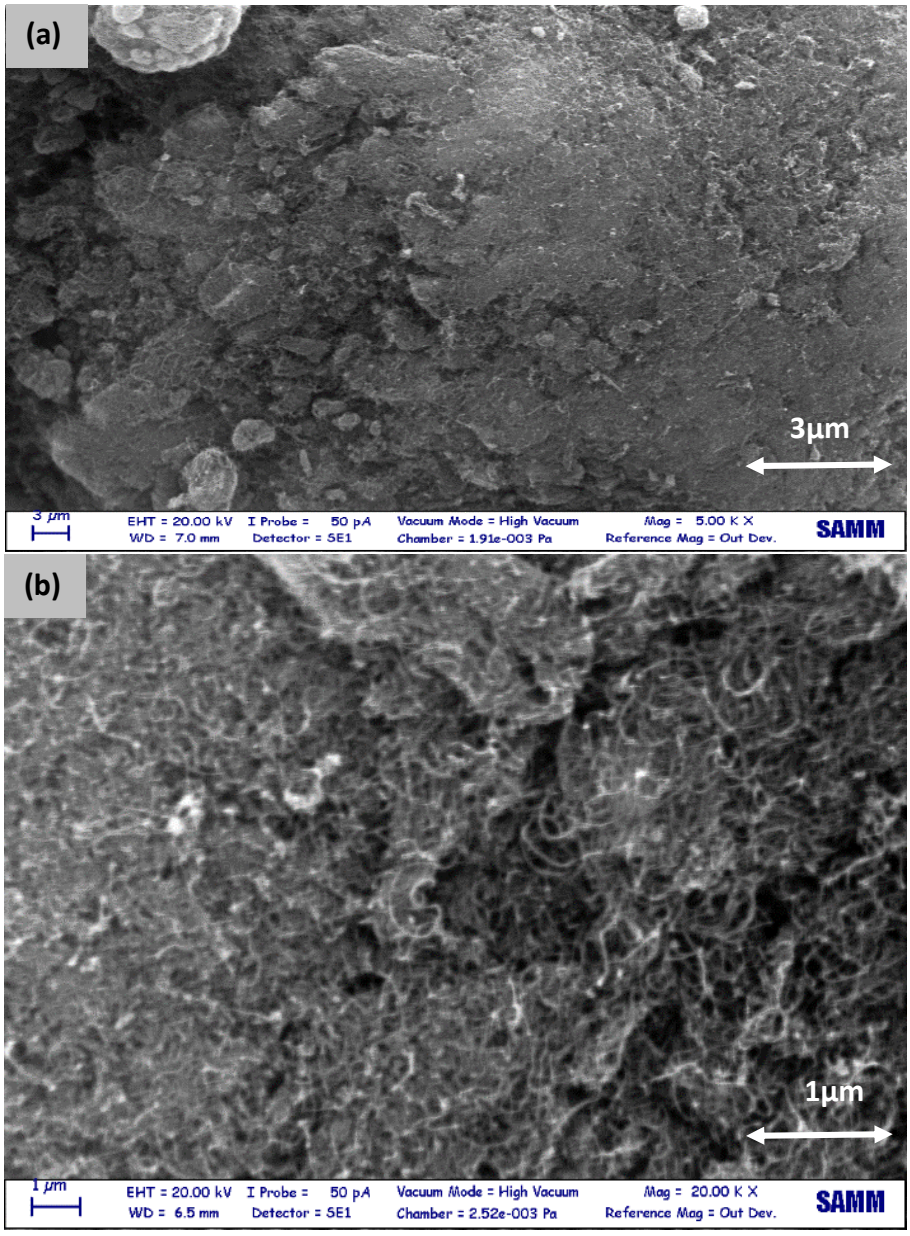

Figure 6 1 SEM images for pristine MWCNTs at magnification of (c) 3µm (d) 1µm

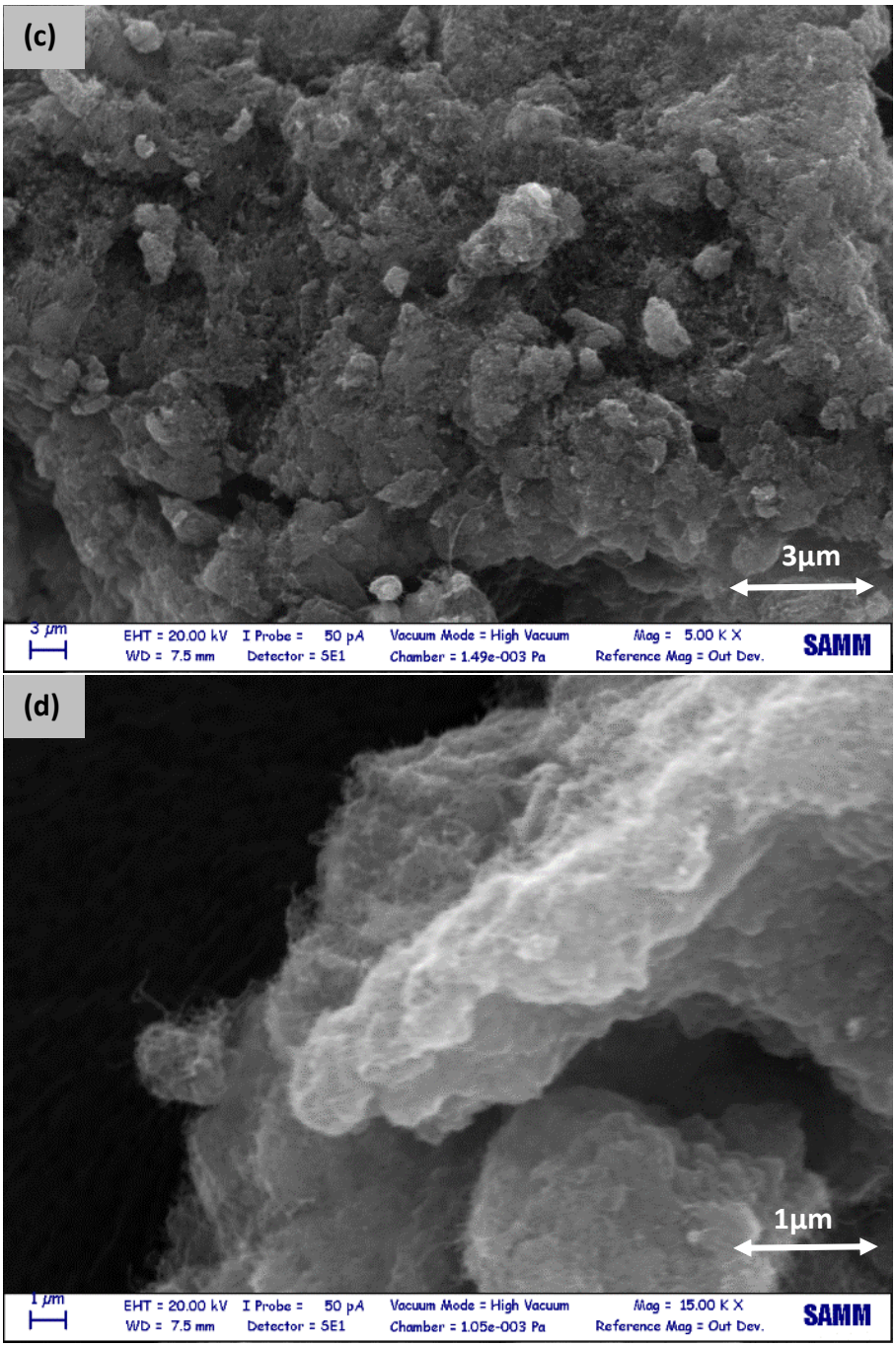

Figure 6 2SEM images for the functionalized MWCNTs at magnification of (c) 3µm (d) 1µm

There is definitely difference between the unfunctionalized and functionalized MWCNTs in terms of addition of functional groups to the tubes. But this difference is not that evident in the SEM micrograph, may be TEM (Tunneling electron microscope) can produce better evidence.

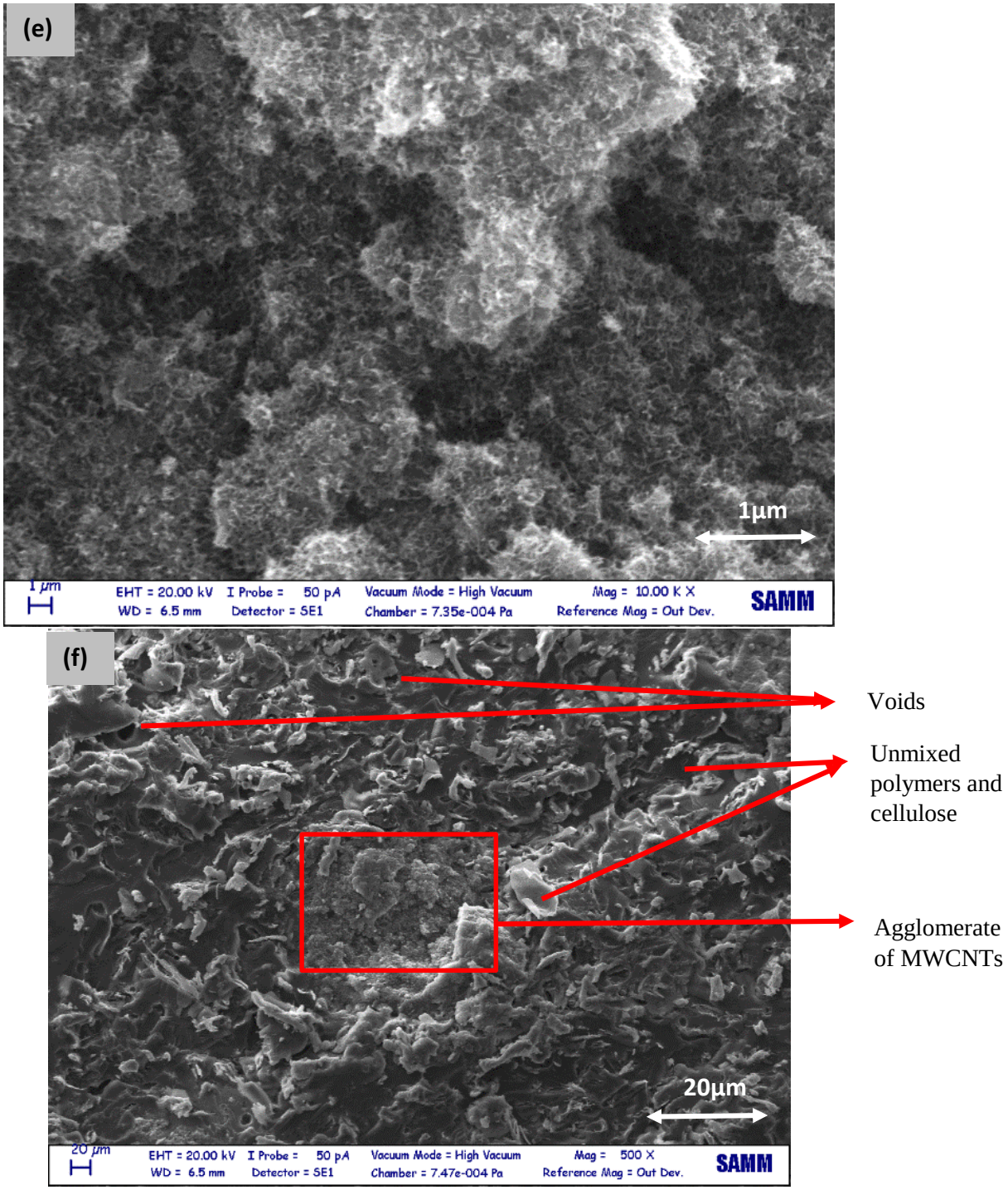

Figure 6 3SEM images for the molded sample containing melamine formaldehyde, phenol formaldehyde, cellulose, MWCNTs at magnification of (e)1µm (f)20µm

The micrograph above show inappropriate dispersion of MWCNTs in the polymer resins, phase segregation between phenolic resins and cellulose is also visible. Some of the voids can also be seen above.

6.2 Tensile Strength

Blue-Hill software was used to interpret the tensile test results. This software was attached to the dynamometer. For the value of yield stress, the maximum of the stress–strain curves was taken. Stress value was divided by strain to obtain modulus E.

Below are the graphs obtained from the tensile tests.

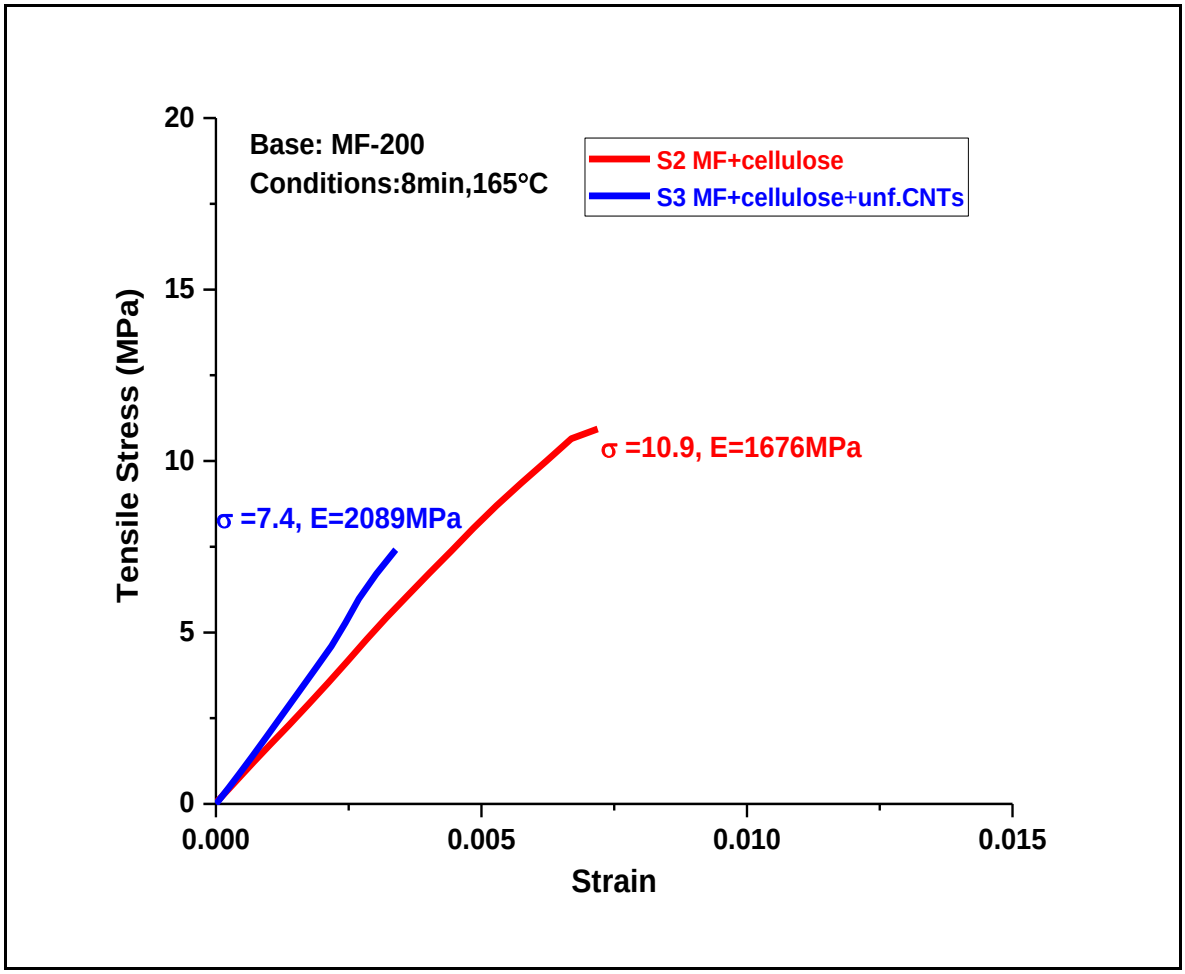

Graph 6 2Trend of tensile stress obtained by molding MF resin with different fillers at conditions of 8minutes and 165ºC

Elastic modulus E and yield stress σ of the molded melamine formaldehyde with cellulose (sample 2) and the one filled with cellulose and unfunctionalized carbon nanotubes (unf. CNTs) (sample 3) has been compared in the graph above, while pristine molded melamine formaldehyde was too brittle for the dog-bone shape and broke before the measurement. These samples were prepared at the temperature of 165ºC and pressed in the mold for about 8 minutes. It can be clearly seen that cellulose in combination with unfunctionalized MWCNTs has increased the modulus more than the sample where only cellulose is reinforcing melamine formaldehyde (sample 2), which means sample 3 has more resistance towards plastic deformation than sample 2.

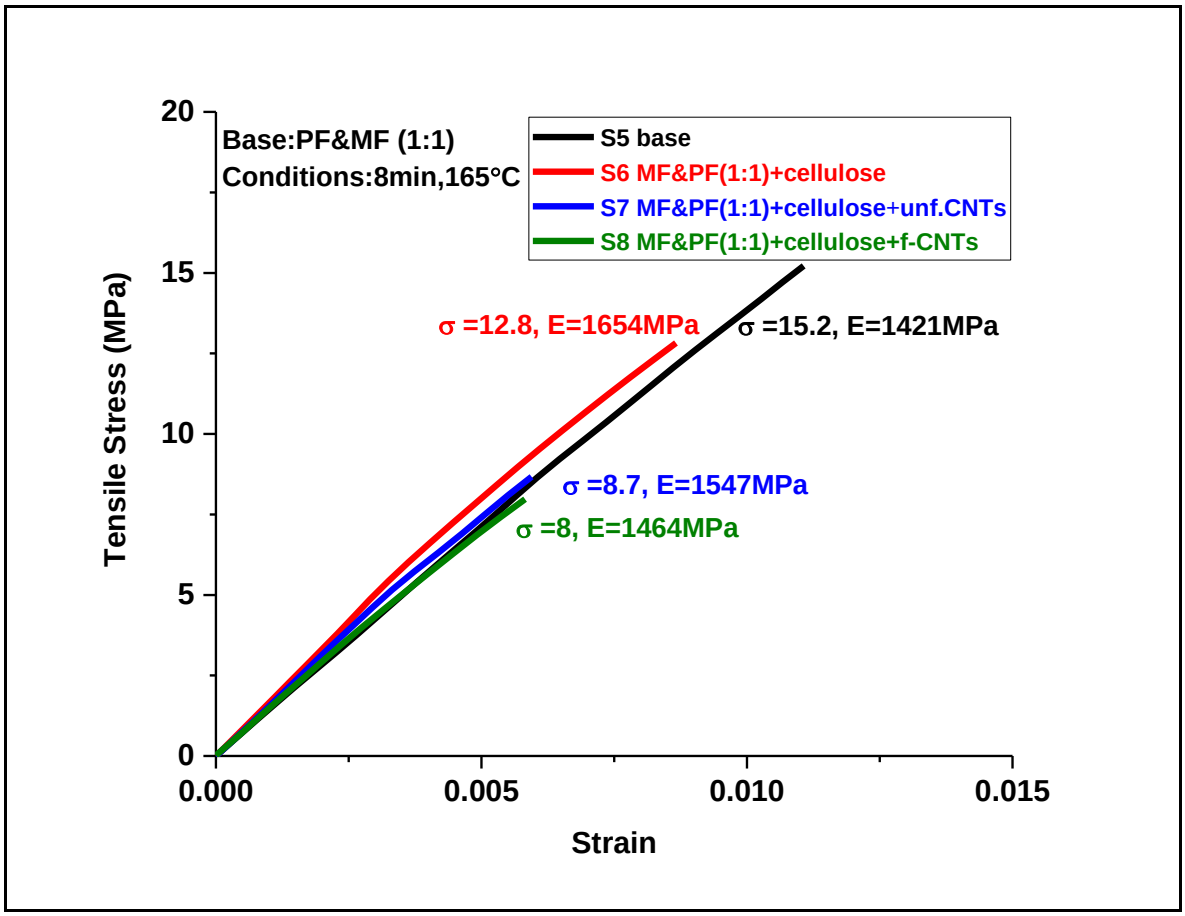

Graph 6 3 Trend of tensile stress obtained by molding PF and MF mixture with different fillers at conditions of 8minutes and 165ºC

As a second set of samples, phenol formaldehyde and melamine formaldehyde (PF and MF) are mixed in the ratio of 1:1 to make a base sample (sample 5), and molded as per conditions of time 8 minutes and temperature of 165ºC. Furthermore, additives like cellulose, unfunctionalized MWCNTs and functionalized MWCNTs were added to the base mixture making samples 6, 7, 8 respectively. All the filled samples (sample 6, 7, 8) have higher elastic modulus E than the base sample (sample 5). A material with high modulus means that it requires high stress to stretch the same distance as a material with low modulus i.e. higher resistance towards plastic deformation. In this case, sample filled with cellulose (sample 6) shows higher modulus and yield stress than the rest of two (sample 7 and 8). For the yield stress σ: as the base mixture gets mixed with fillers, the yield stress is showing a decreasing trend.

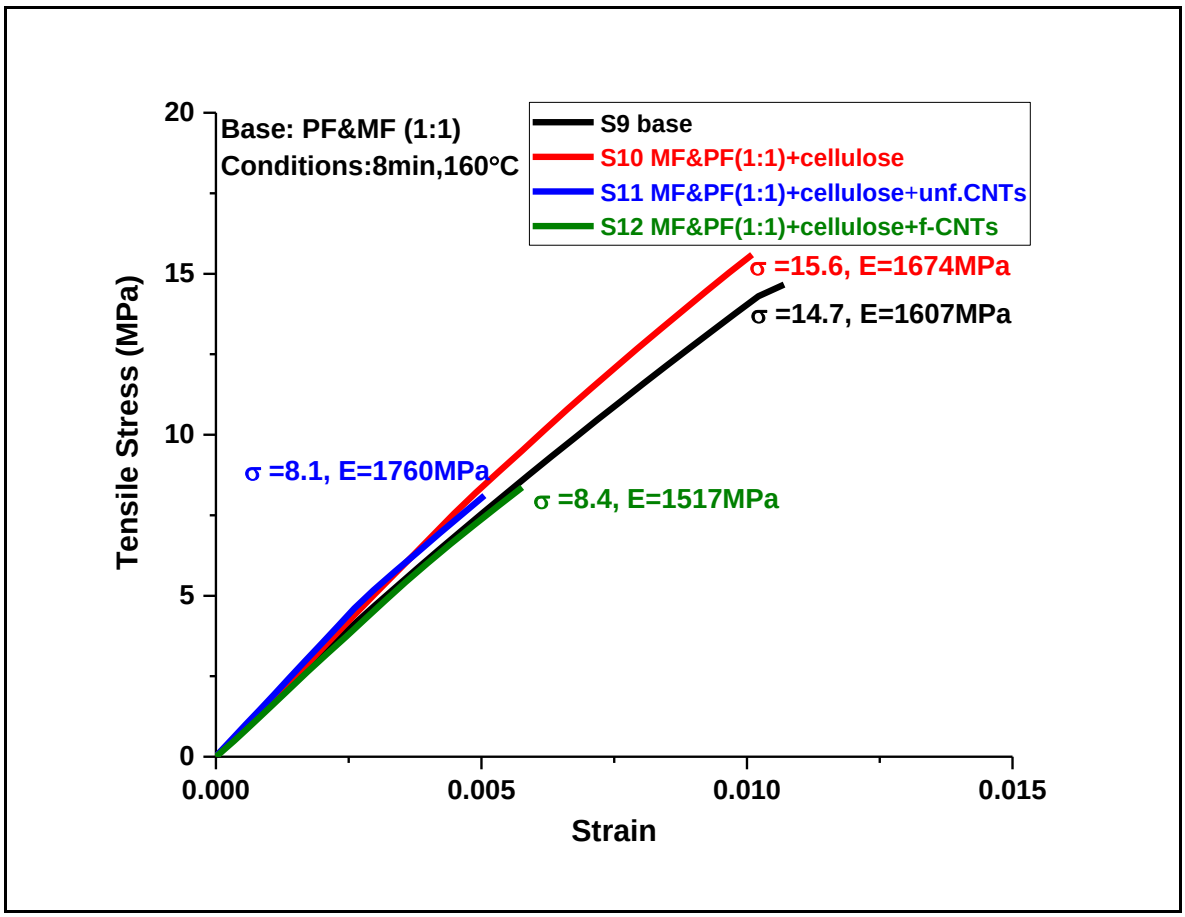

Graph 6 4 Trend of tensile stress obtained by molding PF and MF mixture with different fillers at conditions of 8minutes and 160ºC

As a third set of samples, phenol formaldehyde and melamine formaldehyde (PF and MF) are mixed in the ratio of 1:1 to mold the base sample (sample 9), and molded as per conditions of time 8 minutes and temperature of 160ºC. Furthermore, additives like cellulose, unfunctionalized MWCNTs and functionalized MWCNTs were added to the base mixture making samples 10, 11, 12 respectively. The filled samples (sample 10, 11) have higher elastic modulus E than the base sample (sample 9) showing that these samples need high amount of stress to stretch the same distance as a material with low modulus i.e. they possess higher resistance towards plastic deformation. In this set of samples, sample 12 filled with cellulose and functionalized MWCNTs doesn't show increase in yield stress and elastic modulus as compared to the base sample, thus no improvement in properties. The most probable reason of this behavior could be inadequate mixing of all the ingredients and instead of one-phase mixing, there may be multi-phases in the mixture even after mixing in the ball mill. For the yield stress σ shows no improvement rather a decreasing trend as the fillers are added to base mixture.

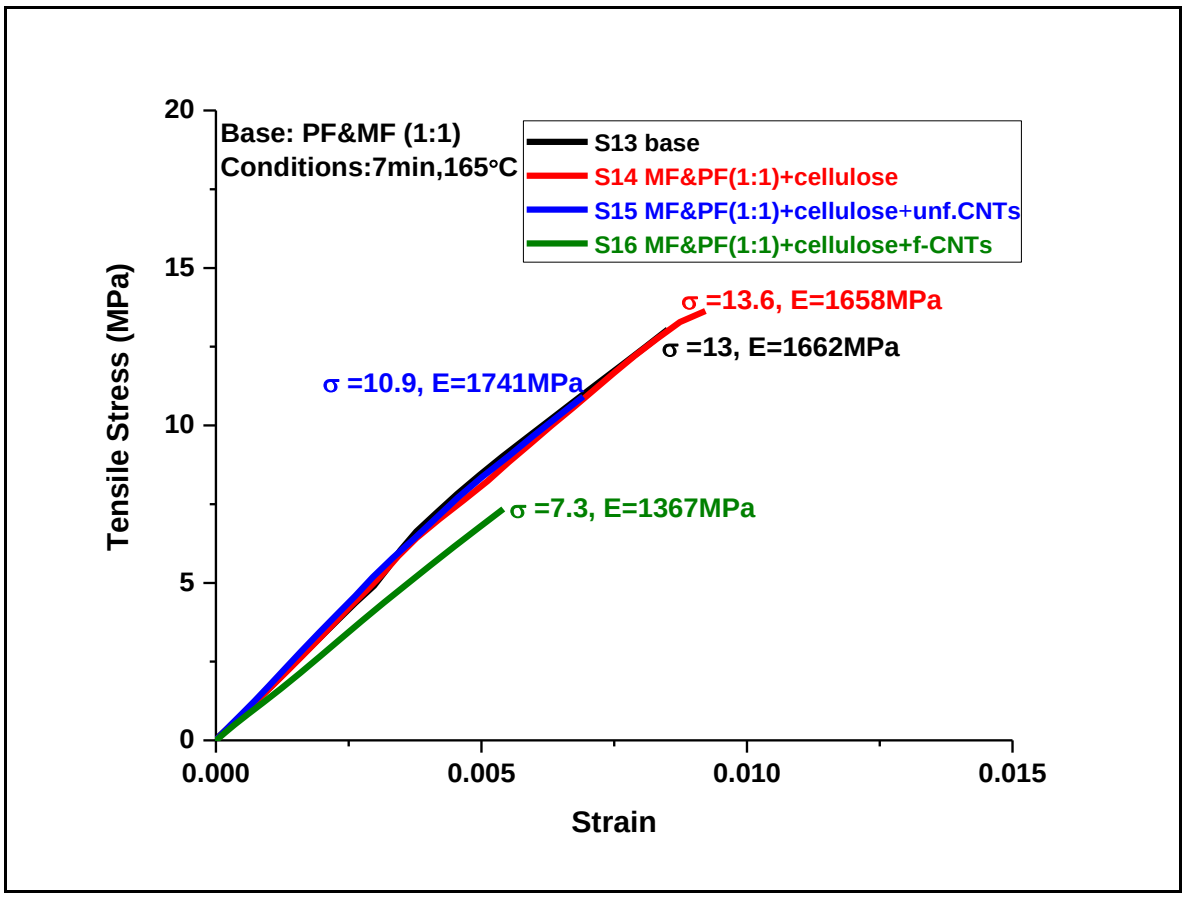

Graph 6 5 Trend of tensile stress obtained by molding PF and MF mixture with different fillers at conditions of 7minutes and 165ºC

As a fourth set of samples, phenol formaldehyde and melamine formaldehyde (PF and MF) are mixed in the ratio of 1:1 to mold the base sample (sample 13), and molded as per conditions of time 7 minutes and molding temperature of 165ºC. Furthermore, additives like cellulose, unfunctionalized MWCNTs and functionalized MWCNTs were added to the base mixture making samples 14, 15, 16 respectively. The sample only filled with cellulose (sample 14) has equal modulus, sample filled with cellulose and functionalized MWCNTs has higher elastic modulus E (sample 15), while the one filled with cellulose and unfunctionalized MWCNTs shows less E than the base sample (sample 13). Yield stress σ usually shows decreasing trend or not so significant improvement by adding fillers to the base mixture.

6.3 Flexural Strength

Blue-Hill software was used to interpret the three-point bending test results. This software was attached to the dynamometer.

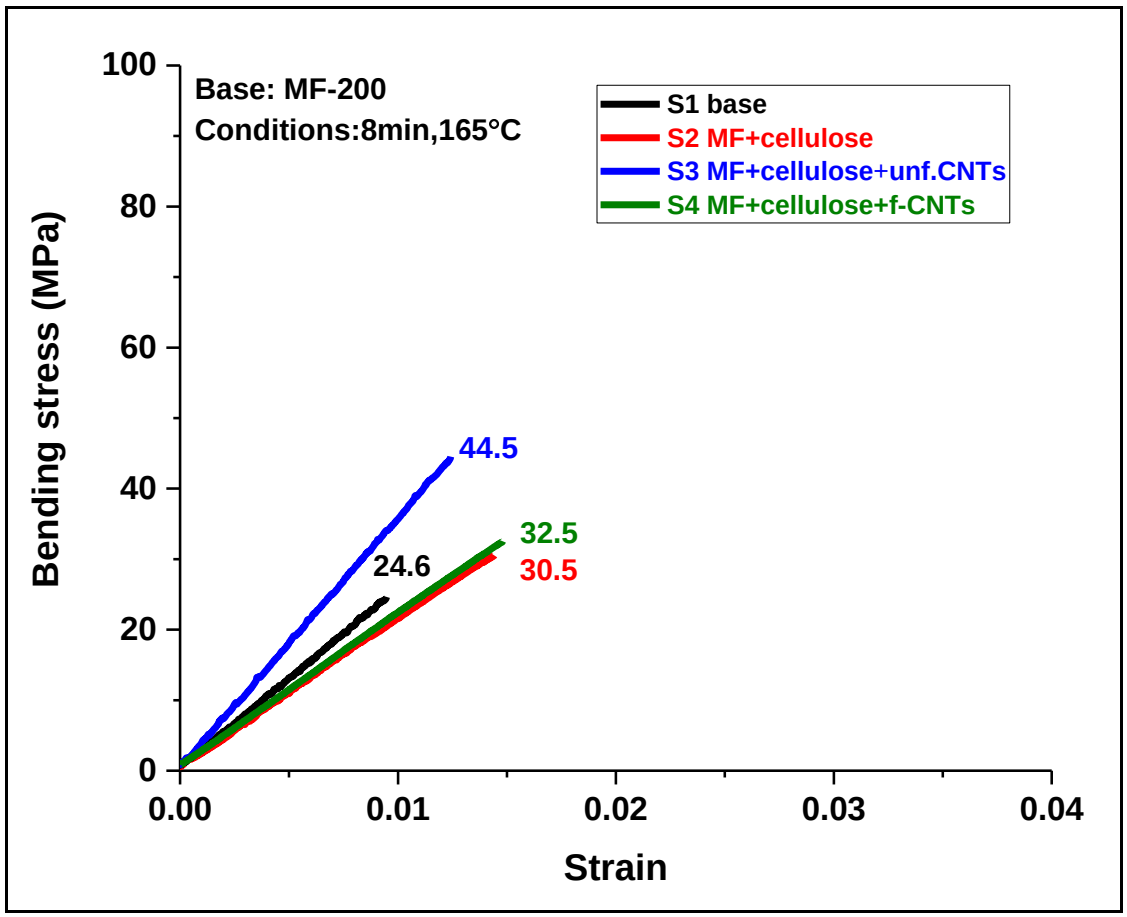

Graph 6 6 Trend of bending stress obtained by molding MF-200 resin with different fillers at 8 minutes and 165ºC

The graph above shows the bending stress obtained by different samples prepared by molding MF-200 (base sample) with different fillers like cellulose alone (sample 2), cellulose and unfunctionalized MWCNTs (sample 3) and cellulose and functionalized MWCNTs (sample 4), at conditions of 8 minutes and 165ºC. The trend dictates that the fillers have improved the bending strength of the samples. Combined effect of unfunctionalized MWCNTs and cellulose with the base sample improves the bending stress the most.

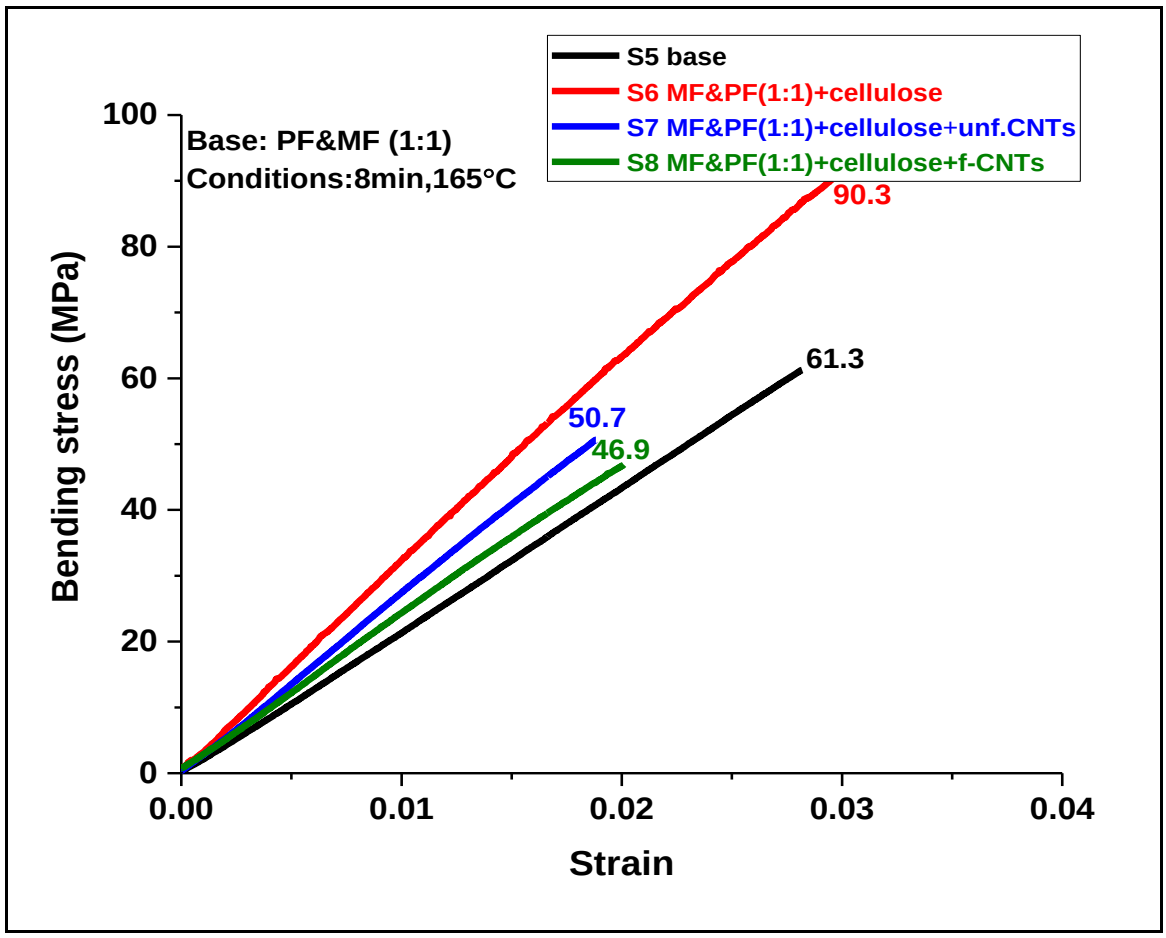

Graph 6 7 Trend of bending stress obtained by molding PF and MF mixture with different fillers at conditions of 8minutes and 165ºC

The graph above shows the bending stress obtained by different samples prepared by molding the mixture of melamine formaldehyde and phenol formaldehyde in 1:1 (base sample) with different fillers like cellulose alone (sample 6), cellulose and unfunctionalized MWCNTs (sample 7) and cellulose and functionalized MWCNTs (sample 8), at conditions of 8 minutes and 165ºC. The trend for this set of samples doesn't dictates that the fillers have improved the bending strength of the samples. In this set of samples, not all fillers are reinforcing the base sample. Cellulose filled base sample (sample 6) shows the most improved bending stress as compared to other filled samples.

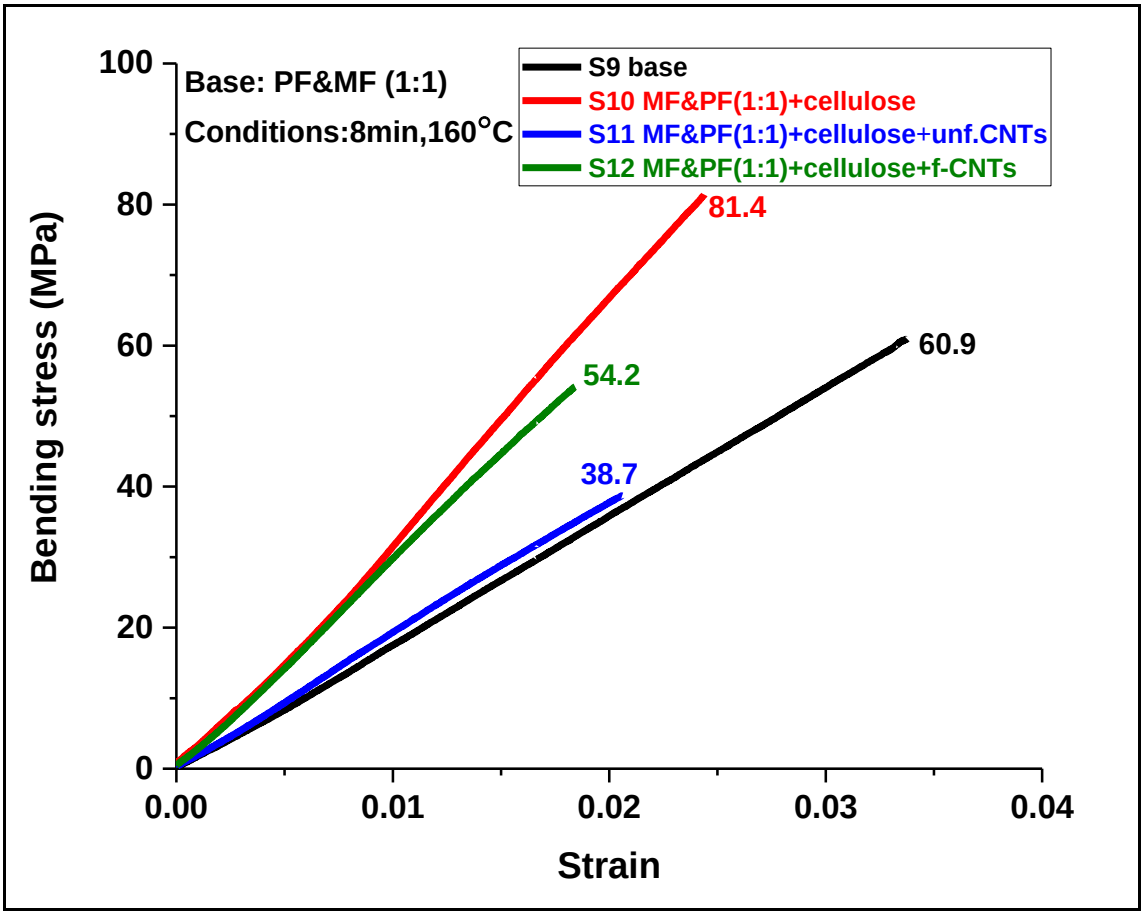

Graph 6 8 Trend of bending stress obtained by molding PF and MF mixture with different fillers at conditions of 8minutes and 160ºC

The graph above shows the bending stress obtained by different samples prepared by molding the mixture of melamine formaldehyde and phenol formaldehyde in 1:1 (base sample) with different fillers like cellulose alone (sample 10), cellulose and unfunctionalized MWCNTs (sample 11) and cellulose and functionalized MWCNTs (sample 12), at conditions of 8 minutes and 160ºC. The trend for this set of samples doesn't dictates that the fillers have improved the bending strength of the samples. In this set of samples, not all fillers are reinforcing the base sample. Cellulose filled base sample (sample 10) shows the most improved bending stress as compared to other filled samples.

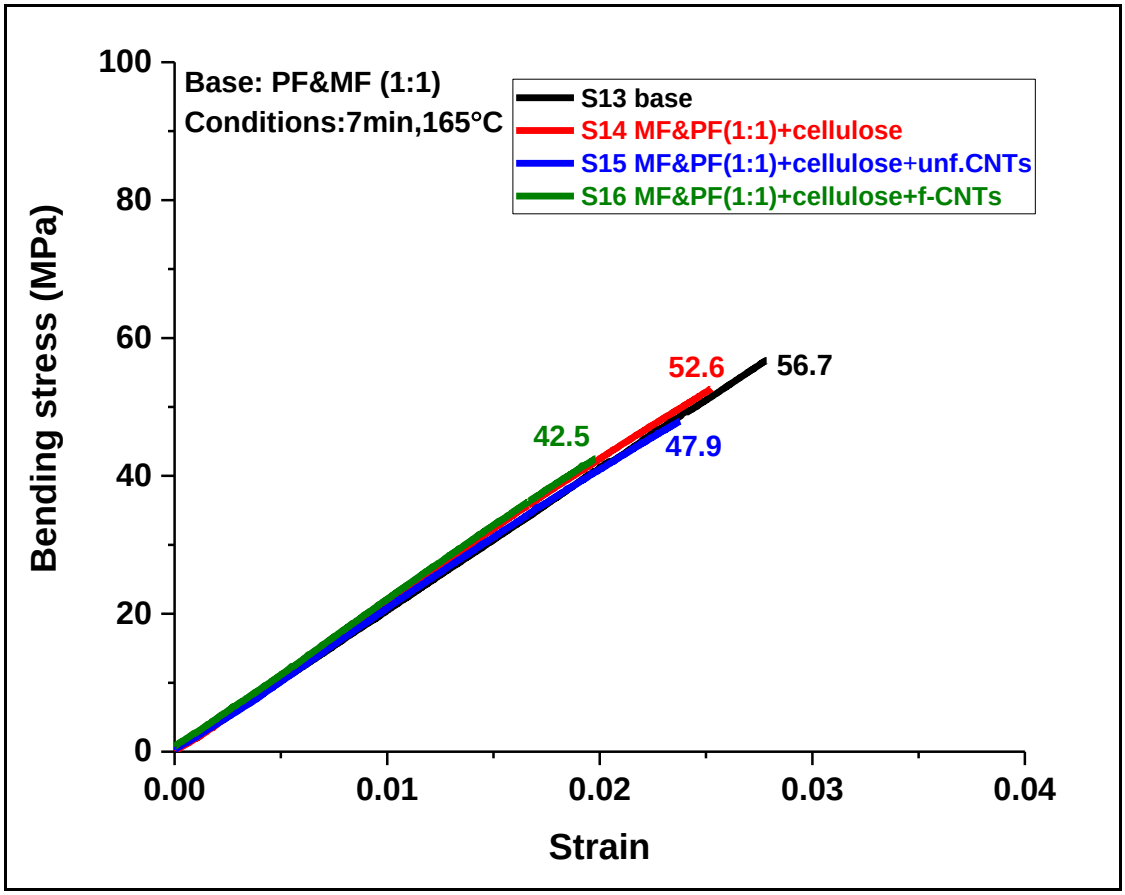

Graph 6 9 Trend of bending stress obtained by molding PF and MF mixture with different fillers at conditions of 7minutes and 165ºC

The graph above shows the bending stress obtained by different samples prepared by molding the mixture of melamine formaldehyde and phenol formaldehyde in 1:1 (base sample) with different fillers like cellulose alone (sample 14), cellulose and unfunctionalized MWCNTs (sample 15) and cellulose and functionalized MWCNTs (sample 16), at conditions of 7 minutes and 165ºC. In this set of samples, all the fillers are unable to improve the bending strength beyond the strength obtained by molding base mixture.

6.4 Calculation of Scratch Hardness:

Pelletier model was used to predict the true contact area, by following steps to determine scratch hardness:

1. For a conical indenter, Rheological factor 'X' can be found using the following expression:

$$X = \frac{E}{\sigma_Y} \tan \beta$$

2. Shape ratio c^2 was computed by these formulas

$$c^2 = \frac{h_c}{h} = 0.25339 \ln X + 0.5017 \quad X < 80$$

$$c^2 = \frac{h_c}{h} = 0.0684 \ln X + 1.2984 \quad X \geq 80$$

3. Recovery angle was calculated as: $\alpha = \frac{1}{b + dX}$

   Where,
   b = 8.54 x10^{-3} and d = 4.3 x 10^{-3}

4. To determine contact radius for the conical part of the indenter, the following formula is used:

$$a_c = \sqrt{2Rh_c - h_c^{\,2}}$$

5. To determine the contact area, Ac, following formula was used

$$A_c = a_c^{\,2}\left(\frac{\pi}{2} + \alpha + \sin\alpha \cos\alpha\right)$$

6. At the end scratch hardness was calculated as:

$$Hc = \frac{Fn}{Ac}$$

The quantities measured during the scratch tests i.e. penetration depth, ratio of residual and penetration depth; and scratch hardness can show the differences between the four set of samples.

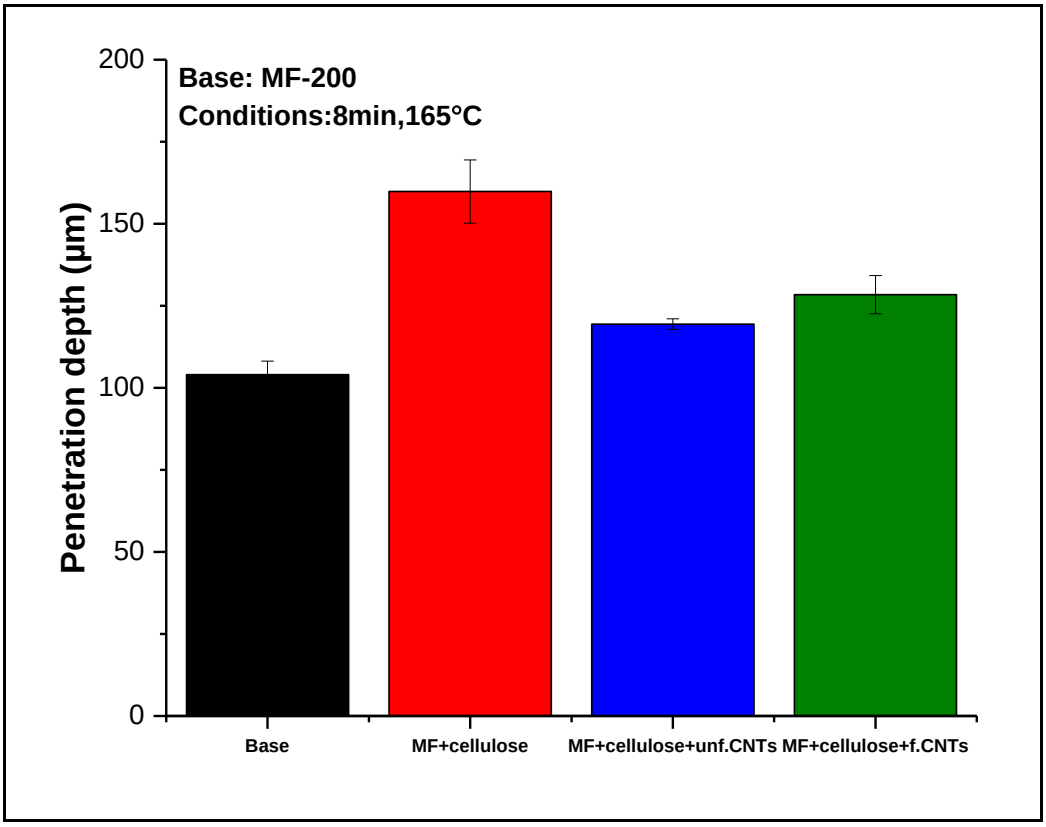

Graph 6 10Trend of penetration depth obtained by molding MF resin with different fillers at conditions of 8minutes and 165ºC

First set of samples were prepared by compression hold molding press at the temperature of 165ºC and for about 8 minutes. Penetration depth of the molded melamine formaldehyde with 20wt. % cellulose (sample 2) is highest amongst all the samples, which was not expected. The reason could be poor interaction between the polymer matrix and cellulose. The sample 4 i.e. the one filled with 20wt. % cellulose and 2wt. % functionalized carbon nanotubes (f. CNTs) and sample 3, i.e the one filled with 20wt. % cellulose and 2wt. % unfunctionalized carbon nanotubes (unf. CNTs) has higher penetration depth than pristine melamine formaldehyde (sample 1), but quite less than sample 2. The reason could be not best interaction between all the fillers and matrix, but definitely the interaction in sample 3 and 4, is much better than in sample 2. Theoretically, penetration depth should decrease as the surface of contact between the polymer matrix and fillers increases. CNTs are supposed to increase the interface interactions more than the cellulose. As scratch test is performed on a small portion of the sample, and if the mixing of the fillers in the matrix is non-uniform throughout the sample, the results tend to change as per the change of location of the scratches.

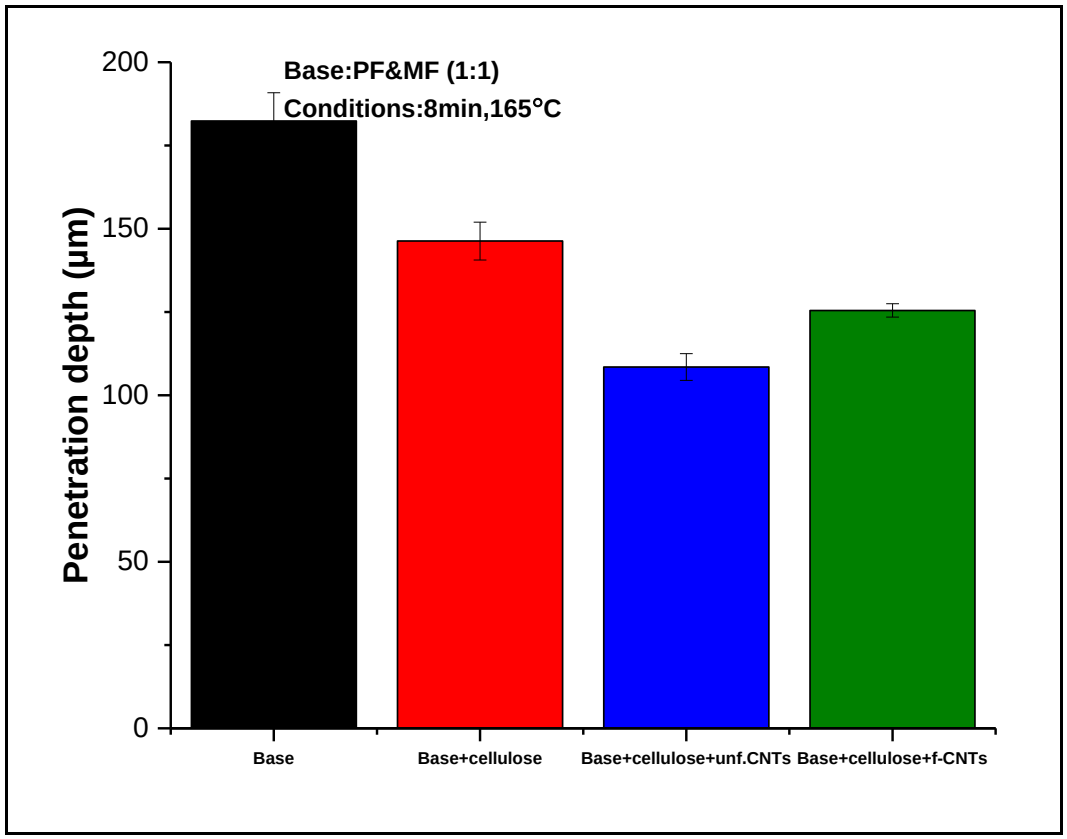

Graph 6 11Trend of penetration depth obtained by molding PF and MF mixture with different fillers at conditions of 8minutes and 165ºC

In the second set of samples, PF and MF are mixed in 1:1 along with the fillers and compressed in the mold at the temperature of 165ºC and for about 8 minutes. Theoretically, penetration depth should decrease as the surface of contact between the polymer matrix and fillers increases. CNTs are supposed to increase the interface interactions more than the cellulose. Penetration depth of the base sample is highest among all, as expected. The filler-matrix interaction in this set of samples seems good, except for the sample 4 i.e the one filled with 20wt. % cellulose and 2wt. % functionalized carbon nanotubes (f. CNTs), its penetration depth should be less than sample 3 i.e. the one filled with 20wt. % cellulose and 2wt. % unfunctionalized carbon nanotubes (unf. CNTs). But nevertheless, the penetration depth of all the filled samples is less than the base sample, thus it indicates improved wear strength.

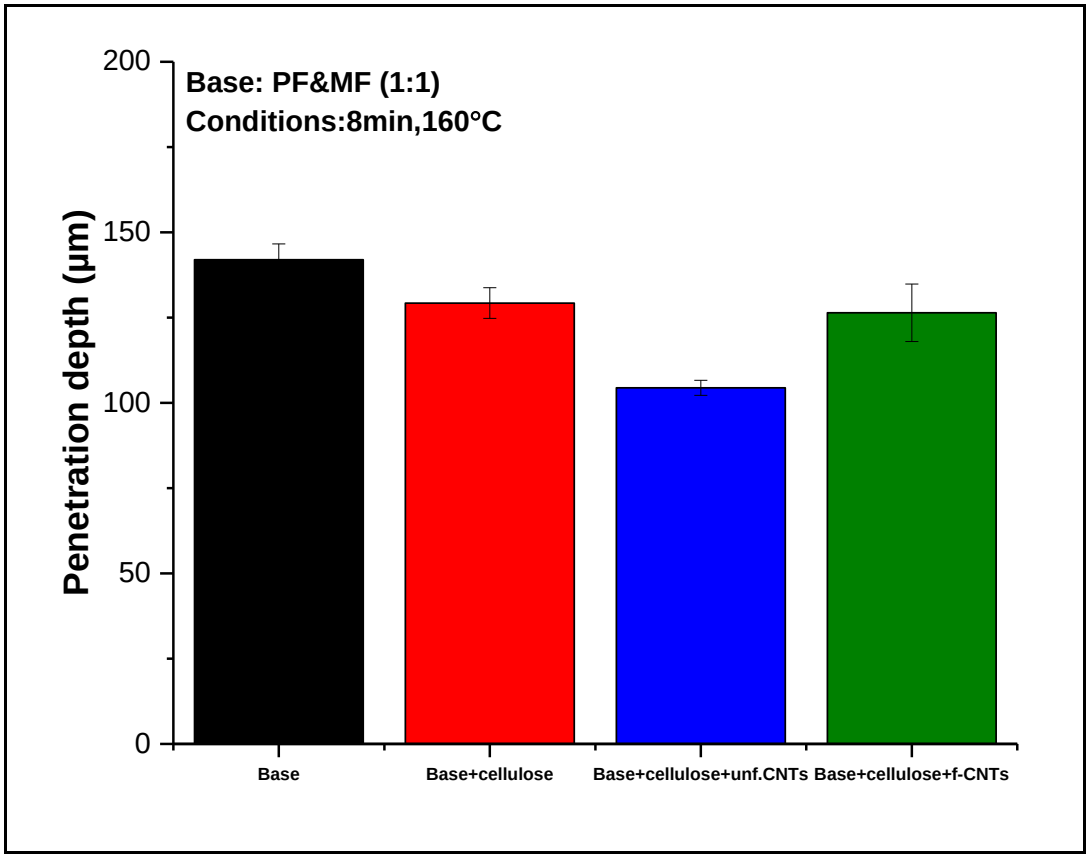

Graph 6 12Trend of penetration depth obtained by molding PF and MF mixture with different fillers at conditions of 8minutes and 160ºC

In the third set of samples, PF and MF are mixed in 1:1 along with the fillers and compressed in the mold at the temperature of 160ºC and for about 8 minutes. Theoretically, penetration depth should decrease as the surface of contact between the polymer matrix and fillers increases. CNTs are supposed to increase the interface interactions more than the cellulose. Penetration depth of the base sample is highest among all, as expected. The filler-matrix interaction in this set of samples seems good, except for the sample 4 i.e the one filled with 20wt. % cellulose and 2wt. % functionalized carbon nanotubes (f. CNTs), its penetration depth should be less than sample 3 i.e. the one filled with 20wt. % cellulose and 2wt. % unfunctionalized carbon nanotubes (unf. CNTs). But nevertheless, the penetration depth of all the filled samples is less than the base sample, thus it indicates improved wear strength.

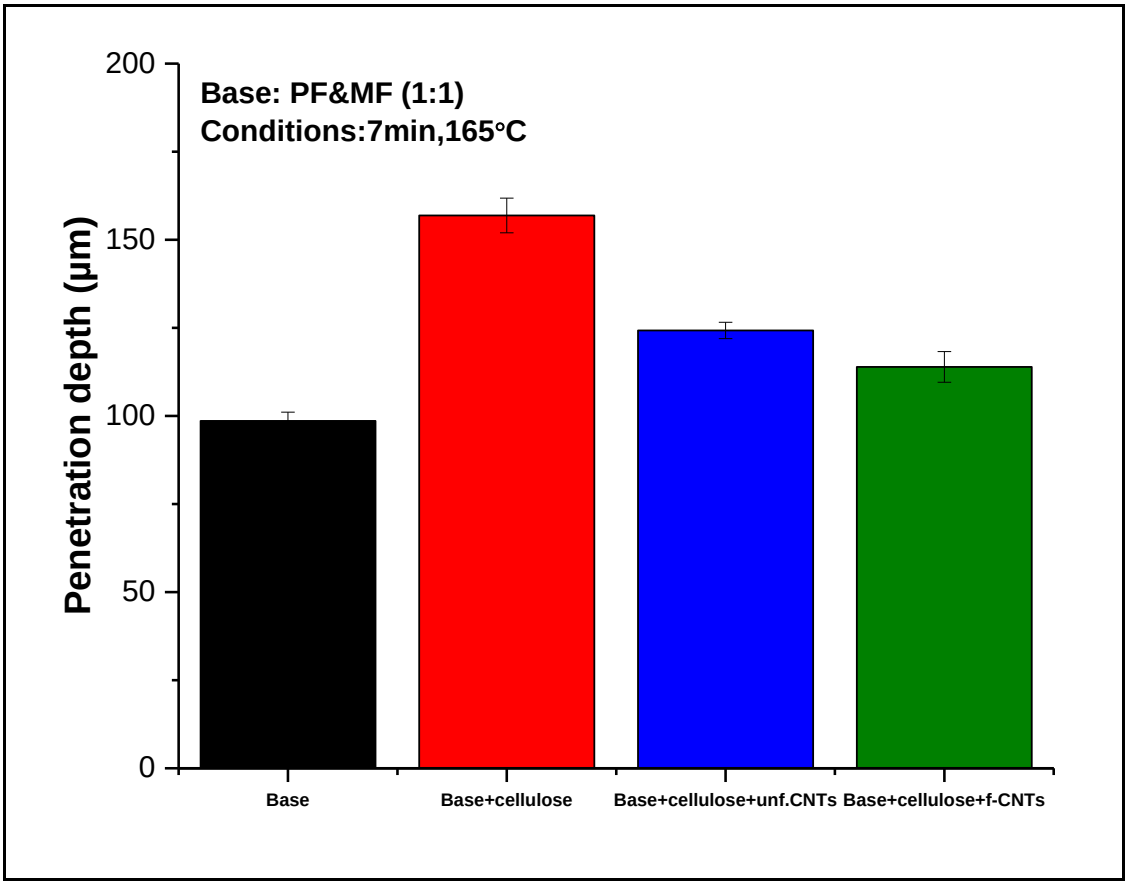

Graph 6 13Trend of penetration depth obtained by molding PF and MF mixture with different fillers at conditions of 7minutes and 165ºC

In the fourth set of samples, PF and MF are mixed in 1:1 along with the fillers and compressed in the mold at the temperature of 165ºC and for about 7 minutes. Penetration depth of sample 2 i.e the one filled with 20wt. % cellulose is highest amongst all the samples, which was not expected. The reason could be poor interaction between the polymer matrix and cellulose. The sample 4 i.e. the one filled with 20wt. % cellulose and 2wt. % functionalized carbon nanotubes (f. CNTs) and sample 3, i.e the one filled with 20wt. % cellulose and 2wt. % unfunctionalized carbon nanotubes (unf. CNTs) has higher penetration depth than the base (sample 1), but quite less than sample 2. The reason could be not best interaction between all the fillers and matrix, but definitely the interaction in sample 3 and 4, is much better than in sample 2. Theoretically, penetration depth should decrease as the surface of contact between the polymer matrix and fillers increases. CNTs are supposed to increase the interface interactions more than the cellulose. As scratch test is performed on a small portion of the sample, and if the mixing of the fillers in the matrix is non-uniform throughout the sample, the results tend to change as per the change of location of the scratches.

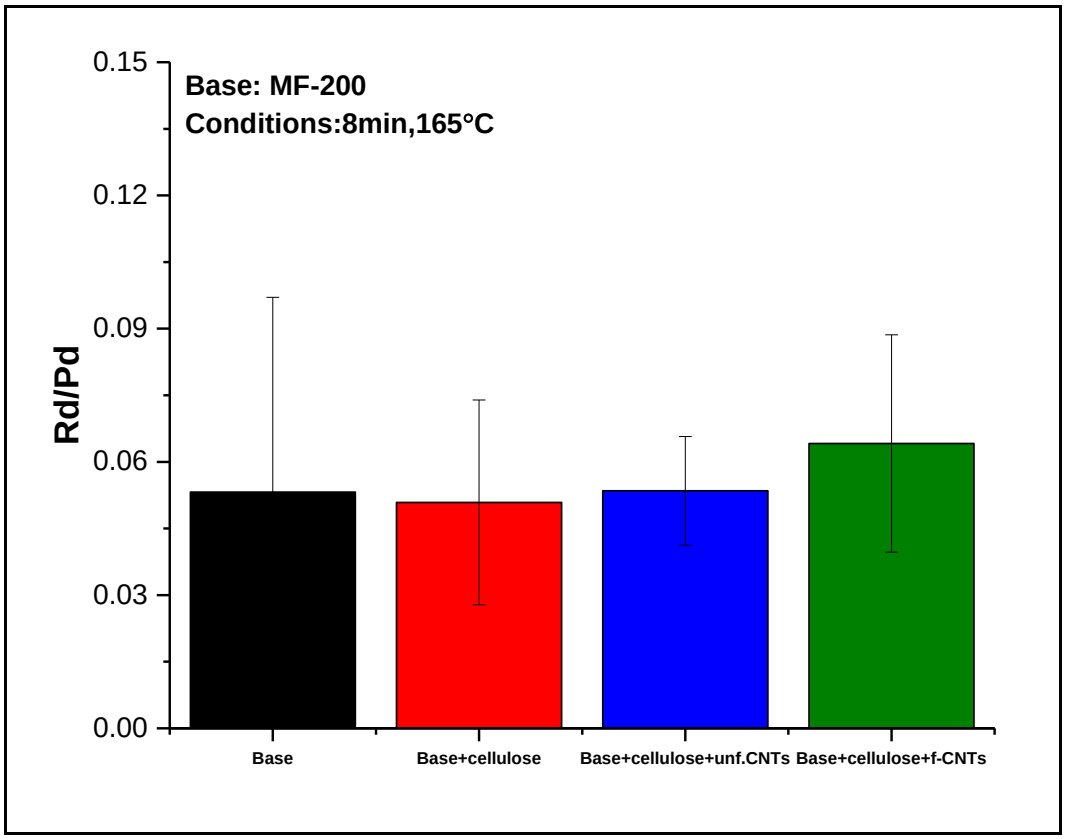

Graph 6 14Trend of ratio of R_d and P_d obtained by molding MF mixture with different fillers at conditions of 8minutes and 165ºC

First set of samples was prepared by hot molding melamine formaldehyde at the temperature of 165ºC and for about 8 minutes. Rd, residual depth is supposed to be small in all the cases, which can be seen in the graph above. Small residual depth means almost complete recovery of the scratch by the material. Ratio of Rd and Pd was expected to be small as well. Addition of the fillers in the base sample should help in the reducing the ratio. Sample 4 i.e the one containing functionalized MWCNTs has slightly higher ratio than the pristine, reason could be agglomeration wt. % of nanotubes is hindering the viscoelastic recovery.

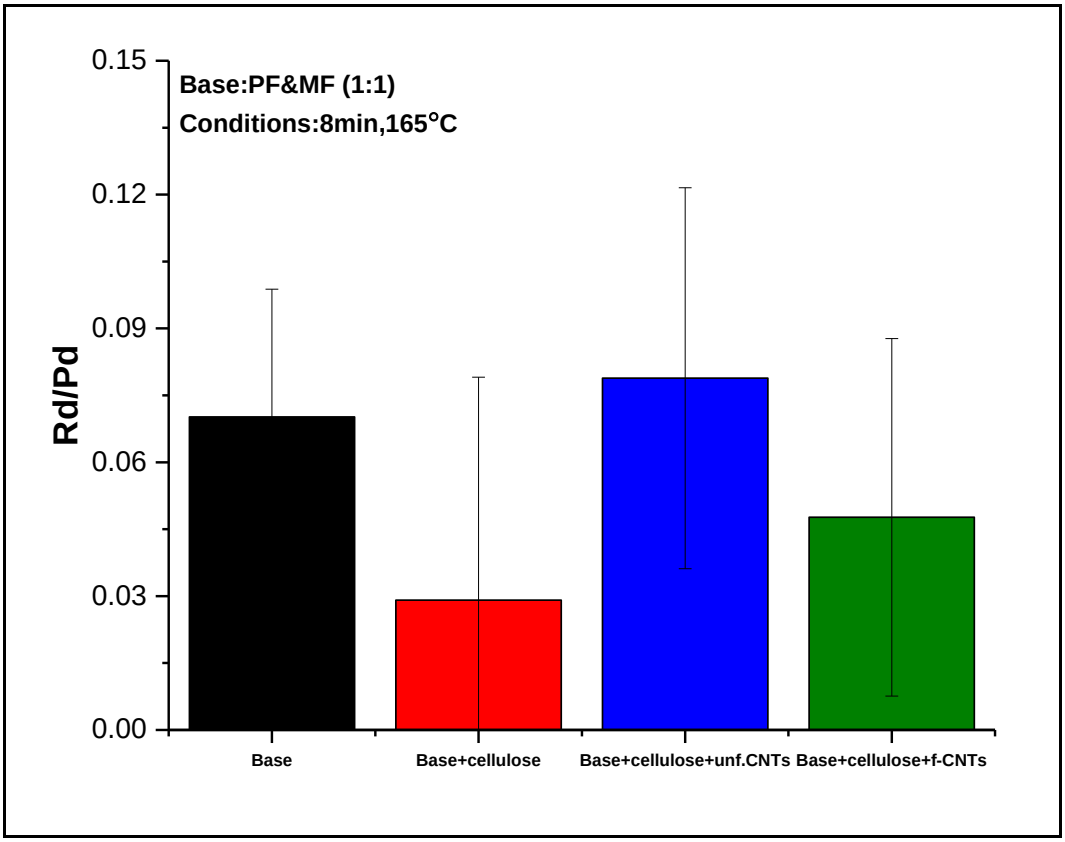

Graph 6 15Trend of ratio of R_d and P_d obtained by molding PF and MF mixture with different fillers at conditions of 8minutes and 165ºC

Second set of samples was prepared by mixing PF and MF in 1:1 inside the compression hot molding press at the temperature of 165ºC and for about 8 minutes. Rd, residual depth is supposed to be small in all the cases, which can be seen in the graph above. Small values leads to large error bars. Small residual depth means almost complete recovery of the scratch by the material. Ratio of Rd and Pd was expected to be small as well. Addition of the fillers in the base sample should help in reducing the ratio. Sample 3 i.e the one containing unfunctionalized MWCNTs has slightly higher ratio than the base sample, but this can be ignored. The reason of not having a trend between the filled samples, sample 2,3 and 4 could be improper mixing and agglomeration of nanotubes that is hindering the viscoelastic recovery.

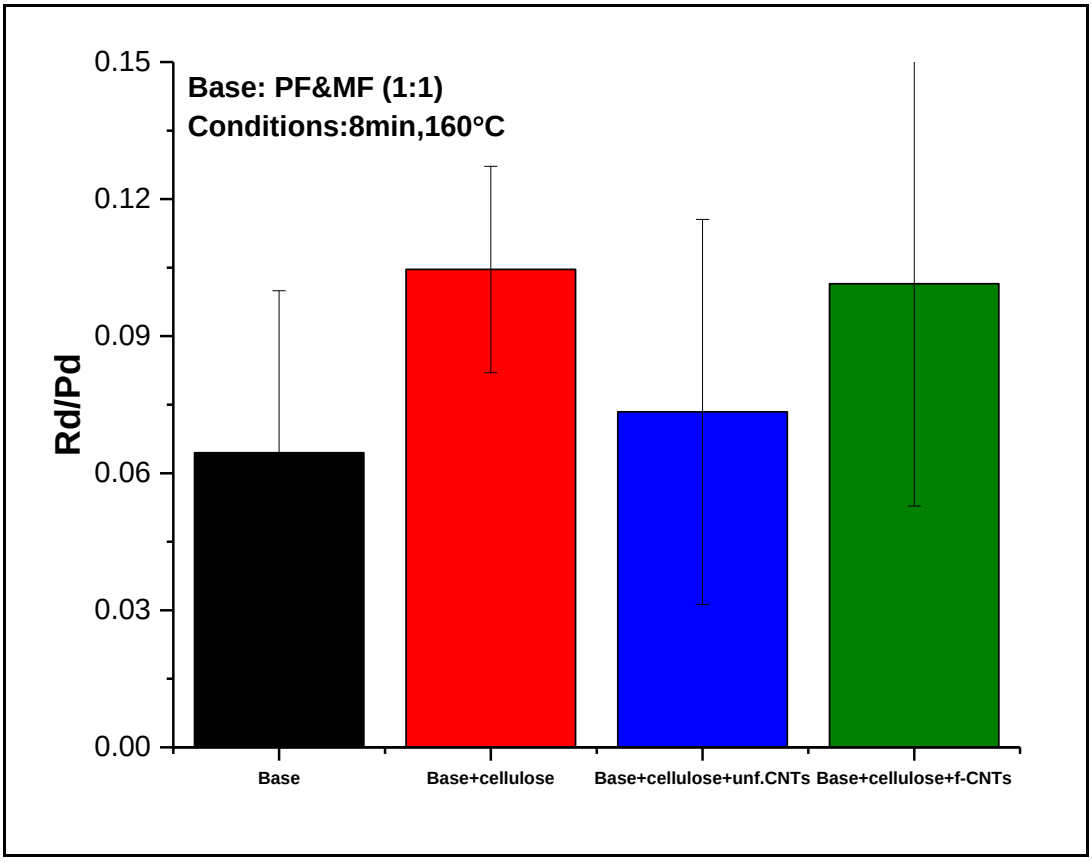

Graph 6 16 Trend of ratio of R_d and P_d obtained by molding PF and MF mixture with different fillers at conditions of 8minutes and 160ºC

Third set of samples was prepared by mixing PF and MF in 1:1 inside the compression hot molding press at the temperature of 160ºC and for about 8 minutes. Rd, residual depth is supposed to be small in all the cases, which can be seen in the graph above. Small residual depth means almost complete recovery of the scratch by the material. Ratio of Rd and Pd was expected to be small as well. Addition of the fillers in the base sample should help in the reducing the ratio, but in this case sample 2 and 4 have higher ratio than the base sample and sample 3 i.e the one filled with 2wt. % cellulose and 2wt.% unfunctionalized MWCNTs. Reason could be improper mixing between the filler and the polymer matrix, in the whole sample or may be in that part of the sample which was scratched.

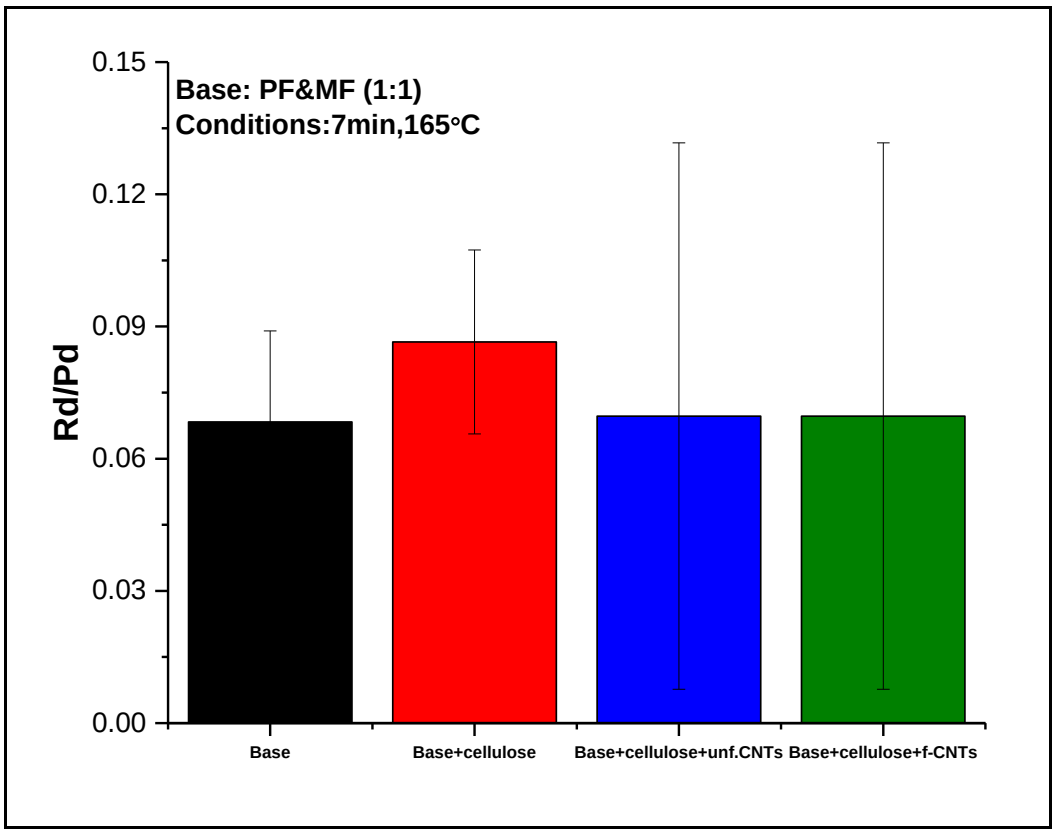

Graph 6 17 Trend of ratio of R_d and P_d obtained by molding PF and MF mixture with different fillers at conditions of 7minutes and 165ºC

Fourth set of samples was prepared by mixing PF and MF in 1:1 inside the compression hot molding press at the temperature of 165ºC and for about 7 minutes. Rd, residual depth is supposed to be small in all the cases, which can be seen in the graph above. Small residual depth means almost complete recovery of the scratch by the material. Ratio of Rd and Pd was expected to be small as well. Addition of the fillers in the base sample should help in the reducing the ratio. But in this sample 3 and 4, aren't reducing rather maintaining the same ratio as base sample. Sample 2 i.e the one containing 20wt. % cellulose has slightly higher ratio than the all of the others, reason could be improper mixing between the filler and the polymer matrix, in the whole sample or may be in that part of the sample which was scratched.

Coefficient of friction μ is a number to quantify and compare the frictional behavior of the materials. It is a dimensionless number.

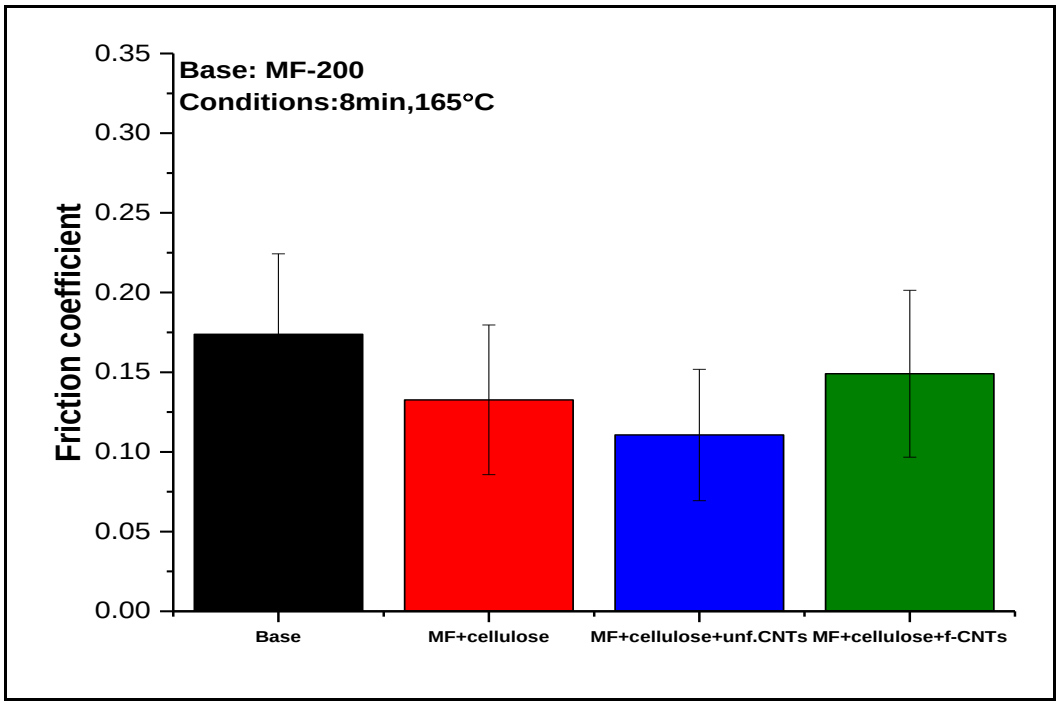

Graph 6 18 Trend of friction coefficient obtained by molding MF with different fillers at conditions of 8minutes and 165ºC

First set of samples was prepared by hot molding melamine formaldehyde at the temperature of 165ºC and for about 8 minutes. As the fillers enhance the interfacial contact between them and the polymer matrix, the friction coefficient should decrease as compared to the base sample, helping polymer chains to stretch easily in the direction of shear. In this case sample 3 i.e the one filled with 20wt. % cellulose and 2wt. % unfunctionalized MWCNTs, shows the best interfacial bonding of the fillers and polymer matrix, thus most reduction in friction coefficient as compared to all others.

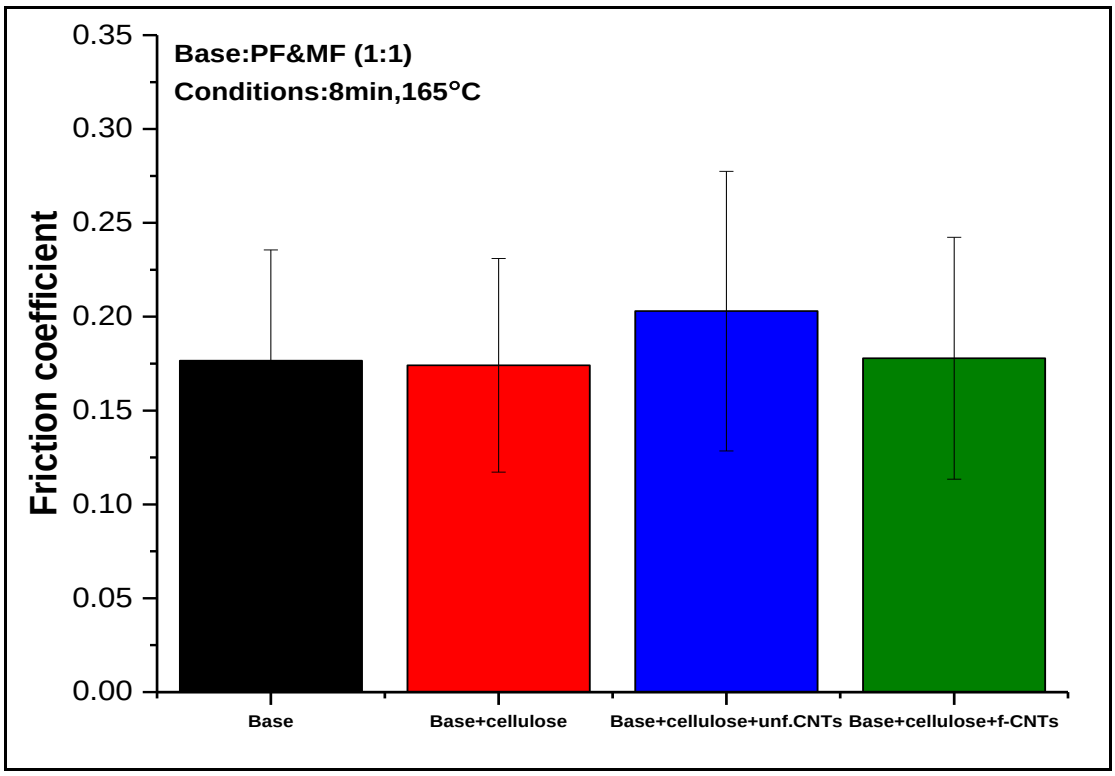

Graph 6 19 Trend of friction coefficient obtained by molding PF and MF mixture with different fillers at conditions of 8minutes and 165ºC

Second set of samples was prepared by hot molding phenol formaldehyde and melamine formaldehyde in 1:1 at the temperature of 165ºC and for about 8 minutes. As the fillers enhance the interfacial contact between them and the polymer matrix, the friction coefficient should decrease as compared to the base sample, helping polymer chains to stretch easily in the direction of shear. In this case sample 3 i.e the one filled with 20wt. % cellulose and 2wt. % unfunctionalized MWCNTs, shows the not so good interfacial bonding of the fillers and polymer matrix, thus having slightly higher friction coefficient as compared to all others. Sample 2 and 4, have almost same friction coefficient as base sample.

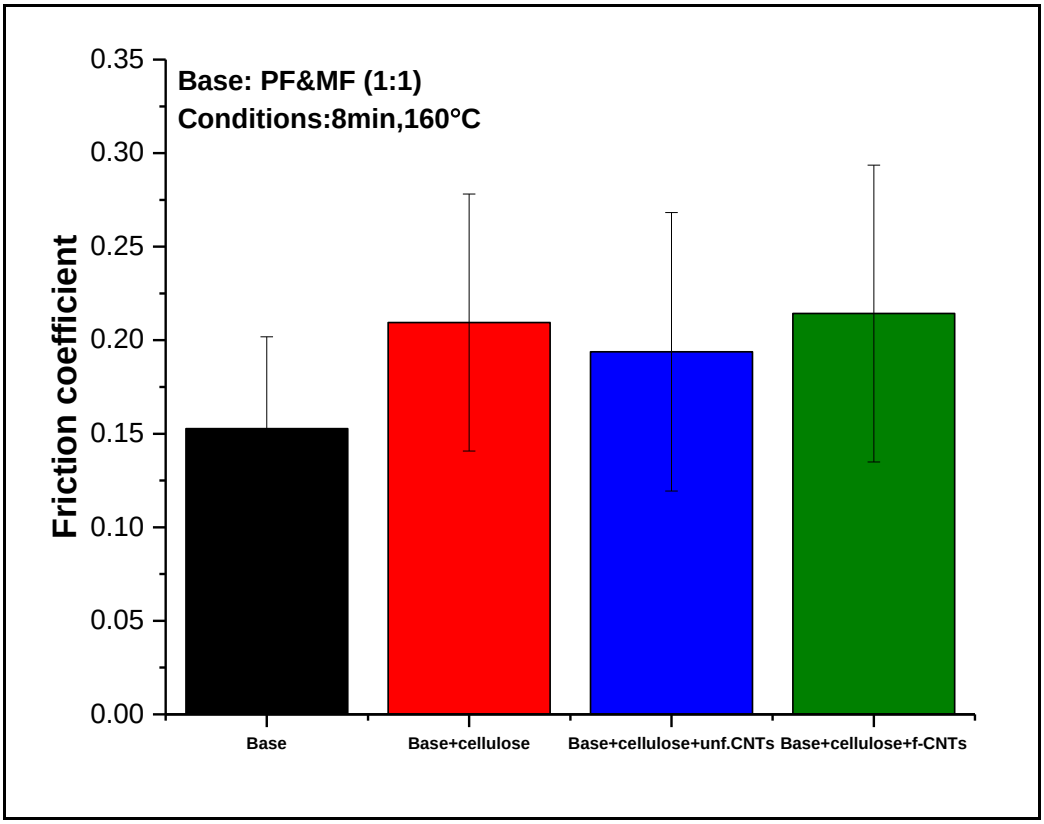

Graph 6 20Trend of friction coefficient obtained by molding PF and MF mixture with different fillers at conditions of 8minutes and 160ºC

Third set of samples was prepared by hot molding phenol formaldehyde and melamine formaldehyde in 1:1 at the temperature of 160ºC and for about 8 minutes. As the fillers enhance the interfacial contact between them and the polymer matrix, the friction coefficient should decrease as compared to the base sample, helping polymer chains to stretch easily in the direction of shear. In this case all the filled samples failed to ease the polymer chain movement, as their friction coefficient is higher than the base sample. Probable reason could be improper mixing between the polymer matrix and fillers, providing less bonding between them.

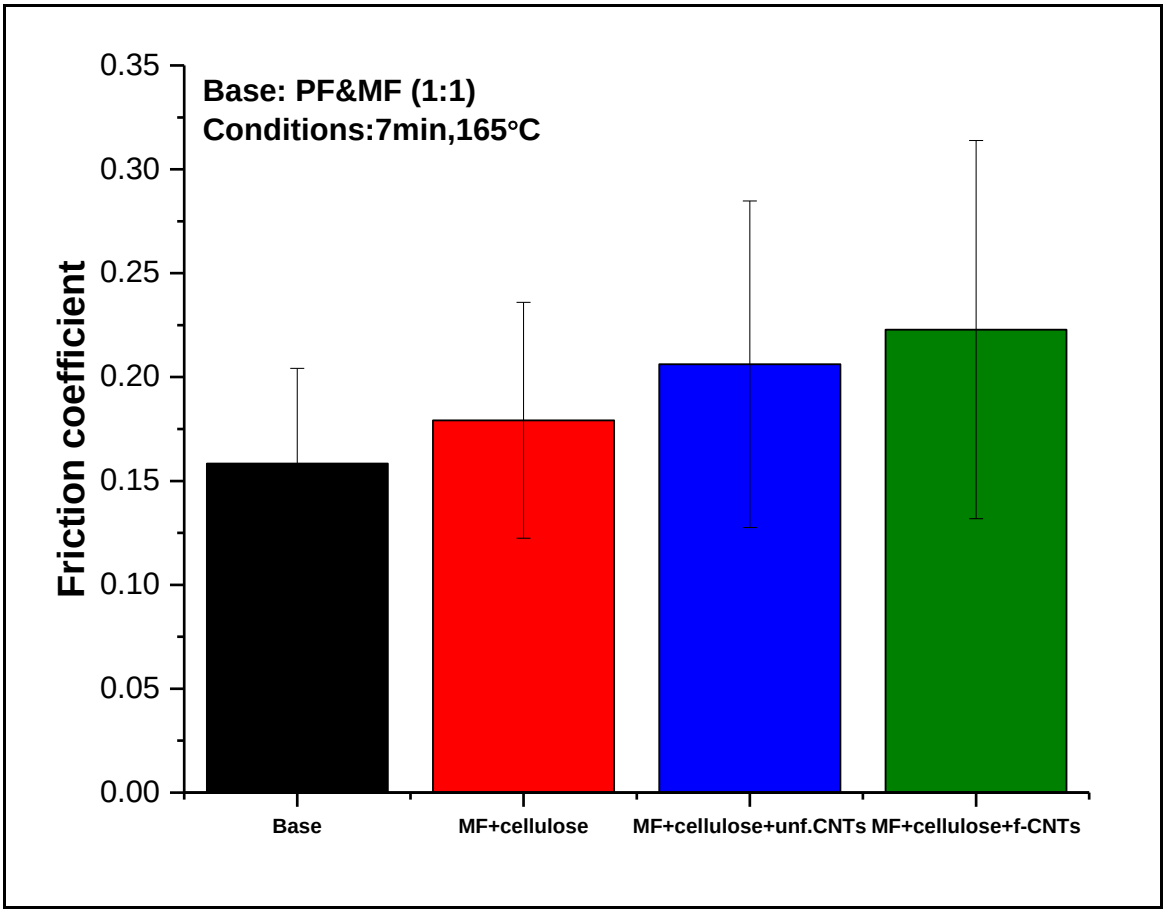

Graph 6 21 Trend of friction coefficient obtained by molding PF and MF mixture with different fillers at conditions of 7minutes and 165ºC

Fourth set of samples was prepared by hot molding phenol formaldehyde and melamine formaldehyde in 1:1 at the temperature of 165ºC and for about 7 minutes. As the fillers enhance the interfacial contact between them and the polymer matrix, the friction coefficient should decrease as compared to the base sample, helping polymer chains to stretch easily in the direction of shear. But in this case, the trend is opposite. All the filled samples failed to ease the polymer chain movement, as their friction coefficient is higher than the base sample. Infact, as the fillers are increasing from sample 2 to 4, friction coefficient is increasing. Probable reason could be improper mixing between the polymer matrix and fillers, providing less interfacial bonding between them.

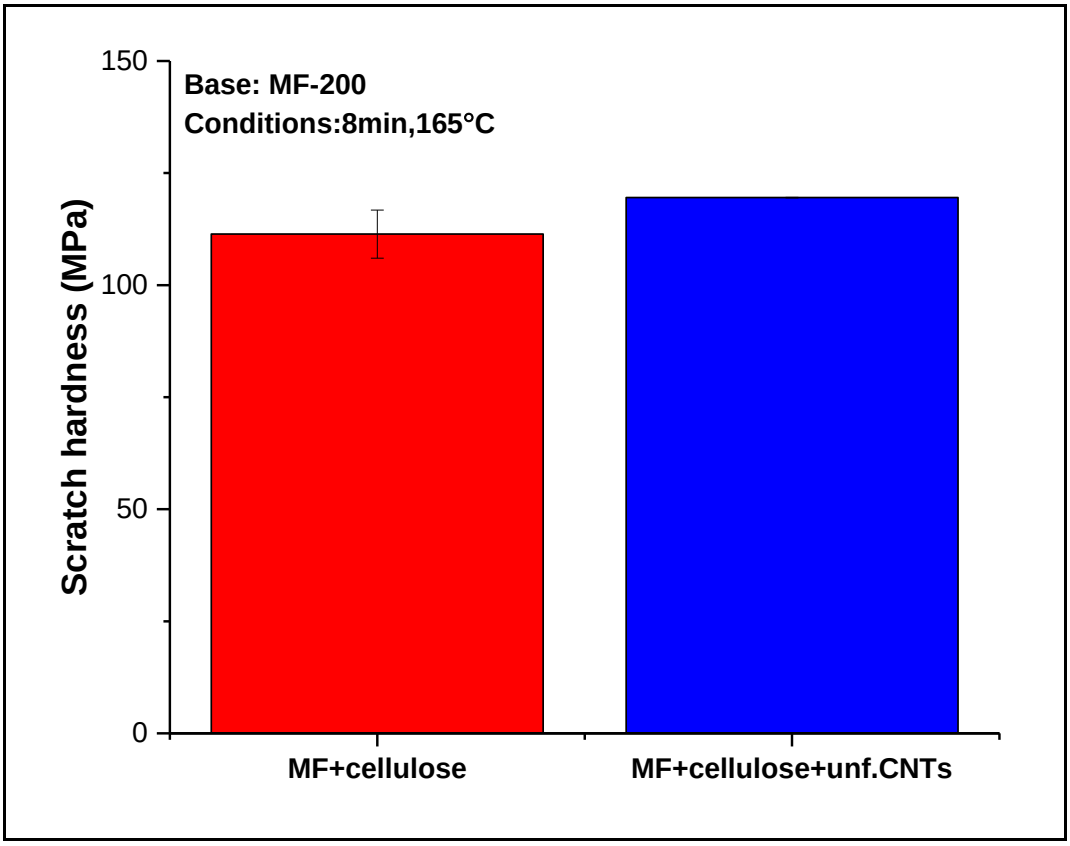

Graph 6 22Trend of scratch hardness obtained by molding MF resin with different fillers at conditions of 8minutes and 165ºC

Scratch hardness of a sample is the response of the material to the contact load exerted by the indenter on it. First set of samples was prepared by hot molding melamine formaldehyde at the temperature of 165ºC and for about 8 minutes. As the fillers enhance the interfacial contact between them and polymer matrix, the scratch hardness i.e. resistance to scratch should increase as the filling increase. In this case, base sample and the one filled with 2wt.% functionalized MWCNTs, being so brittle didn't survive the tensile tests, that's why their scratch hardness wasn't calculated. While comparing the two filled samples, sample with 20wt. % cellulose and 2 wt.% unfunctionalized MWCNTs seems to have better scratch hardness than the one that only has cellulose, reason could be larger modulus of the latter.

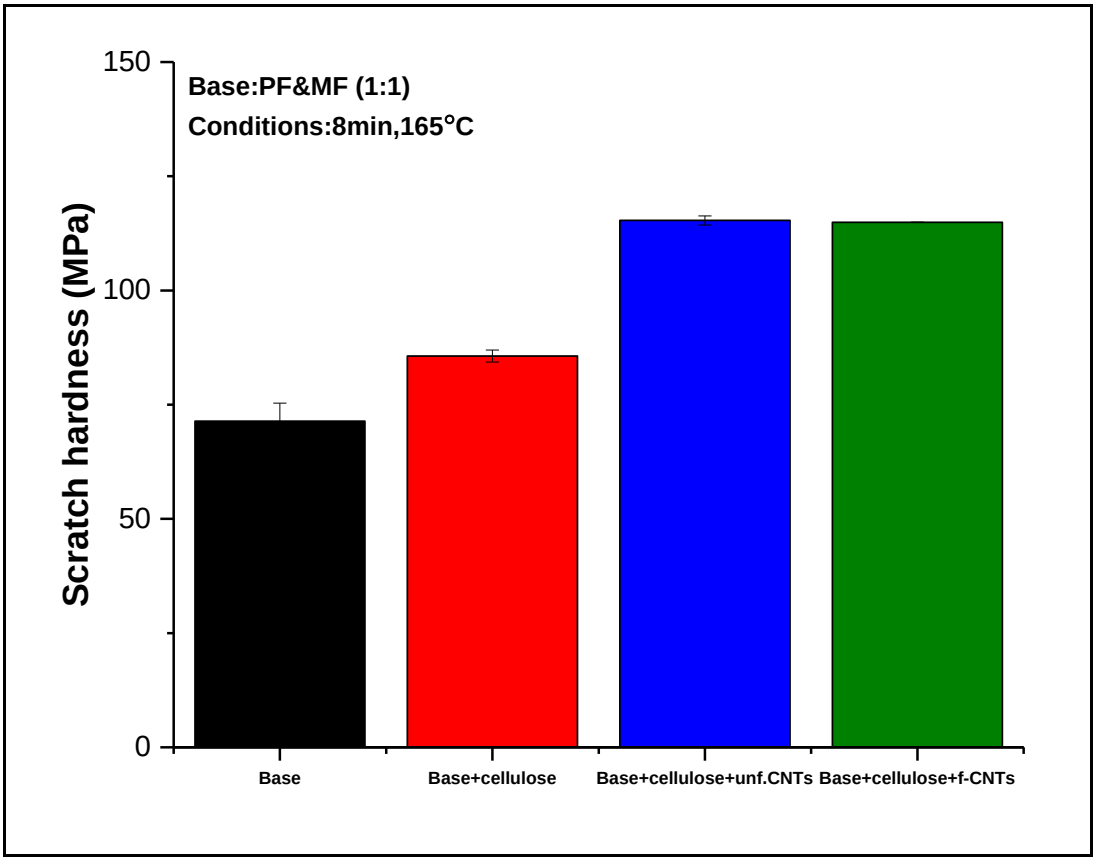

Graph 6 23Trend of scratch hardness obtained by molding PF and MF mixture with different fillers at conditions of 8minutes and 165ºC

Second set of samples was prepared by hot molding phenol formaldehyde and melamine formaldehyde in 1:1 at the temperature of 165ºC and for about 8 minutes. As the fillers enhance the interfacial contact between them and the polymer matrix, the scratch hardness in this case is increasing regularly with increasing the filler content and filler bonding with the polymer matrix, as shown in the graph above.

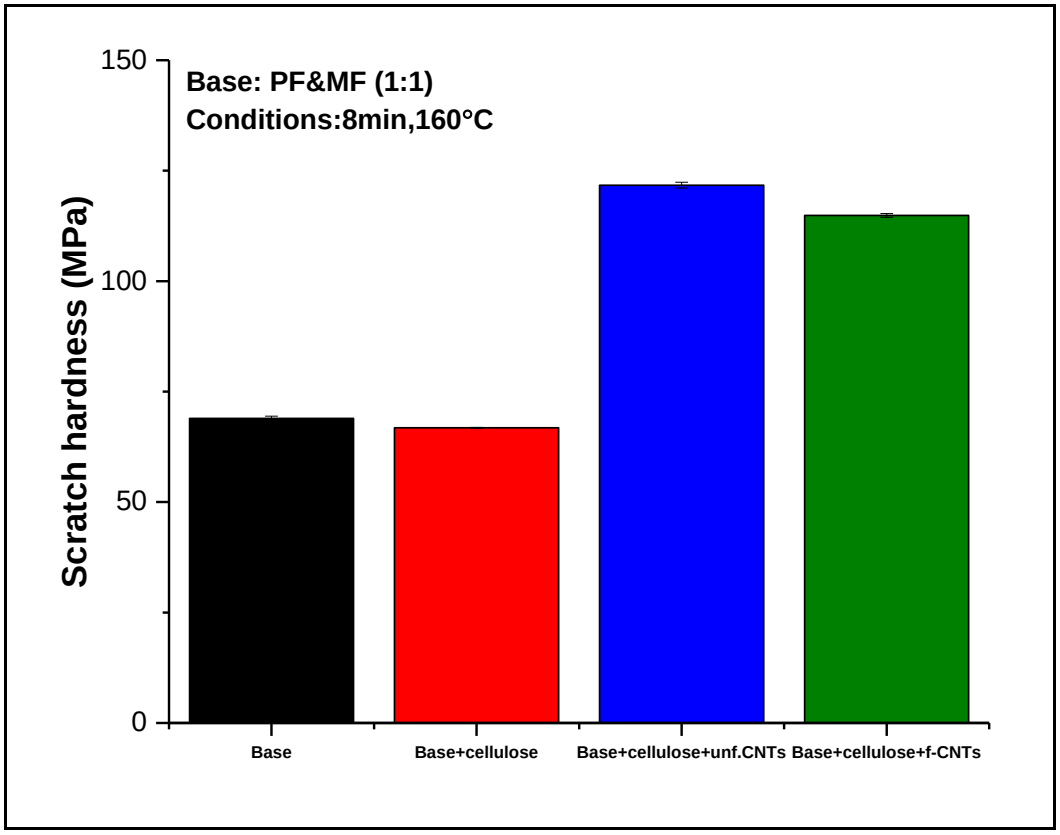

Graph 6 24Trend of scratch hardness obtained by molding PF and MF mixture with different fillers at conditions of 8minutes and 160ºC

Third set of samples was prepared by hot molding phenol formaldehyde and melamine formaldehyde in 1:1 at the temperature of 160ºC and for about 8 minutes. Scratch hardness of the samples filled with cellulose and unfunctionalized MWCNTs/ functionalized MWCNTs has significantly improved as compared to the base sample and the one filled with cellulose.

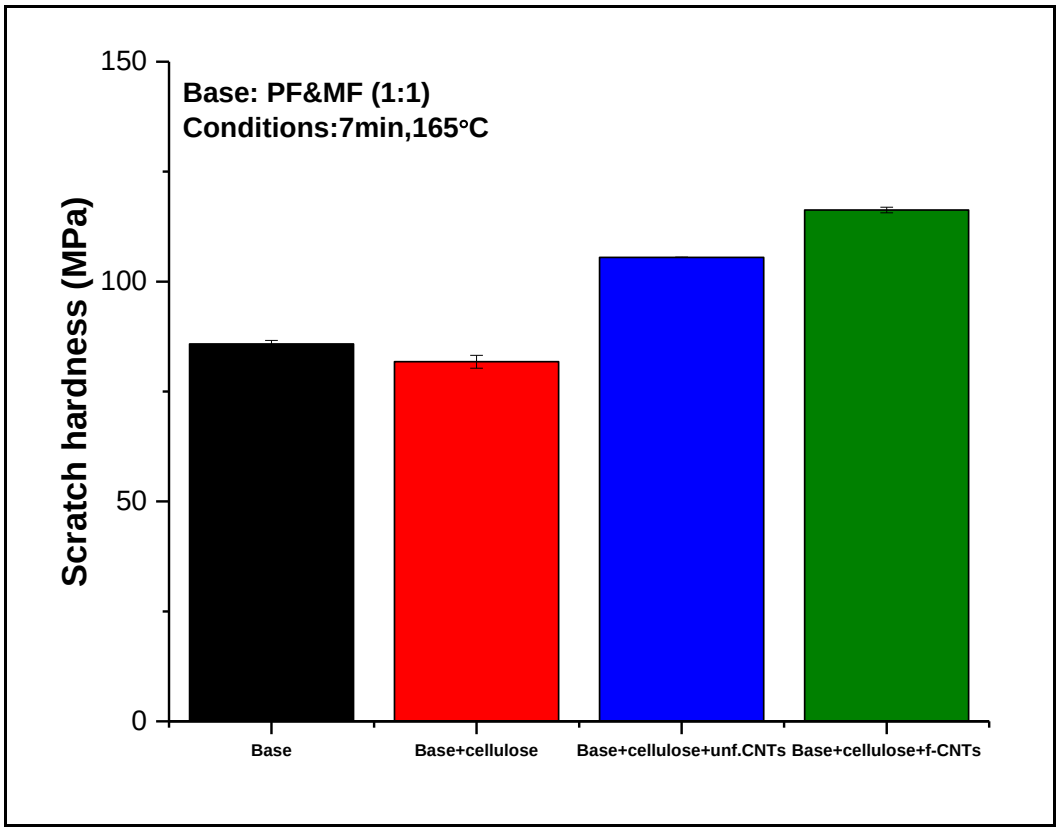

Graph 6 25 Trend of scratch hardness obtained by molding PF and MF mixture with different fillers at conditions of 7minutes and 165ºC

Fourth set of samples was prepared by hot molding phenol formaldehyde and melamine formaldehyde in 1:1 at the temperature of 165ºC and for about 7 minutes. Scratch hardness of the samples filled with cellulose and unfunctionalized MWCNTs/ functionalized MWCNTs has improved as compared to the base sample and the one filled with cellulose.

To get the better idea of the degree of reinforcement by the fillers, it is a good idea to compare scratch hardness with the maximum tensile stress obtained with each of the sample set. The maximum tensile stress is 'apparent' tensile stress as it is determined as per the conventional definition of yield point, which is identified as the relative maximum in stress-strain curve.

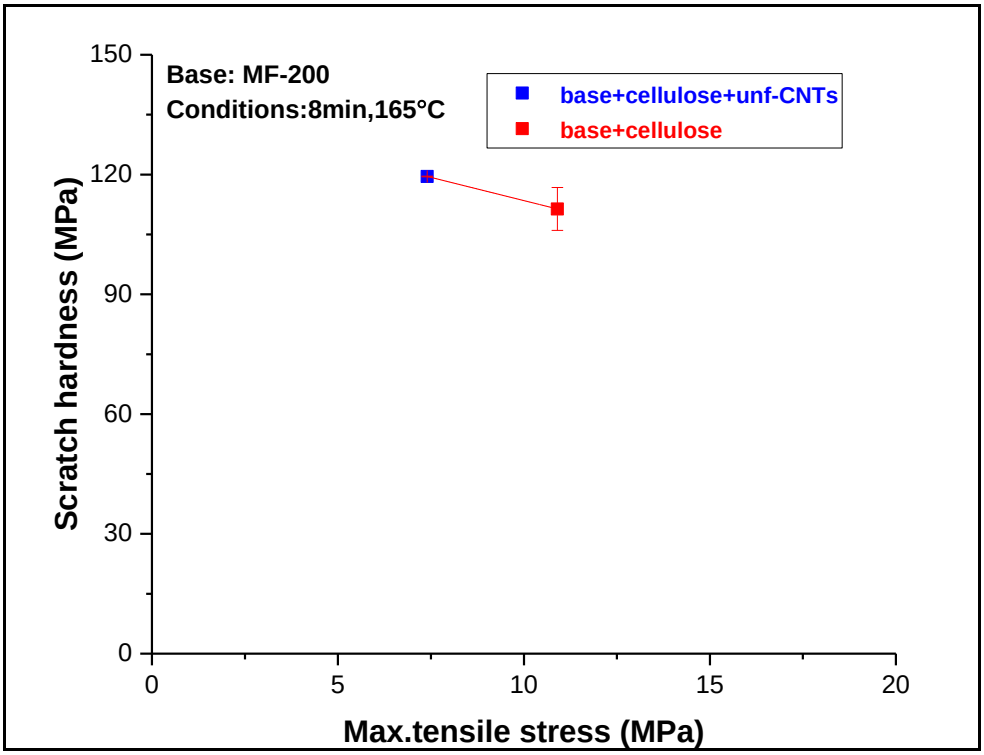

Graph 6 26Correlation between scratch hardness and maximum tensile stress for the first set of samples

First set of samples was prepared by hot molding melamine formaldehyde at the temperature of 165ºC and for about 8 minutes. It can be observed that the incorporation of the cellulose and unfunctionalized MWCNTs in the base has increased the scratch hardness more than the sample that is filled with cellulose only. But the trend is opposite in the case of maximum tensile stress for these samples.

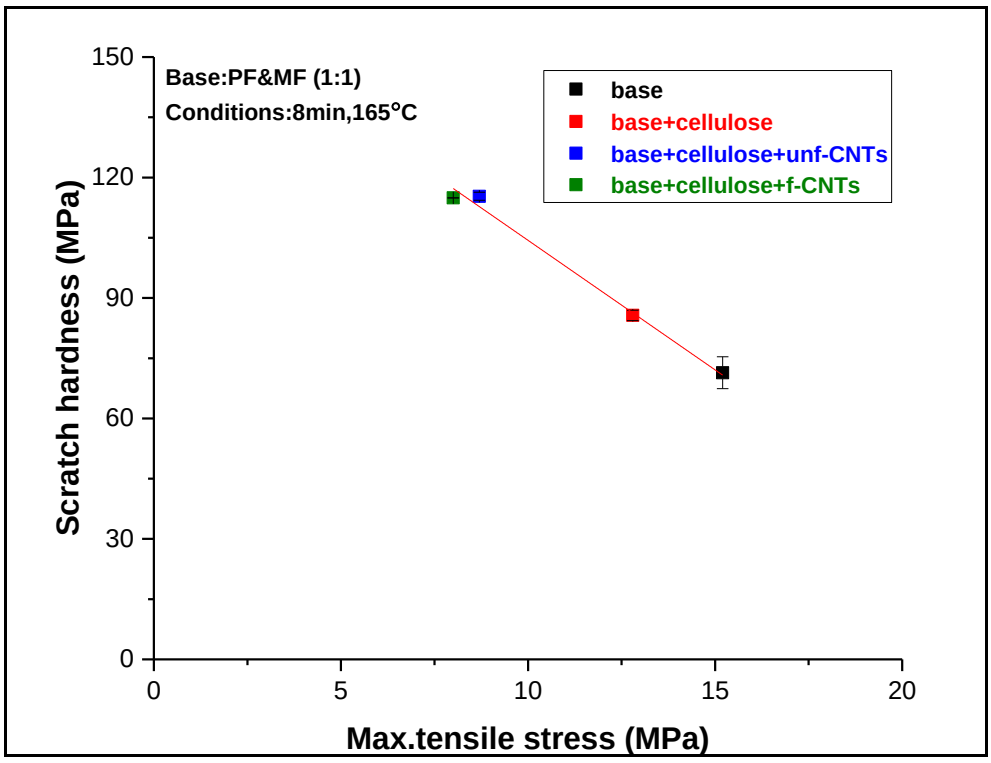

Graph 6 27Correlation between scratch hardness and maximum tensile stress for the second set of samples

Second set of samples was prepared by hot molding phenol formaldehyde and melamine formaldehyde in 1:1 at the temperature of 165ºC and for about 8 minutes. It can be observed that the incorporation of the fillers has increased the scratch hardness as the sample filled with cellulose and functionalized MWCNTs shows the maximum scratch hardness. In this case, scratch hardness displays a regular increasing trend as the filler content increases. But these fillers were unable to increase the maximum tensile stress of the samples as compared to the base sample. This concludes the fact that increase in scratch hardness doesn't necessarily mean an overall enhancement of the mechanical properties.

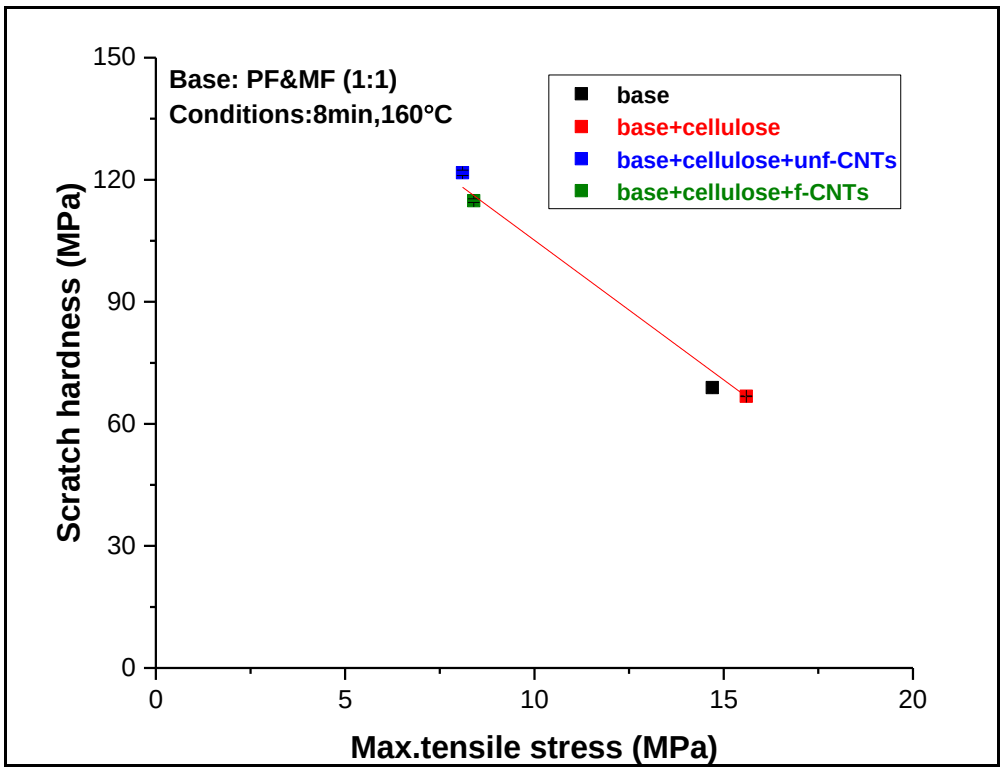

Graph 6 28Correlation between scratch hardness and maximum tensile stress for the third set of samples

Third set of samples was prepared by hot molding phenol formaldehyde and melamine formaldehyde in 1:1 at the temperature of 160ºC and for about 8 minutes. It can be observed that the incorporation of the unfunctionalized and functionalized MWCNTs along with cellulose improves the scratch hardness more than the base sample and the sample that is filled with cellulose alone. The reason could be better interaction between the fillers and polymer matrix. But the trend for the maximum tensile stress is completely opposite. This concludes the fact that increase in scratch hardness doesn't necessarily mean an overall enhancement of the mechanical properties.

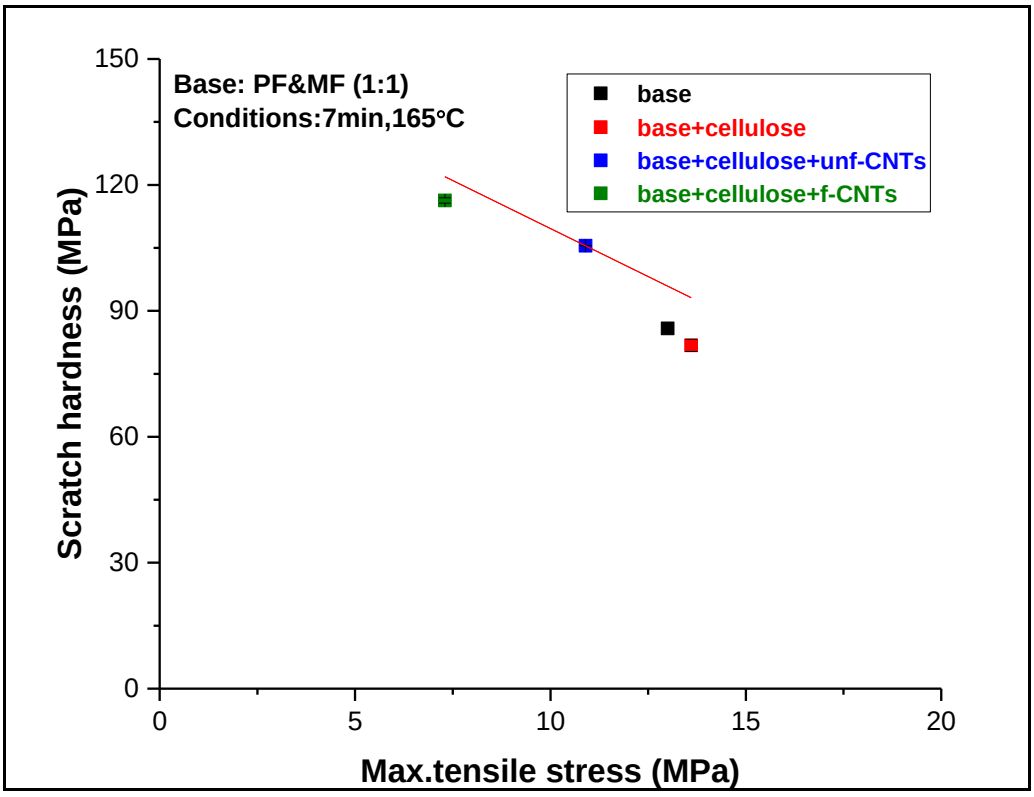

Graph 6 29 Correlation between scratch hardness and maximum tensile stress for the fourth set of samples obtained

Fourth set of samples was prepared by hot molding phenol formaldehyde and melamine formaldehyde in 1:1 at the temperature of 165ºC and for about 7 minutes. It can be observed that the maximum scratch hardness is obtained by incorporating functionalized MWCNTs along with cellulose in the base sample. But increasing the filler content didn't improve the maximum tensile stress. This concludes the fact that increase in scratch hardness doesn't necessarily mean an overall enhancement of the mechanical properties.

The graphs relating scratch hardness and maximum tensile stress indicates that incorporating the rigid fillers inside the polymer matrix, results in the change in scratch deformation mode from ductile ploughing to the brittle fracture, but this effect makes scratch much more visible. The fillers like CNTs which are harder than the matrix, either slightly decrease or does not affect the yield stress much [45]. Also the lack of strong interfacial bonding between the fillers and the polymer matrix didn't let the fillers toughen the polymer matrix well. Nonetheless, these results concludes that at least the composite samples prepared in this work show improvement in resistance to scratch penetration.

CHAPTER 7- CONCLUSIONS AND FUTURE OUTLOOKS

7. 1 Conclusion

The effect of incorporation of different types and certain amount of fillers i.e. 20wt. % of cellulose, 2wt % of unfunctionalized MWCNTs and 2wt % of functionalized MWCNTs in the polymer matrix of pure melamine formaldehyde and 1:1 of melamine formaldehyde and phenol formaldehyde was investigated in this research work, when these sample mixtures were hot compression molded in the time and temperature conditions of 8 minutes 165ºC, 8 minutes 160ºC and 7minutes 165ºC under the constant pressure of 75kg/cm^2 (7.35MPa).

The chemical functionalization of the MWCNTs was pretty reasonable, in this work as desired functional groups were obtained through FTIR (graph 1). In all the set of samples, the base sample filled with cellulose and unfunctionalized MWCNTs possess better tensile modulus out of all. Residual depth in all set of samples was less, so fillers didn't alter the viscoelastic nature of polymer matrix i.e. they didn't hinder the scratch recovery. The scratch hardness showed increasing trend with the increase in the fillers, but they tend to have brittle behavior of scratch as well.

Agglomeration of MWCNTs inside the composite is a dominant problem in this work, which appeared because of their lack of dispersion inside the polymer matrix. This has to be solved either by some other surface pre-treatment of CNTs that can ensure better filler-matrix bonding or by another appropriate mixing method providing high mechanical shear mixing instead of ball milling.

Since polymers do not always guarantee better strength and hardness for better wear resistance, to obtain desired tribological performance of the material, optimization of different parameters like polymer-filler type and ratio, process conditions, treatment/proper mixing of polymer matrix-fillers for better interaction is required.

7.2 Future Outlooks

Dispersing MWCNTs in an organic solvent like hexafluoroisopropanol (HFIP) first [46], before adding to the powder mixture of thermosetting resins may help with the adhesion, but this has to be analyzed. Another way to improve the interfacial adhesion between the CNTs and polymer matrix could be melt mixing in an extruder by monitoring the viscosity increase of the matrix during the process to prevent the coagulation of the nanotubes.

Ceramic powders like SiO2, SiC, ZnO, TiO2, Al2O3, Si3N4 and CuO can also act as reinforcing filler with thermosetting polymers that can help to enhance both mechanical strength and abrasion resistance, thus better tribological properties.

Though incorporating electrical conductivity in the composite for the slip ring, is beyond the scope of this research work, and needs further work. Incorporating metal particles that could adhere well with other fillers and polymer matrix can serve the purpose.

Appendix:

MOLDING CONDITIONS	SAMPLE NUMBER	COMPOSITION	TENSILE TEST	THREE-POINT BENDING	SCRATCH TEST
8 minutes, 165ºC	S1	**Base:** MF-200	Not done	σ = 24.6 MPa	Not done
	S2	MF+20% cellulose	σ =10.9 MPa E= 1676 MPa	σ = 30.5 MPa	Scratch hardness = 111.4 MPa
	S3	MF+20% cellulose + 2% unfunctionalized MWCNTs	σ =7.4 MPa E= 2089 MPa	σ = 44.5 MPa	Scratch hardness = 119.5 MPa
	S4	MF+20% cellulose + 2% functionalized MWCNTs	Not done	σ = 32.5 MPa	Not done
8 minutes, 165ºC	S5	**Base:** MF&PF (1:1)	σ = 15.2 MPa E= 1421 MPa	σ = 61.3 MPa	Scratch hardness = 71.4 MPa
	S6	MF&PF (1:1)+20% cellulose	σ = 12.8 MPa E= 1654 MPa	σ = 90.3 MPa	Scratch hardness = 85.7 MPa
	S7	MF&PF (1:1)+20% cellulose + 2% unfunctionalized MWCNTs	σ = 8.7 MPa E= 1547 MPa	σ = 50.7 MPa	Scratch hardness = 115.3 MPa
	S8	MF&PF (1:1)+20% cellulose + 2% functionalized MWCNTs	σ = 8 MPa E= 1464 MPa	σ = 46.9 MPa	Scratch hardness = 114.9 MPa
8 minutes, 160ºC	S9	**Base:** MF&PF (1:1)	σ = 14.7 MPa E= 1607 MPa	σ = 60.9 MPa	Scratch hardness = 68.9 MPa
	S10	MF&PF (1:1)+20% cellulose	σ = 15.6 MPa E= 1674 MPa	σ = 81.4 MPa	Scratch hardness = 66.8 MPa
	S11	MF&PF (1:1)+20% cellulose + 2% unfunctionalized MWCNTs	σ = 8.1 MPa E= 1760 MPa	σ = 38.7 MPa	Scratch hardness = 121.7 MPa
	S12	MF&PF (1:1)+20% cellulose + 2% functionalized MWCNTs	σ = 8.4 MPa E= 1517 MPa	σ = 54.2 MPa	Scratch hardness = 114.9 MPa

7 minutes, 165ºC	S13	**Base:** MF&PF (1:1)	σ = 13 MPa E= 1662 MPa	σ = 56.7 MPa	Scratch hardness = 85.8 MPa
	S14	MF&PF (1:1)+20% cellulose	σ = 13.6 MPa E= 1658 MPa	σ = 52.6 MPa	Scratch hardness = 81.8 MPa
	S15	MF&PF (1:1)+20% cellulose + 2% unfunctionalized MWCNTs	σ = 10.9 MPa E= 1741 MPa	σ = 47.9 MPa	Scratch hardness = 105.5 MPa
	S16	MF&PF (1:1)+20% cellulose + 2% functionalized MWCNTs	σ = 7.3 MPa E= 1367 MPa	σ = 42.5 MPa	Scratch hardness = 116.3 MPa

REFERENCES

[1] L. Stobinski, B. Lesiak, L. Kövér, J. Tóth, S. Biniak, G. Trykowski, J. Judek, *'Multiwall carbon nanotubes purification and oxidation by nitric acid studied by the FTIR and electron spectroscopy methods'*, Journal of Alloys and Compounds 501 (2010) 77–84

[2] Pinar Kurkcu, Luca Andena, Andrea Pavan, *'An experimental investigation of the scratch behaviour of polymers: 1. Influence of rate-dependent bulk mechanical properties'*, Wear 290–291 (2012) 86–93

[3] In-Yup Jeon, Dong Wook Chang, Nanjundan Ashok Kumar and Jong-Beom Baek, *'Carbon Nanotubes - Polymer Nanocomposites'*, Chapter 5:''Functionalization of Carbon Nanotubes'', (2011)

[4] A.Pizzi Pizzi, *'Melamine–Formaldehyde Adhesives'*, Chapter 32, (2003)

[5] R. Koehler, Kunststoffe Tech. 11: 1 (1941); Kolloid Z. 103: 138 (1943).

[6] R. Frey, Helv. Chim. Acta 18: 491 (1935).

[7] Dyana Ambrose, Sulafudin Vukusic, Ahmed A. Abdala, '*Melamine formaldehyde: Curing studies and reaction mechanism'*, Polymer Journal (2013) 45, 413–419

[8] Hirsch, A., *'Functionalization of Single-Walled Carbon Nanotubes'*. Angew, Chem, Int. Ed. (2002), 41, (11), 1853-1859.

[9] Sinnott, S.B, '*Chemical Functionalization of Carbon Nanotubes'*, Journal of Nanoscience and Nanotechnology J. Nanosc. Nanotechnol. 2, (2002),113-123

[10] Bianco, A.; Prato, M.; Kostarelos, K. & Bianco, A. *'Functionalized Carbon Nanotubes in Drug Design and Discovery'*. Acc. Chem. Res. 41, (2008), (1), 60-68.

[11] Mickelson, E.T.; Huffman, C.B.; Rinzler, A.G.; Smalley, R.E.; Hauge, R.H. & Margrave, J.L. *'Fluorination of single-wall carbon nanotubes',* Chem. Phys. Lett. 296, (1998), (1-2), 188-194.

[12] Kelly, K.F.; Chiang, I.W.; Mickelson, E.T., et al. *'Insight into the mechanism of sidewall functionalization of single-walled nanotubes: an STM study'*, Chem. Phys. Lett. (1993), 313, 445–450

[13] Stevens, J.L.; Huang, A.Y.; Peng, H.; et al., *'Sidewall amino-functionalization of SWNTs through fluorination and subsequent reactions with terminal diamines'*,Nano Lett. (2003), 3, 331–336.

[14] Ma, P.-C.; Siddiqui, N.A.; Marom, G. & Kim, J.-K. '*Dispersion and functionalization of carbon nanotubes for polymer-based nanocomposites: A review'.* Composites: Part A 41, (2010) 1345-1364.

[15] Islam, M.F.; Rojas, E.; Bergey, D.M.; Johnson, A.T.; Yodh, A.G., *'High Weight Fraction Surfactant Solubilization of Single-Wall Carbon Nanotubes in Water'*, Nano Lett. 3 (2), (2003), 269-273

[16] Tagmatarchis, N. & Prato, M.J., '*Functionalization of carbon nanotubes via 1,3-dipolar cycloadditions',* J. Mater. Chem. 14, (2004), 437–439.

[17] Liu, J.; Rinzler, A.G.; Dai, H.; Hafner, J.H.; Bradley, R.K.; Boul, P.J.; et al. '*Fullerene Pipes*' Science 280, (1998) 1253-1256.

[18] Yu, R.; Chen, L.; Liu, Q.; Lin, J.; Tan, K.-L.; Ng, S.C.; Chan, H S.O.; Xu, G.-Q. & Hor, T.S.A. '*Platinum Deposition on Carbon Nanotubes via Chemical Modification*', (1998)

[19] Sham, M.-L. & Kim, J.-K., *'Surface functionalities of multi-wall carbon nanotubes after UV/Ozone and TETA treatments'*, Carbon 44, (2006) (4), 768-777.

[20] Klumpp, C.; Kostarelos, K.; Prato, M.; & Bianco, A., *'Functionalized carbon nanotubes as emerging nanovectors for the delivery of therapeutics'*, Biochim. Biophys. Acta, (BBA) - Biomembranes 1758, (2006) (3), 404-412.

[21] Lifei Chen, Huaqing Xie and Wei Yu, Chapter 9: *'Functionalization Methods of Carbon Nanotubes and Its Applications'*, Carbon Nanotubes Applications on Electron Devices, Prof. Jose Mauricio Marulanda (Ed.), (2011) ISBN: 978-953-307-496-2

[22] Salavati-Niasari, M., & Bazarganipour, M., '*Covalent functionalization of multi-wall carbon nanotubes (MWNTs) by nickel(II) Schiff-base complex Synthesis, characterization and liquid phase oxidation of phenol with hydrogen peroxide',* Applied Surface Science, Vol.255, No.5, (2008),pp. 2963-2970, ISSN 0169-4332

[23] Pantarotto, D., Partidos, C.D., Graff, R., Hoebeke, J., Briand, J.P., & Prato, M., *'Synthesis, structural characterization, and immunological properties of carbon nanotubes functionalized with peptides'*, Journal of the American Chemical Society, Vol.125, No.20, (2003), pp. 6160-6164, ISSN 0002-7863

[24] Zeng, Y.L., Huang, Y.F., Jiang, J.H., Zhang, X.B., Tang, C.R., Shen, G.L., & Yu, R.Q., '*Functionalization of multi-walled carbon nanotubes with poly(amidoamine) dendrimer for mediator-free glucose biosensor*' Electrochemistry Communications, Vol.9, No.1, (2007) pp.185-190, ISSN 388-2481

[25] Lee Mohana Reddy, A., & Ramaprabhu, S, *Design and fabrication of carbon nanotube-based microfuel cell and fuel cell stack coupled with hydrogen storage device,* International Journal of Hydrogen Energy, Vol.32, (2007) No.17, pp.4272-4278, ISSN 0360-3199

[26] H. Pelletier, C. Mendibide, A. Riche, ''Mechanical characterization of polymeric films using depth-sensing instrument: correlation between viscoelastic plastic properties and scratch resistance'', Progress in Organic Coatings, (2007) 62162–178.

[27] K.L. Johnson,*'' The correlation of indentation experiments"*, Journal of the Mechanics and Physics of Solids 18, (1970) 115–126.

[28] J.L. Bucaille, E. Felder, G. Hochstetter, *''Mechanical analysis of the scratch test on elastic and perfectly plastic materials with the three-dimensional finite element modelling"*, Wear 249, (2001) 422–432.

[29] Mersen, *''Technical guide: Carbon brushes for motors and generators''*,

[30] Renown electric motors & repair Inc., *''Renown Electric's Guide to Carbon Brushes for Motors & Generators"*.

[31] N. Satyanarayana, K.S.S. Rajan, S.K. Sinha, L. Shen, *''Carbon nanotube reinforced polyimide thin-film for high wear durability"*, Tribol. Lett. 27, (2007) 181-188.

[32] J. Cumings, A. Zettl, *''Low-friction nanoscale linear bearing realized from multiwall carbon nanotubes"*, Science 289, (2000) 602-604.

[33] Accessed from official website: https://www.fratelligalli.com/Galli-Vaccum-Ovens-21GV-English.htm

[34] Edited by Hanna Dodiuk, Sidney H. Goodman, Handbook of thermoset plastics, Third edition, Pdl handbook series, Elsevier, (2014)

[35] U.S. Environmental Protection Agency. Integrated Risk Information System (IRIS) on Formaldehyde. National Center for Environmental Assessment, Office of Research and Development, Washington, DC. (1999)

[36] N.K. Myshkin, M.I. Petrokovets, A.V. Kovalev, '*Tribology of polymers: Adhesion, friction, wear, and mass-transfer',* Tribology International 38, (2005) 910–921

[37] Bely VA, Sviridenok AI, Petrokovets MI, Savkin VG. *'Friction and wear in polymer-based materials',* Oxford: Pergamon Press; (1982) p. 416.

[38] K. Friedrich, '*Polymer composites for tribological applications'*, Advanced Industrial and Engineering Polymer Research 1, (2018) 3-39

[39] K. Holmberg, A. Erdemir,*' Influence of tribology on global energy consumption, costs and emissions'*, Friction 5 (2017) 263-284.

[40] T. Santos, G. Vasconcelos,W. de Souza, M. Costa, E. Botelho, '*Suitability of carbon fiber-reinforced polymers as power cable cores: Galvanic corrosion and thermal stability evaluation',* Mater. Design 65 (2015) 780–788.

[41] X.-Q. Pei, R. Bennewitz, A.K. Schlarb, *'Mechanisms of friction and wear reduction by carbon fiber reinforcement of PEEK'*, Tribol. Lett. 58 (2015) 1–10.

[42] C. Sanchez, B. Julian, P. Belleville, M. Popall, Applications of hybrid organic–inorganic nanocomposites. J. Mater. Chem., 15 (2005) 3559–3592.

[43] Klaus Friedrich, Alois K.Schlarb, Editor: B.J. Briscoe, *'Tribology of polymeric nanocomposites'*, Tribology and interface engineering series, No.55, (2008)

[44] Luis F. Giraldo, Betty L. Lo´ pez, Witold Brostow*, ''Effect of the Type of Carbon Nanotubes on Tribological Properties of Polyamide 6'',* (2009), Polymer Engineering and Science

[45] Pinar Kurkcu, Luca Andena, Andrea Pavan, *'An experimental investigation of the scratch behaviour of polymers: 2. Influence of hard or soft fillers*, Wear 317 (2014) 277–290

[46] Akira Igarashi, Toshinari Terasawa, Mihoko Kanie Takeshi Yamanobe, Tadashi Komoto, 'A Morphological Study Of The Effect Of Carbon Nanotube Filler On Tribology Of Phenol/Formaldehyde Resin-Based Composites', (2005), Polymer Journal, Vol. 37, No. 7, pp. 522–528